A Study of the Effects of Sensory State on Rhesus Monkey Postural Control

by

Lara A. Thompson

B.S., Mechanical Engineering
University of Massachusetts Lowell (2003)

M.S., Aeronautical and Astronautical Engineering
Stanford University (2005)

Submitted to the Department of Health Sciences and Technology
In Partial Fulfillment of the Requirements for the Degree of

Doctor of Philosophy in Biomedical Engineering

at the

MASSACHUSETTS INSITUTE OF TECHNOLOGY

September 2013

Signature of Author _____
Department of Health Sciences and Technology
August 21, 2013

Certified by _____
Richard F. Lewis
MD, Associate Professor of Otology and Laryngology
Thesis Supervisor

Accepted by _____
Emery N. Brown
MD, PhD/Director,Harvard-MIT Program in Health Sciences and Technology
Professor of Computational Neuroscience and Health Sciences and Technology

A Study of the Effects of Sensory State on Rhesus Monkey Postural Control

by
Lara A. Thompson

Submitted to the Department of Health Sciences and Technology on August 21, 2013
in Partial Fulfillment of the Requirements for the Degree of Doctor of Philosophy in
Biomedical Engineering

ABSTRACT

Although many take the seemingly simple ability to balance in order to maintain posture for granted, approximately 8 million American adults have chronic balance impairment issues derived from vestibular dysfunction. For patients suffering from severe vestibular dysfunction, maintaining balance in daily activities, such as walking on an uneven surface at night, turning one's head, or attempting to stand on a moving surface, can prove extremely challenging. Unfortunately, many vestibular-loss sufferers are left with limited treatment options and can become permanently debilitated. In order to aid the vestibular-impaired population in partially restoring postural stability, it is important to develop rehabilitative solutions.

For subjects suffering from severe bilateral vestibular loss, but with intact eighth nerve function, the invasive vestibular prosthesis is a potential rehabilitative solution. This must be developed and fully characterized in non-human primates in parallel with human implementation. In this research, we characterized the postural response of a severely vestibular-lesioned non-human primate instrumented with a prototype invasive vestibular prosthesis. We showed that the severely vestibular-impaired animal aided by the prosthesis was able to utilize the partially restored vestibular cues to increase its stability compared to the severely-impaired state.

We also explored the impact on balance of (1) supplying an additional cue (light-touch) and (2) compensative strategies that the subject develops when suffering from mild or severe vestibular-impairment. We determined that the severely-impaired animal decreased its trunk sway when provided the light-touch cue, however a mildly-impaired animal did not. We also determined that an animal with mild vestibular impairment spontaneously compensated for its vestibular loss to stabilize itself both for stationary support surface conditions and for support surface perturbations. This thesis is the first time that animal posture measures for different levels of vestibular impairment have been used in conjunction with a feedback controller model to investigate the postural control mechanisms used.

The results reported within this thesis begin to establish the baseline database of primate postural responses to a wide variety of test situations for different levels of vestibular impairment that will be needed for further investigation and evaluation of rehabilitative solutions, such as prototype vestibular implant systems.

Thesis Supervisor: Richard F. Lewis
Title: Associate Professor of Otology and Laryngology (Neurology)

To my parents

Acknowledgements

I would like to thank my thesis supervisor, Dr. Richard Lewis, for his guidance and expertise and also for the allowing me the opportunity to be part of a diverse, unique, interesting, and truly novel set of research involving characterization of postural effects in vestibular loss and prosthesis assisted rhesus monkeys. I also thank the National Institutes of Health (NIH) for funding this research. I would like to thank my thesis committee: Drs. Donald Eddington, James Lackner, Daniel Merfeld, and Adam Goodworth for their guidance, assistance, and aid in the development of my thesis research. Finally, I would like to thank the Jenks Vestibular Diagnostic Laboratory and the entire Jenks Vestibular Physiology Laboratory for their efforts, expertise, and insights in guiding the research.

On a more personal note, I would like to thank my teachers, close friends and family for years of their support and encouragement. There are numerous friends and teachers, too many to list here, that have taught me various life-lessons that I will be forever grateful for. I would like to thank both my immediate and extended family for their love and support. I would like to thank my parents, Charles and Tita Thompson, for showing me not only through words, but also by example, that through diligence, hard work, and perseverance that all things are possible and that every wall has the potential to be a door. I would like to thank my sister, Danielle Thompson-Reynolds, for her support, encouragement, and advice. I would also like to thank my brother, Charles W. Thompson, for his love and support. Last but not least, I would like to thank my grandparents, Charles and Eiko Thompson and Jamie and Rosario Bersamira, for teaching me that by having an education, not only do we expand our own knowledge, but gain the ability to give back to others.

Table of Contents

List of Figures

List of Tables

I. Introduction

1.1 Motivation for Research

Everyday life depends on the posture needed to maintain balance. Without this we would risk falls leading to injury and possibly even death. Approximately 8 million American adults have chronic balance impairment issues derived from vestibular dysfunction (NIDCD 2008). Vestibular loss can arise due to congenital anomalies, genetic diseases, exposure to ototoxic drugs, age-related hair cell degeneration, and other idiopathic causes. People suffering from severe vestibular dysfunction experience equilibrium disorders that can cause unsteady balance in daily activities such as walking in dim lighting or on uneven surfaces, bending to pick something up, or the simple task of turning one's head. Although some patients may develop compensatory strategies over time, vestibular-loss sufferers that are unable to do so are left with limited treatment options and can become permanently debilitated. Possible rehabilitation solutions (in order of most to least invasive) include: 1) an invasive vestibular prosthesis (e.g., Gong and Merfeld 2002) that is aimed at restoring vestibular function, 2) non-invasive balance aids or devices (e.g., Back-y-Rita 2003; Peterka et al. 2006) that supply information to the subject about their body orientation (e.g., via tactile sensation) in order to serve as partial substitutes for the missing vestibular information, and 3) a set of posture strategies that the subject develops (either on their own or with expert training) in order to compensate for their vestibular dysfunction (e.g., increased muscle stiffening (as in Carpenter et al. 2001; Horak et al. 1994)).

For subjects suffering from severe bilateral vestibular loss, but who still have intact eighth nerve function, the invasive vestibular prosthesis may supersede the second and third rehabilitation strategies listed above. This most invasive rehabilitative solution must be developed and fully characterized in non-human primates prior to, or in parallel with, human implementation. In Chapter VI, we characterized the postural response of a severely vestibular-lesioned non-human primate (the rhesus monkey) that was instrumented with a prototype invasive vestibular prosthesis. An invasive vestibular prosthesis that encoded angular head velocity (via electric stimuli delivered to the semicircular canal afferents) was implemented, and we show that this information was integrated by the central nervous system (CNS) to provide the severely-impaired animal a more accurate estimate of head orientation. Because both head orientation cues and neck proprioceptive cues are needed in order for the animal to estimate its trunk position (e.g., Mergner 1983; Stapley 2006), the partially restored head orientation information (derived from the integration of the partially restored head velocity cues via the vestibular prosthesis) enabled the severely-impaired animal to reduce its trunk sway.

The second rehabilitation solution (sensory substitution) was not addressed explicitly, but we did explore the impact of providing an additional light-touch cue (via an earth-mounted juice reward dispenser) to animals with either mild or severe vestibular loss (Chapter V). These analyses showed that the severely-impaired animal decreased its trunk sway when provided the light-touch cue, however the mildly-impaired animal did not. We hypothesize that the mildly-impaired animal spontaneously and successfully compensated for the mild impairment (see below) in its animal farm environment and did not make use of the additional cue during testing.

In the least invasive rehabilitation scenario, the vestibular-loss patient develops a new posture control strategy (either on their own or with training) that compensates for the vestibular dysfunction and restores stability. Here we show that an animal with mild vestibular impairment can spontaneously compensate for its vestibular loss and stabilize itself both for stationary support surface conditions (Chapter III) and for support surface perturbations (Chapter IV). In this thesis, measures related to the posture of rhesus monkeys in three sensory states (i.e., normal, mild vestibular impairment, and severe vestibular impairment) were used in conjunction with a feedback control model that allowed us to investigate the postural control mechanisms used (i.e., long-latency sensory mediated mechanisms and/or intrinsic/short-latency mechanisms) by these animals. Taken together, the analysis of the measured data and the modeling results are related to the third rehabilitative solution outlined above.

In clinical practice, a broad range in severity of vestibular dysfunction exists across vestibular-loss sufferers. While previous studies have focused predominantly on quantifying the balance of subjects with either normal vestibular function or severe vestibular dysfunction, differences in the posture of normal, mildly-impaired, and severely-impaired subjects have not been characterized. Understanding how different levels of vestibular function affect the postural control mechanisms (e.g., the ability or inability of the subject to adjust postural strategy in order to compensate) should help to determine the most beneficial rehabilitative solution for the patient. The results reported here also begin to establish the baseline database of primate postural responses to a wide variety of test situations and in different sensory states that will be needed for the evaluation of prototype vestibular implant systems.

1.2 Background and Significance

1.2.1 Previous posture studies

Input stimuli to the three main sensory systems for posture (i.e., the visual system, somatosensory system, and vestibular system[1]) are encoded in neural responses that are integrated by the postural control system to yield an output postural response. For human and non-human subjects suffering from equilibrium disorders of peripheral vestibular origin, maintaining balance may prove to be challenging for situations involving: limited visual or somatosensory cues (Horak et al. 1990), decreased base-of-support[2] (e.g., Horak and Macpherson 1996), large amplitude head-turns (Stapley et al. 2006) and rotations of the support surface (e.g., Macpherson et al. 2007; Peterka 2002). Thus, previous studies have utilized quiet-stance, head-turns, and tilts of the support surface to determine the effects of vestibular dysfunction on posture.

1.2.1.1 Quiet-Stance

Quiet-stance is the simplest experimental condition used to evaluate the effects of the visual, somatosensory, and vestibular systems on posture and has been used both in human and animal studies. Quiet-stance refers to the condition in which both the visual surround and support surface are stationary and the subject attempts to stand as still as possible. Horak et al. (1990) have shown that humans with bilateral vestibular loss are able to maintain sway within normal range as long as they receive cues from visual or somatosensory systems. Furthermore, it has been shown that humans with bilateral vestibular loss have difficulty balancing when visual and somatosensory cues are unavailable or unreliable (e.g., Black and Nashner 1984). Thus, daily activities, such as

standing or walking in dimly-lit environments on uneven or compliant surfaces, would prove challenging for those suffering from vestibular dysfunction.

It has been previously shown that humans with severe bilateral vestibular dysfunction in an environment with limited visual cues could reduce their center-of-pressure $(COP)^2$ sway when they were allowed a light (< 1 N) finger-tip touch to a surface. Without this additional contact cue, none of the vestibular-loss subjects could stand in the dark without falling, but all the normal subjects could. However, when provided a light-touch cue, bilateral vestibular-loss subjects were significantly more stable in the dark than normal subjects in the dark without the touch cue. These findings showed that an additional cue (i.e., light-touch to a stationary surface) was effective in attenuating body sway in the absence of vestibular and visual information (Lackner et al. 1999).

Although there can be a broad range of vestibular function (from normal function to severe dysfunction) across subjects, the effects of utilizing a light-touch cue on posture have been determined exclusively for either normal or severe vestibular-loss humans (as in Lackner et al. 1999). The benefit of providing an additional sensory cue (e.g., light-touch) to an animal with an intermediate level of vestibular dysfunction (i.e., mild bilateral vestibular hypofunction or "mBVH") compared to an animal with severe vestibular dysfunction (i.e., severe bilateral vestibular hypofunction or "sBVH") has not previously been determined. Therefore, it was important to determine if a subject with a mild level of vestibular dysfunction could benefit (e.g., stabilize its trunk) by an additional sensory cue (e.g., light-touch). More specifically, could an animal with mild vestibular loss reduce its trunk sway when provided a light-touch cue in darkness? Also,

we aimed to determine if a severe vestibular-loss animal would make use of the light-touch cue and demonstrate a greater benefit (i.e., greater reduction in trunk sway) compared to the animal in the mild vestibular-loss state.

During quiet-stance testing, normal and labyrinthectomized cats had similar COP sway (Thomson et al. 1991). This study is mentioned here because it the most relevant to our studies involving characterization of the different levels of vestibular function in the rhesus monkey. However, the severely vestibular-lesioned cats were not tested in conditions of weak visual and somatosensory cues or decreased base-of-support, which may have revealed postural instability. Furthermore, only COP (derived from vertical ground reaction force data) was measured and not body movements directly (e.g., displacement of the center-of-mass) which could have revealed increases in body sway. In order to move beyond the limitations of previous quiet-stance cat studies, we did the following: 1) varied somatosensory cues by providing relatively strong or weak surface cues (i.e., thin, hard rubber surface or a thick, compliant foam surface, respectively), 2) varied mediolateral stance width to provide either a large (18 cm) or small (9 cm) base-of-support, 3) measured the animal's head and trunk movements (via position sensors), as well as ground reaction forces (via platform tri-directional force sensors). Furthermore, unlike human and animal studies that focused on either normal subjects or subjects with severe vestibular loss, we addressed the effects of three levels of vestibular dysfunction (i.e., normal, mild dysfunction, and severe dysfunction) on the animal's postural response to the quiet-stance experimental test conditions. We hypothesized that an animal with mild vestibular hypofunction (mBVH) may be able to compensate for its loss by increasing muscle stiffness (via long-latency and/or intrinsic/short-latency mechanisms),

thereby allowing the animal to sway within normal range, but that an animal with severe vestibular hypofunction (sBVH) would have increased sway and possibly be unable to compensate.

1.2.1.2 Head-Turn

It is well known that vestibular dysfunction can have a profound affect on standing balance in some conditions but not others. For both human and non-human subjects with severe vestibular loss, maintaining balance while turning the head is difficult. When asked to turn their head while walking, human bilateral vestibular-loss sufferers exhibit ataxic gait. In order to compensate for their loss, bilateral vestibular-loss humans may adopt a strategy where the head is "fixed" and not moving relative to the trunk (Herdman 1994). Furthermore, cat studies show that labyrinthectomized animals thrust their bodies to the ipsilateral side of the head-turn (opposite the response of normal animals), which led to imbalance and falls (Stapley et al. 2006). Based on previous human perception studies (e.g., Mergner 1983; 1991), it was hypothesized that since the vestibular-lesioned animal no longer received head-in-space (vestibular) cues, but still received head-on-trunk (neck proprioceptive) cues, the animal calculated an erroneous estimate of trunk-in-space (or trunk position) which led to imbalance and falls. While previous studies focused on either normal or severe vestibular-loss test subjects, they did not address postural responses to head-turns for subjects with various levels of vestibular dysfunction.

We investigated the effects of the degree of vestibular function on the postural response to head-turns. Head-in-space information was varied between sensory states: normal, mild bilateral vestibular loss (mBVH), severe bilateral vestibular loss (sBVH),

and severe bilateral vestibular loss aided by a vestibular prosthesis (sBVH + STIM-ON). The effect of partially restored vestibular information (via a vestibular prosthesis) on an animal's posture while undergoing head-turns has not previously been studied and further understanding could have implications for humans with severe vestibular loss.

The vestibular prosthesis used was a semicircular canal prosthesis that mimicked canal function in that it encoded angular head velocity through modulated electrical pulses to the eighth cranial nerve (introduced in Section 2.3.1. and discussed in Chapter VI). We hypothesized that the relatively high angular velocity head-turns in the plane of the one-dimensional vestibular prosthesis (as opposed to the quiet-stance and platform roll-tilt experimental stimuli where the head was relatively stationary or moving at low velocities) would show the effects of the prosthetic stimulation on trunk sway. Although the prosthesis used was a semicircular canal prosthesis that transduced angular head velocity, and not a prosthesis that restored sensation to the otoliths (the primary vestibular organs that sense linear acceleration and gravity necessary for standing balance), there has been considerable evidence that shows that canal cues can contribute to the estimate of head orientation relative to gravity (e.g., Angelaki et al. 1999; Merfeld et al. 1999). We hypothesized that partially restored head orientation (vestibular) cues combined with the information of the head relative to the trunk (neck proprioceptive) cues would enable the animal in the sBVH +STIM-ON state to better estimate trunk position than in the sBVH sensory state.

We hypothesized that an animal that was mildly impaired would be able to compensate for its moderate vestibular loss and control trunk sway within normal range during head-turns. However, based on previous studies (e.g. Stapley et al. 2006) we

presumed that an animal that was severely impaired would be relatively unstable and suffer increased trunk sway when turning its head to targets. Lastly, we hypothesized that an animal with severe bilateral vestibular loss aided by a vestibular prosthesis (sBVH + STIM-ON) would have partial restoration of head rotational cues, resulting in a better estimate of head orientation, and thus a more accurate estimate of trunk position compared to the sBVH animal. The partially restored head orientation (vestibular) information in combination with the existing head relative to the trunk orientation (neck proprioceptive) information would lead to a more accurate estimate of trunk position. This was hypothesized to cause decreased trunk sway for the animal sBVH + STIM-ON state compared to the sBVH sensory state. The degree to which the prosthesis affects posture in a severely impaired animal is an initial, but crucial, step in documenting the potential benefits of the prosthesis to severe vestibular-loss humans.

1.2.1.3 Platform tilts

A posture task more difficult for severe vestibular-loss sufferers than stationary platform conditions (e.g., quiet-stance and head-turns) was dynamic tilts of the support surface. To determine the posture response to support surface tilts as a function of amplitude (i.e., stimulus-response curve) and also the transfer function of the postural control system, a pseudorandom input platform tilt has been applied in several human studies (e.g., Goodworth et al. 2009, 2010; Peterka 2002). Peterka (2002) showed that for normal human subject's root-mean-square (RMS) center-of- mass $(COM)^2$ body sway saturates (or increases non-linearly) as platform tilt amplitude increases. The saturation of the normal subject's response as stimulus amplitude increases is attributed to the normal test subject's ability to increase orientation to earth-vertical as opposed to the

platform surface. This orientation to earth-vertical prevents normal humans from falling at the larger amplitude tilts in both the sagittal and frontal planes (Goodworth and Peterka 2010; Peterka 2002). As tilt amplitude increases, the normal human orients more with earth-vertical and less with the tilting platform. The sensory reweighting hypothesis predicts that normal humans weight their graviceptive (or earth-vertical) cues more heavily than their proprioceptive (or support surface) cues as stimulus amplitude increases. However, human subjects with severe bilateral vestibular loss do not exhibit the same reweighting of graviceptive cues with increases in stimulus amplitude (likely due to their severe vestibular impairment). Instead, they rely more heavily on their proprioceptive cues, and orient increasingly more with the support surface (Peterka 2002). Therefore, their stimulus-response curves remain close to linear and do not saturate. At larger amplitudes, this response results in instability and falls. Characteristics that are seen in the RMS stimulus-response curves can also be seen in the gain-phase relationships of the system transfer functions. For larger stimulus amplitudes, normal humans orient their COM with earth-vertical (i.e., gain = body tilt from upright/stimulus tilt approaches zero) as opposed to the platform. However, bilateral vestibular-loss subjects oriented their COM with the platform (i.e., gain = body tilt from upright/stimulus tilt is greater than or equal to one).

Postural responses to pseudorandom tilt stimuli have not been published for quadrupeds. Instead, ramp and hold rotations (Macpherson et al. 2007) and discrete sinusoidal inputs (e.g., Beloozerova et al. 2003; Brookhart et al. 1965) have been used. Macpherson et al. (2007) examined bilateral vestibular-loss cats during ramp and hold pitch and roll rotations of the support surface (~ 6 deg). The normal postural response

was to maintain limb alignment with earth-vertical. However, the control strategy of the vestibular-loss cats was opposite that of normal cats in that the animal rotated with the platform surface as opposed to aligning with earth-vertical. This strategy led to instability and falls. Similar to Peterka's (2002) study in humans, the large body sway for vestibular-loss cats in response to platform tilt suggests that muscle activation patterns were opposite those of normal subjects (i.e., abnormal response magnifies body sway leading to destabilization) and consequently the lesioned animal became unstable. The concept of sensory reweighting (described above) could be investigated by use of a feedback controller model (e.g., Peterka 2002). More specifically, model parameter graviceptive and proprioceptive weights could be investigated as a function of platform tilt amplitude to either prove or dispute the hypothesis.

We hypothesized that a normal, and also mildly impaired (mBVH), animal's trunk response to platform tilt would exhibit sway saturation, and furthermore, that sensory reweighting would be present. Sensory reweighting means that the animal would place a larger reliance (weight) on graviceptive cues that orient it with earth-vertical and place decreased reliance on proprioceptive cues that orient it with the platform at the larger platform tilt amplitudes. By modifying a previously developed human postural feedback control model (described in Chapter IV),, we were able to test the sensory re-weighting hypothesis for the animal's hindtrunk.

1.2.2 Balance Aids and Vestibular Prostheses

Vestibular hypofunction can occur as a result of congenital anomalies, genetic diseases, exposure to ototoxic drugs, age-related hair cell degeneration, and other causes. Patients with bilateral vestibular hypofunction suffer from visual, perceptual, and postural

deficits (e.g., blurred vision while walking and during head movements, chronic disequilibrium, and postural imbalance) (e.g., Lewis et al. 2007). Because the inputs to the vestibuloocular and vestibulospinal reflexes are limited or unavailable in vestibular-loss sufferers, they are unable to stabilize their eye and body movements. Although partial compensation may develop over time, those who are unable to do so are left with very limited treatment options. Thus, there has been a pressing need for development of rehabilitative solutions, and both non-invasive and invasive solutions have been investigated.

Non-invasive approaches (such as "balance aids") do not emulate vestibular function but instead are used as a means to augment postural reflexes by serving as a sensory addition or sensory substitute. Some examples of non-invasive solutions are: 1) tactile stimulation applied to the subject's torso (e.g., Peterka et al. 2006), 2) sound presented by headphones (e.g., Dozza et al. 2005), and 3) electrical stimulation of the tongue (e.g., Bach-y-Rita 2003; Tyler et al. 2003). While these solutions may aid in augmenting posture reflexes, they cannot fully emulate vestibular function nor do they restore visual reflexes (e.g., vestibuloocular reflex (VOR)).

Invasive approaches ("vestibular prostheses" or "vestibular implants") excite neurons of the vestibular system and are aimed at restoring vestibular function. The vestibular system responds to head movements that are both angular (via the semicircular canals) and linear (via the otolith organs). Although a prosthesis that restores full vestibular function (i.e., to both the otoliths and the semicircular canals) would be ideal, this technology is not yet feasible (e.g., directing electrical stimulation to the otoliths is hindered by the opposing polarities of the otolith hair cells). Instead past and current

investigations have involved the use of a semicircular canal prosthesis aimed at restoring rotational cues. Gong and Merfeld (2002) created a one-dimensional prosthesis that was able to restore the angular VOR in a guinea pig with a plugged semicircular canal. To explore the effects the prosthesis on eye movements in non-human primates, squirrel monkeys with severe vestibular dysfunction have been used (e.g., Lewis et al. 2010; Merfeld et al. 2007). Furthermore, development of a three-dimensional prosthesis used to restore rotational cues to three semicircular canals has been investigated in chinchillas (e.g., Della Santina et al. 2006; Fridman et al. 2010) and rhesus monkeys (e.g., Chiang et al. 2011). While previous studies investigated the effects of invasive semicircular canal prostheses on eye movements, their impact on posture had not been examined until recently.

The effects of postural responses to electrical stimulation (via a unilateral semicircular canal prosthesis in the right ear) were studied in human subjects suffering from Meniere's disease (Phillips et al. 2013). The vestibular-loss humans were studied for quiet-stance (with tandem foot placement) in the eyes-open or eyes-closed conditions. While undergoing prosthetic stimulation to a particular canal, the force-plate derived COP response was measured. The results showed that canal stimulation elicited postural responses with directional selectivity. For example, for the right posterior semicircular canal, head acceleration towards the right ear in the LARP plane (pitch back and roll right), is naturally excitatory. However, electric stimulation localized to the right posterior canal was interpreted (by the subject) as a sudden, unexpected rotation of the body within the this plane which caused a postural reflex to pitch the body forward and roll left to stabilize against the sensed perturbation. Another finding was that sway

response modulated with modulation of the stimulation current. However, a limitation of the prosthesis was that eye movements were not consistent with postural responses. More specifically, in all subjects the direction of the elicited eye movements changed as a function of stimulation current level (possibly due to increases in current spread at higher current levels), but the direction of the postural response was not observed to change. However, this study served as an initial step towards the feasibility and implications of a vestibular prosthesis in regards to posture.

The prosthesis used in the present study stimulated the semicircular canal (angular head velocity sensor) afferents of the right posterior canal, and was not a prosthesis that restored sensation to the otoliths (linear acceleration and gravity sensors). However, there has been considerable evidence that canal cues combine with otolith cues to differentiate between head translations and head tilts (e.g., Angelaki et al. 1999). More specifically, semicircular canals combine with otolith cues to estimate head orientation relative to gravity. As opposed to studying the COP of eyes-open and eye-closed quiet-stance conditions (as in Phillips 2013), we aimed to study the effects of head-turns to illuminated targets (in a severely impaired animal instrumented with the prosthesis) on trunk sway. We hypothesized that partially restored head orientation (vestibular) cues combined with the information of the head relative to the trunk to give the animal in the sBVH + STIM-ON state a better estimate of trunk position thereby causing a reduction in trunk sway compared to the animal in the severely impaired (sBVH) sensory state.

1.3 Document Organization

In addition to the introduction, this thesis includes five main chapters:

Chapter II

Chapter II describes the general methods used in this body of thesis research.

Chapter III

Chapter III characterizes posture by utilizing a stationary platform (e.g., to implement the quiet-stance condition). Measures of RMS trunk roll and ground reaction forces are shown for the normal and mildly-impaired (mBVH) rhesus monkey. Together, these results show that a mild vestibular-impaired animal (R2) decreases sway and increases forces exerted on the platform compared to a normal animal. Because intrinsic/short-latency stiffness orients the animal upright on a stationary surface, we hypothesize that by increasing (intrinsic/short-latency) muscle stiffness the animal with a mild vestibular impairment is able to compensate for its vestibular deficit. Results were interpreted with the aid of a feedback controller model. Model-predicted trunk sway measures (Prieto et al. 1996) were closely matched (within 10% error) to trunk sway measures derived from the measured data for the normal and mBVH states of R2. An increase in model-estimated intrinsic/short-latency stiffness for the mBVH state compared to the normal state was consistent with the stiffening hypothesis. Unlike the normal and mildly-impaired animal (R2), it was hypothesized that the severely-impaired (sBVH) animal (R1) would not be able to fully compensate (i.e., exhibit increased sway) because increases in intrinsic/short-latency stiffness would be insufficient to offset the destabilizing effects of diminished sensory feedback from the vestibular system. We further hypothesized that the magnitude of the trunk sway was substantial enough that (long-latency) neural feedback (as opposed to intrinsic/short-latency mechanisms (Loram et al. 2007)) control became more dominant in the response (e.g., Peterka 2002). Implementation of the feedback controller model was used to test this hypothesis and to

explain the sBVH results. Model-predicted sway measures, and those derived from experimental data, were in close agreement.

Chapter IV

Chapter IV characterizes posture utilizing a moving platform with a dynamic, pseudorandom ternary sequence (PRTS) roll-tilt (input) stimulus. Normal and mBVH results were described in terms of stimulus-response curves (i.e., trunk RMS roll as a function of stimulus amplitude) and transfer functions (i.e., gain, phase, and coherence). In the normal animal, saturation hindtrunk roll for an increase in stimulus amplitude (or sway saturation) was measured. The animal in the mBVH state still exhibited some sway saturation, but to a lesser extent than seen in the normal animal. We hypothesized that the normal animal increased its graviceptive sensory weight (orientation to earth-vertical) for an increase in stimulus amplitude. It had not been previously addressed, or even explored, whether a feedback control model (based on humans) could be implemented to determine meaningful interpretations of monkey data. A feedback controller model was used to explore physiologic model parameter estimates and relate them to the normal and mBVH measured results. For normal and mBVH sensory states, the feedback controller model was also used to test the sensory reweighting hypothesis: increased weighting of graviceptive cues at the larger stimulus amplitudes. This was the first feedback model of its kind that characterized normal and vestibular-impaired monkey data.

Chapter V

The purpose of Chapter V was to study the effect of the degree of vestibular impairment on the animal's ability to make use of a light-touch cue. One juice reward configuration provided the animal a light-touch stationary reference, while the other did

not. One rhesus monkey (R2) was studied in the mildly impaired (mBVH) sensory state and other animal (R1) in a severely impaired (sBVH) sensory state. We determined that the animal in the sBVH state was able to utilize light-touch cues to greater attenuate its trunk sway than the animal in the mBVH state.

Chapter VI

Chapter VI characterizes the effects of the prosthesis on posture during head-turns toward illuminated targets. Rhesus monkey trunk position (trunk-in-space) in response to head-turns was measured for an animal (R1) receiving two levels of head-in-space (vestibular) information (i.e., sBVH and sBVH + STIM-ON). The prosthetic stimulation during head-turns partially restored head velocity information that the CNS integrated to provide the severely-impaired animal a more accurate estimate of head orientation. The animal in the sBVH + STIM-ON sensory state had decreased trunk sway compared to the animal in the sBVH state. The results imply that partial restoration of head-in-space cues (via the prototype vestibular prosthesis), combined with normal neck proprioceptive (or head-on-trunk) cues, can provide a severely-impaired animal a more accurate estimate of trunk position (or trunk-in-space) and, as a result, a reduction in trunk sway.

1.4 Introductory Material

Postural control is maintained by sensory integration of three main sensory systems: the somatosensory system, the visual system, and the vestibular system.

1.4.1 Somatosensory System

The somatosensory system includes proprioceptors and tactile sensors (i.e., somatoreceptors).

In order to control our motor performance, perception of our body image is needed. The term "proprioceptors" has been used to describe a set of somatosensory afferents that convey information about the position and movements of body parts relative to one another. Among proprioceptors, muscle spindles have been regarded as the most important (e.g., Matthews 1988). Muscle spindle receptors are interspersed throughout muscles. The rate of firing of spindle receptors depends on both the length and movement (velocity) of the muscle. Spindle afferents fire rapidly during muscle stretch, however they also fire tonically when muscle length is constant (Matthews 1988). Muscle spindle receptors, such as those within the leg, provide important information for postural control (Horak and Macpherson 1996). For example, if the muscle spindles within the leg are stretched, the firing rate increases which transmits to the CNS the information that can be used to estimate degree of body tilt and hence trunk position. Located within the tendons are another type of stretch receptor (i.e., the Golgi tendon organ). Tendon organs lie in series with the muscle and respond whenever the muscle contracts. Together, muscle spindles and Golgi tendon organs provide the sensory segment of basic (spinal) reflexes for stabilizing a joint and aid in maintaining posture and locomotion.

The outputs of subcutaneous touch and pressure receptors can be used by the brain to determine body position with respect to an external reference. Pressure receptors are stimulated in the feet when standing on a support surface or stimulated in the fingertip when touching an object. Mechanoreceptors respond to sensations of touch and pressure on the soles of the feet, hands, and body. Furthermore, there are mechanoreceptors within the skin that are sensitive to stretch. For example, shearing forces on the feet due

to platform tilts cause the mechanoreceptors in the skin of the foot to change their firing rate, thus giving information about velocity and perturbation of the support surface (Horak and Macpherson 1996). Furthermore, Edin (2002, 2004) showed the importance of skin mechanoreceptors for joint movements and postures. Movements at nearby joints activate afferents originating from skin mechanoreceptors on the back of the human hand and these afferents provide information of both the static and dynamic aspects of joint movements (Edin 2002). This study held implications for mechanoreceptors in other areas of the body. Edin (2004) obtained microneurographic recordings from the afferents innervating the area of skin deformed by movements at the knee joint. Because the knee joint is one of the largest joints in the body, and is also subjected to large torques on a regular basis, control of the knee is imperative for postural stability. Edin (2002, 2004) showed that because skin receptors are capable on conveying relevant high-fidelity information, they play a significant role in proprioception.

1.4.2 Visual System

The visual system allows us to perceive our own motion and our position relative to the world around us. Unlike nonvisual sensory systems, such as the vestibular system, and to a lesser extent the somatosensory system, visual inputs do not habituate during constant velocity motion (Previc 2004). However, the visual system has a long latency compared to the nonvisual orientation systems. For example, the vestibular system can relay signals for eye movement control in < 7 ms (e.g., Huterer and Cullen 2002) as opposed to the visual system that can relay to the visual cortex in ~100 ms (Previc 2004). Thus, for low frequency movement visual signals provide reliable sensory information used to help stabilize oneself. During higher frequency activities (e.g., brisk walking,

jogging or running), we rely on "interactive" reflexes between the visual and vestibular systems, to stabilize our visual field in response to head or body movements. The vestibuloocular reflex (VOR) uses signals from the vestibular organs to control the position of the fovea and therefore hold images stable during high frequency or rapid head rotations.

The visual system is task and context dependent. In general, the visual input dominates both at low frequencies of body sway and when the visual system is in conflict with the somatosensory and vestibular systems (Horak and Macpherson 1996).

1.4.3 Vestibular System

The vestibular system within the inner ear contributes to equilibrium and spatial orientation. The vestibular system senses rotations via the semicircular canals and linear accelerations via the otolith organs. Both the canals and the otoliths can be modeled as heavily damped linear second-order systems, which respond to angular velocity or tilt angle and linear acceleration, respectively.

The three semicircular canals are approximately orthogonal to each other, and are called the horizontal (or lateral), the anterior (or superior) and the posterior (or inferior) semicircular canals. For yaw rotations (rotation about the vertical axis) there is movement of fluid within the horizontal semicircular canal. For pitch (rotations in the sagittal plane, about the interaural axis) or roll (rotations in the frontal plane, about the nasooccipital axis) the anterior and posterior canals are activated. When the head rotates, the movement of fluid, or endolymph, through the canal duct deflects a gelatinous structure called the cupula, which contains hair cells. When the hair cell stereocilia are deflected towards the kinocillium, gating channels open and depolarize the hair cell (i.e.,

K+ ions of the endolymph flow into and depolarize the hair cell). This causes vesicular release that leads to synaptic transmission on the hair cell afferent fibers. This process is called mechano-electric transduction.

While the semicircular canals respond to rotations, the otolith organs, consisting of the utricle and the saccule, sense linear acceleration and gravity. Because of their orientations, the utricle is sensitive to horizontal movements and the saccule is sensitive to vertical movements. Within the otolith organs, the otoconia crystals in the otoconia layer rest on a viscous gel layer, and are heavier than their surroundings. During linear acceleration, stereociliary bundles of the hair cells deflect and mechano-electric transduction occurs.

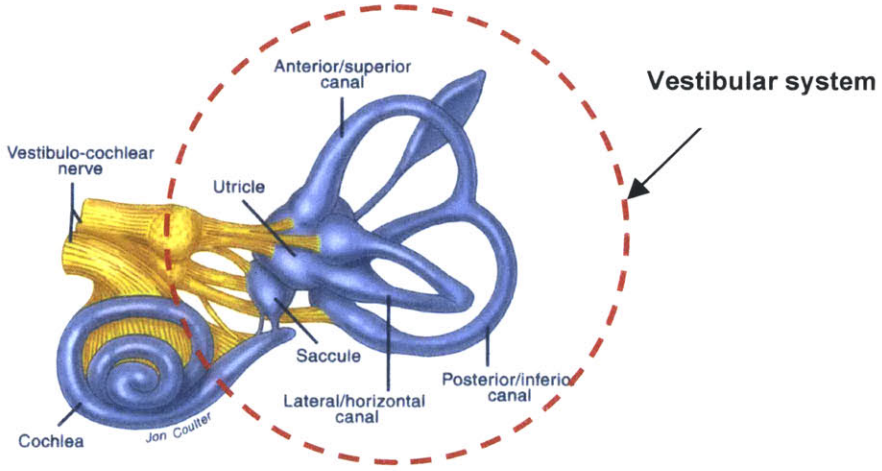

Figure 1.1 The inner ear (The Balance Center of Maryland 2013).

The vestibular system plays an important role in posture in that activation leads to several body and limb reflexes that result in stabilization of the head and body. Vestibular signals are sent to the vestibular nuclei. From there, two vestibulospinal tracts (i.e., the lateral vestibulospinal tract and medial vestibulospinal tract) descend from the brainstem and are important in regulation of posture via action of proximal and axial

muscles (Cheung 2004).

1.4.4 Postural Orientation and Postural Equilibrium

The previous section briefly described the three main systems involved with posture. In this section, I discuss two important behavioral goals of the postural control system: orientation and equilibrium.

Postural orientation is the relative positioning of body segments with respect to one another, and it can be aimed at aligning the trunk, limbs, head, or gaze to a variety of reference frames. Postural orientation can change (e.g., based on the specific task, specific behavioral goals, and postural references). Postural references may include the following: 1) a visual reference, 2) a somatosensory reference (e.g., contact with an external object), 3) a vestibular reference (e.g., based on gravitoinertial forces and perceived earth-vertical), and 4) an internal representation of body orientation (e.g., based on prior experience or memory). Because the trunk determines the positioning of limbs relative to objects with which one may wish to interact, trunk position is one of the most important controlled variables of postural orientation (Horak and Macpherson 1996). During complex motor tasks, head and neck position affect the perception of the trunk in space. Thus, animals may tend to stabilize their head in space (e.g., to simplify interpretation of visual and vestibular information).

Postural equilibrium is the state where the net forces acting on the body are balanced. One of the main goals of postural equilibrium is to control the position and velocity of the trunk, where most of the body mass resides. Center-of-mass (COM) is the point at which the entire distributed mass of the body is balanced. Destabilizing influences, such as gravity, produce external forces on the body. In order to control the

position of the COM and maintain equilibrium, internal (body) forces attempt to counteract destabilizing, external forces. The musculoskeletal system has a large number of degrees of freedom and thus the transformation of muscle contraction to forces and then to movement of the COM is mechanically complex (Horak and Macpherson 1996). Although there are not simple relationships between the muscle contractions and forces generated at the joints, the overall "goal" is to move the COM into the region of stability by applying the appropriate forces (under the feet) on the support surface. Vertical ground reaction forces of the support surface (i.e., the forces that are opposing the forces exerted by the animal on the support) are used to determine center-of-pressure (COP). COP is the weighted average of all the pressure over the surface area in contact with the ground (e.g., bottom of the feet), and is the location of the (resultant) vertical ground reaction force vector (Winter 1995).

In static equilibrium, the body's vertical projection of the COM lies within the base-of-support. The base-of-support is the area that is bounded by the body's points of contact with the support surface (e.g., the area between the feet). Static stability is proportional to the following: 1) base-of-support area, 2) (vertical) distance from COM to support base, and 3) body weight (Horak and Macpherson 1996). Quadrupeds have a base-of-support that is large relative to COM height. A larger base-of-support allows for a larger area within which the COM can move without loss of equilibrium. Thus, compared to quadrupeds (e.g., cats and rhesus monkeys), bipedal humans are relatively unstable because their base-of-support is small and COM is high. During dynamic equilibrium, such as locomotion, the body COM projection rarely lies within the base-of-support.

In order to maintain postural orientation and postural equilibrium, a postural strategy is formulated. Postural strategy is a high-level plan formulated by the nervous system for one or more postural goals (e.g., trunk orientation, gaze fixation, or energy expenditure). Postural strategy is described, for example, in terms of kinematics and muscle synergies. The appropriate strategy will depend on task and context (i.e., one set of goals may take precedence over another set of goals). And for a given task, there are multiple successful strategies because the musculoskeletal system has more degrees of freedom than are necessary to achieve a specific task or goal (Horak and Macpherson 1996). Alongside the postural strategy, a neural strategy applies a hierarchy on the appropriate controlled (postural) variables to achieve one solution for a particular task.

---

[1] Readers unfamiliar with the visual, somatosensory, and vestibular systems are referred to the introductory material in Section 1.4.

[2] Readers unfamiliar with posture nomenclature (e.g., base-of-support, center-of-pressure, and center-of-mass) are referred to the introductory material in Section 1.4.4.

II. Methods

2.1 Introduction

This chapter provides an overview of the methods used for this thesis research. It describes the species used, the sensory states (defined in terms of vestibular function) in which measures were made, the rhesus monkey balance platform, and the experimental test conditions used.

For this research, non-human primates (i.e., rhesus monkeys) were used. Posture was studied for various levels of vestibular function: normal, mild bilateral vestibular hypofunction (mBVH), severe bilateral vestibular hypofunction (sBVH), and severe bilateral vestibular hypofunction aided by a prototype vestibular prosthesis (sBVH + STIM-ON). The animal stood on a balance platform that was equipped with force sensors that were used to measure ground reaction forces, and the animal wore position sensors to measure displacements of the head, foretrunk, and hindtrunk. The experimental test conditions implemented have been used previously in human and/or cat studies (described in Chapter I) to test the balance of those with normal vestibular function and severe vestibular deficits. The balance platform setup allowed for a variety of input experimental conditions (i.e., quiet-stance, head-turn, and pseudorandom roll-tilt stimuli) used to quantify the animals' postural responses. Thus, the experimental conditions highlighted in this chapter were implemented to characterize the postural control system. The hypotheses, results, and interpretation of the measured data for the experimental conditions discussed in this chapter are described in Chapters III, IV, V, and VI.

2.2 Explanation of Species Used

A major thrust of this thesis research was to aid in developing rehabilitative solutions (e.g., an invasive vestibular prosthesis) for those suffering from vestibular loss. People suffering from severe vestibular dysfunction experience equilibrium disorders that can cause unsteady balance during daily activities (e.g., turning one's head or walking in dimly-lit environments). Although some patients may develop compensatory strategies over time, vestibular-loss sufferers that are unable to do so are left with limited treatment options and can become permanently debilitated. As previously stated in the Chapter I, possible rehabilitation solutions include: 1) an invasive vestibular prosthesis aimed at restoring vestibular function, 2) non-invasive balance aids that supply information to the subject about their body orientation (e.g., via tactile sensation) in order to serve as partial substitutes for the missing vestibular information, and 3) a set of posture strategies that the subject develops (either on their own or with expert training) in order to compensate for their vestibular dysfunction. For investigation of the second and third rehabilitative solutions, humans could serve as potential test subjects (as opposed to animal test subjects). However, the first rehabilitative solution (the invasive vestibular prosthesis) needed to be developed and fully characterized in a non-human primate prior to, or in conjunction with, human implementation.

Although the second and third rehabilitative solutions (above) could be investigated in humans, the advantage to using animal test subjects (e.g., rhesus monkeys) for the experiments described in this thesis was that animal test subjects had the potential to serve as their own control (as opposed to human studies where normal and severe vestibular-loss patients were different individuals). By characterizing the

posture of animals in normal, mild, and severe vestibular impaired states, as well as a severely impaired vestibular state aided by a vestibular prosthesis, allowed us to establish a database on the effects of different levels of vestibular function on posture. This knowledge would aid future vestibular-loss human posture studies, including those aimed at the development of the vestibular prosthesis.

Although human testing would be the most direct path to characterization of the first rehabilitative solution (the invasive vestibular prosthesis), animal test subjects were used for the experiments discussed in this thesis. Non-human primates (rhesus monkeys) were used because they were more similar to humans than e.g., guinea pigs (Gong and Merfeld 2000; 2002) or chinchillas (e.g., Della Santina et al. 2006) that had been used previously to characterize the effects of an invasive prosthesis on eye movements. The use of non-human primate test subjects allowed for a broader and more extensive range of the research experiments that were needed leading up to human implementation of the vestibular prosthesis. Utilizing the rhesus monkey allowed us to characterize animal behaviors (e.g., the main focus of this thesis: postural responses) [1] for systematically varied levels of vestibular function (e.g., normal, mBVH, sBVH, and sBVH + STIM-ON). It also allowed us to further develop the prosthesis itself and prosthesis implantation procedures (e.g., surgical risks during placement or removal, assessment of infection, implant failure and lifespan (not discussed further here)). By developing this knowledge base (in non-human primates), this decreases the possible risks and enhances the potential benefits associated with future implementation of the invasive prosthesis in humans.

Another advantage to using the rhesus monkey as a test subject was that there is a large background database on the physiology of the vestibular system for this species that could aid in interpretation of the results from these experiments. Because the rhesus monkey was a frontal eye species with binocular foveate vision, we were able to quantify level of vestibular function by a well-known reflex: the vestibuloocular reflex (VOR). These reflexive eye movement responses (i.e., the vestibuloocular reflex (VOR)) are linked to semicircular canal and otolith function and were quantified in response to sinusoidal inputs. The monkey's sensory state (e.g., normal, mBVH, sBVH, and sBVH + STIM-ON) was defined in terms of the VOR gain (ratio of eye velocity to head velocity).

Training and manageability were other reasons that the rhesus monkey was ideal and favorable for use as compared to other potential non-human animal models. The experimental conditions described here required animals that could be trained to perform complex tasks (e.g., standing on a compliant foam surface or balancing on a platform undergoing the pseudorandom platform tilt stimulus). Currently, there are no published data on animals, other than humans, undergoing pseudorandom platform tilts, and it is unlikely that either lower primates or non-primates could be trained to perform these sets of experiments. Also, the rhesus monkey's manageable size, as opposed to larger non-human primates such as chimpanzee or ape, made them favorable animals for this research. Lastly, the principal investigator (Richard F. Lewis) had extensive experience (>17 years) working with alert, behaving rhesus monkeys and training them to perform complex tasks.

The obvious, mechanical difference between the rhesus monkey and humans is that the rhesus monkey is a habitual quadruped in comparison to the human, a habitual

biped. Initially, it was proposed to conduct the experiments with the animal standing as a biped. Because the bipedal balance task turned out to be more difficult to implement than anticipated, and also because it was a stance not habitual to the animal, we proceeded with the rhesus monkey in its natural (quadrupedal) stance (Lewis et al. 2007).

Our preliminary analysis of normal monkey postural responses to pseudorandom tilts showed similarities to that of human responses. This moderated our concerns about the quadruped/biped differences. Rhesus monkey RMS roll of the trunk as a function of pseudorandom roll-tilt amplitude (i.e., stimulus-response curves) showed striking similarity to those seen in normal humans (Peterka 2002) in that the trunk sway generally followed the platform tilt waveform, remained relatively constant across repeated cycles, contained power primarily at the stimulated frequencies, and saturated with increases in stimulus amplitude. Furthermore, the normal animal's upper to lower trunk (foretrunk to hindtrunk) phase difference as a function of stimulus frequency showed that foretrunk and hindtrunk are in phase at low frequencies but out of phase at higher frequencies (see Chapter IV). This preliminary finding was similar to the normal human upper body and lower body responses to mediolateral pseudorandom tilt (Goodworth and Peterka 2010). These examples show that although the monkey was a habitual quadruped, the similarities between human and monkey responses to pseudorandom tilts indicate that monkey should provide a useful subject in the testing and development of a vestibular prosthesis.

2.3 Sensory States

Two rhesus monkeys (R1 and R2) were studied in various sensory states. R2 was studied in the normal and mBVH sensory states and R1 was studied in the control, sBVH,

and sBVH + STIM-ON sensory states.[2] As stated in Chapter I, previous posture studies in both animal and humans have focused on normal function and severe vestibular dysfunction. In the work reported here, we characterize rhesus monkey posture responses to a range of experimental conditions for levels of vestibular function (normal, mBVH, sBVH, and sBVH + STIM-ON).

In order to damage the vestibular hair cells while preserving the eighth nerve for electric stimulation, ototoxic drugs (i.e., the aminoglycosides intratympanic gentamicin and intramuscular streptomycin) were administered (see Section 3.3.1 for details). The dosages of the ototoxic drugs were based on the animals' weight (R1: 7.9 kg and R2: 6.7 kg). The angular vestibuloocular reflex, or VOR, (a simple and direct measure of semicircular canal function) was used to quantify sensory state. Figure 2.1 describes the various sensory states in terms of the percent reduction of VOR compared to the baseline state for each animal.

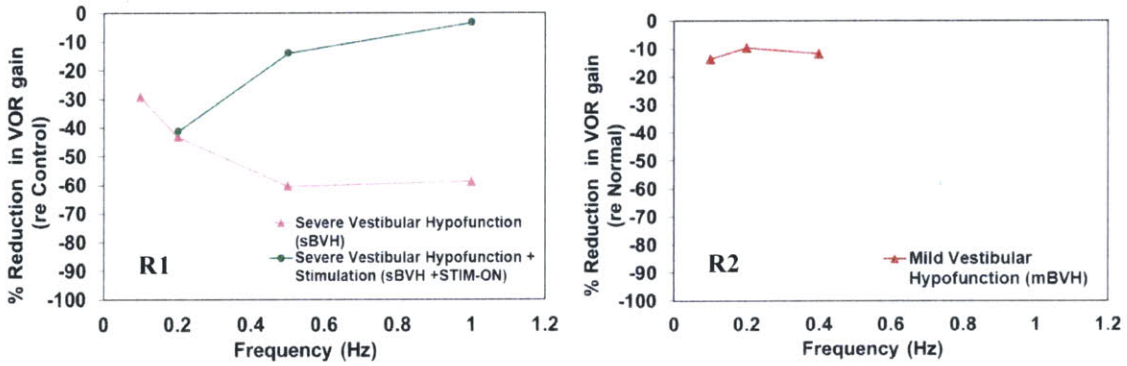

Figure 2.1 Sensory states of R1 (left) and R2 (right) shown as a percent reduction from baseline values of VOR gain.

2.3.1 Vestibular Prosthesis

The details of the prosthesis design and implementation have been previously published (Gong and Merfeld 2002; Lewis et al. 2010; Merfeld et al. 2007) and will only

be described briefly. The study described in Chapter VI of this thesis utilized a one-dimensional, semicircular canal prosthesis in which the electrode was placed in the ampulla of the right posterior canal in the rhesus monkey, R1. Although a one-dimensional prosthesis is described here, current ongoing research involves implementation of a three-dimensional prosthesis to stimulate all three canals in one ear.

The one-dimensional prosthesis sensed head velocity that was high-pass filtered (~0.03 Hz cutoff frequency, time constant of 5 s), to mirror the function of a normal rhesus monkey semicircular canal. The filtered head velocity was used to modulate the current pulse rate of the electric stimulus so that increasing (or decreasing) head velocity results in increases (or decreases) in spike rate (similar to the normal physiology of the canal and ampullary nerve). The tonic, baseline pulse rate was 250Hz with a pulse amplitude of 90 microamperes with 200 μs pulse duration. The rate was modulated to provide a bidirectional cue (i.e., head-turns that were ipsilateral to the stimulating electrode increased the rate of stimulation while head turns that were contralateral to the stimulating electrode decreased rate of stimulation). The modulation itself was based on a hyperbolic tangent function that saturated at higher angular velocities, but was approximately linear for mid-range velocities.

2.4 Equipment and Training

2.4.1 Balance platform apparatus

Figure 2.2 displays the rhesus monkey balance platform used for the studies described in this thesis. Each of the four platform footplates was equipped with tri-directional force sensors (ME-Meßsysteme GmbH, KD24S, Hennigsdorf, Germany) used to quantify ground reaction footplate forces. A 16-bit analog-to-digital converter (ADC)

with 5 V full-scale voltage range was used. The quantization error of the ADC was ~ 1.53 $x10^{-5}$ V. The calibrated force sensor directional sensitivities were quantified as the following: ~21 N/V (vertical), ~14 N/V (anterior-posterior), and ~14 N/V (mediolateral). Therefore, the measurement error (in N) associated with quantization error were the following: ~ $1.53x10^{-3}$ N (vertical) and ~ $1.07x10^{-3}$ N (anterior-posterior and mediolateral). Also, based on manufacturer specifications, each force sensor had a nominal output of 0.5 mV/V +/- 0.1 % at the nominal force of +/- 100 N (i.e., an operating force range 200 N). For a 5V source, the mean of nominal output of the sensor is 2.5 mV with +/- 0.0025 mV deviation. We can convert the sensor deviation (0.0025 mV) to N using the calibrated sensitivities. The sensor error was the following: 5 x 10^{-5} N (vertical) and 3.5 x 10^{-5} N (anterior-posterior and mediolateral). These measurement and sensor error values are orders of magnitude smaller than the reaction forces that we expected to measure for the animal (e.g., shear forces were expected to be > ~ 0.5 N and vertical forces > ~15 N). Force data were sampled at 200 Hz for the quiet-stance and head-turn experimental conditions and at a rate of 600 Hz for the pseudorandom tilt experimental condition, using LabVIEW (National Instruments Corporation, Austin, TX). These sampling rates are much greater (> 10 x) than the frequencies expected for the fluctuations in force measurements of the animal and therefore satisfied the Nyquist sampling criterion.

To measure the motion of the head, foretrunk, and hindtrunk, three, six-degree of freedom sensors (miniBIRD, Ascension Technology Corporation, Milton, VT) were sampled at 100 Hz for the quiet-stance and head-turn experiments and at 150 Hz for the pseudorandom platform tilt experiment. These frequencies were much greater than the

frequencies expected for body-sway (< ~ 10 Hz) and therefore satisfied the Nyquist sampling criterion. Angular ranges of the sensors were +/- 180° (yaw and roll) and +/- 90° (pitch). Factory specifications of the position sensors were described as resolutions relative to the mid-range transmitter (i.e., static resolution for position was 0.5 mm and static resolution for orientation was 0.1° at 30.5 cm from a mid-range transmitter). Since the sensors were within close proximity to the transmitter, we assumed the factory specification of 0.1° to be the measurement resolution. We were initially expecting body motions to generally be > ~ 0.1°, and so it was anticipated that this resolution was satisfactory. For our experimental measurements we observed the following angular deviation ranges from the mean: head-mounted quiet-stance (hindtrunk: ~0.07 to ~0.15°; foretrunk: ~0.17 to ~0.32°), head-turns (foretrunk: ~4 to ~14 °), PRTS (hindtrunk: ~0.1 to ~1.2°).

In order to limit visual cues, all test sessions were conducted in dim lighting with a black tarp surround. When recording test sessions, infrared illuminators (48-LED Illuminator Light Cctv Ir Infrared Night Vision) were used in conjunction with a pair of Kodak (movie) cameras with infrared lenses. The cameras were positioned to image the front and side of the animal to record: 1) animal behavior and 2) human handling artifacts within a given test session.

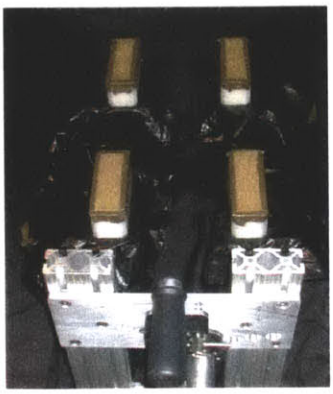

Figure 2.2 Rhesus monkey balance platform (Lewis et al. 2007).

The stationary platform allowed for changes of the base-of-support and also of the support surface material (quiet-stance experiment). The stationary platform was also used in conjunction with illuminated targets placed on the surround to evoke animal head movements (head-turn experiment). Furthermore, the platform allowed for dynamic tilts in the roll axis (pseudorandom stimulus experiment).

Depending on the posture experiment, the balance system included three different reward configurations illustrated in Figure 2.3: a vertical, earth-mounted juice reward system (that provided a light-touch cue), a head-mounted juice reward system (no light-touch cue), a platform-mounted juice reward system (that was attached to, and moved with, the balance platform). The earth-mounted reward configuration used a flexible mouth tube attached to a rod in front of the balance platform. The head-mounted reward configuration used a juice tube clipped to the monkey's headcap and, with flexible tubing, was routed to the monkey's mouth. The head-mounted reward system allowed the monkey to freely move its head during the test session. By moving directly with the platform, the platform-mounted juice reward configuration motivated the animal to stand on the tilting platform without providing it a stationary (re earth), reference cue.

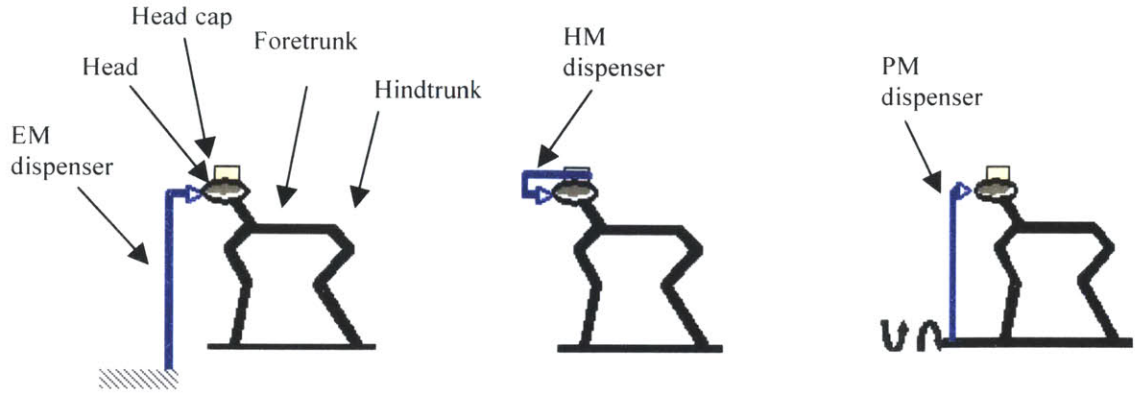

Figure 2.3 Schematic of the juice reward configurations. Earth-mounted, EM, dispenser (left), head-mounted, HM, dispenser (middle), and platform-mounted, PM, dispenser (right).

The measurement system used in this research was novel. It allowed for various configurations (i.e., including alteration of footplate cues and base-of-support, and alteration of light-touch cues via the juice reward configurations) that were not addressed in previous normal and vestibular-lesioned animal studies. Also, the platform was motorized thereby allowing the pseudorandom roll-tilts to serve as an input to the postural control system. In previous studies, this stimulus had only been used to characterize human posture.

The measurement system used in this research was novel. It allowed for various configurations (i.e., including alteration of footplate cues and base-of-support, and alteration of light-touch cues via the juice reward configurations) that were not addressed in previous normal and vestibular-lesioned animal studies. Also, the platform was motorized thereby allowing the pseudorandom roll-tilts to serve as an input to the postural control system. In previous studies, this stimulus had only been used to characterize human posture.

2.4.2 Animal training

The animal was trained, by use of a juice reward system, to stand free of human or mechanical restraint on the balance platform. In order to familiarize the animal with its surroundings, the animal was initially brought into the fully-lit training room and was seated in a (constrained) plexiglass chair. While in the chair, the animal acclimated to the environment while receiving juice. After about a week, the animal was released from the chair and began training on the platform. The animal technicians attached a very loosely tethered training leash to a neck collar worn by the animal. One animal technician placed the animal on the platform, while the other positioned each foot on the appropriate footplate (to encourage the animal to stand in its natural quadrupedal stance). An earth-mounted juice dispenser was located at the front of the platform and the experimenter manually triggered juice. When the animal had each foot on the appropriate footplates, a juice reward was provided. Because the juice reward was given only if the animal placed each foot on the correct footplate, the animal learned to stand on the platform in order to receive a reward. R1 took several days to learn how to stand on the platform without human restraint, however R2 was able to stand freely on the platform on the first day of training. The animal was considered to be comfortable standing if only minor (and occasional) position adjustments were provided by the animal technicians. At that point, the juice-reward was set to automatic triggering such that when the animal exerted a minimum of 500 g (or ~ 1 lb.) vertical force on each of the footplates, it received juice as a reward. After the animal was able to do this for several days, it was outfitted with a harness (to hold the position measurement sensors). Once the animal felt comfortable wearing the harness (i.e., was not distracted by it or trying to remove it), the position sensors were placed on the harness. After a few days of being comfortably instrumented,

the tethered training leash was removed, the training room lights were dimmed and earth-mounted quiet-stance data could be collected.

After the animals were able to associate standing on the platform with receiving a juice reward, they were readily trained in the head-mounted juice reward configuration and the platform-mounted juice reward configuration. The head-mounted juice reward configuration required minimal training. The platform-mounted configuration was very similar to the earth-mounted juice-reward configuration, and so the animal already knew how to do the task. However, standing on the moving (tilting) platform required additional training. Initially, the motor was left on to acclimate the animal to the new acoustic environment and also vibrations from the motor being turned on. The animal stood and drank with the motor on. After ~2 weeks, small platform tilts (e.g., 0.5° and 1° pp) were introduced. After one more week, the animal was able to be introduced to the larger roll-tilts and was able to stand on the platform freely. At this point, data could be collected.

2.5 Experimental Stimulus Conditions

Input conditions to the three main sensory systems for posture (i.e., the visual system, somatosensory system, and vestibular system) are integrated to yield a measurable output postural response.

In this research, experimental stimulus conditions were implemented that have previously proven to be challenging to humans and/or cats with vestibular dysfunction: quiet-stance, head-turns, and pseudorandom roll-tilts. These stimuli (described in Sections 2.5.1, 2.5.2, and 2.5.3) allowed us to vary the input condition level of difficulty (e.g., by providing a range of sensory system cues) and measure the animal's force and

body position responses. By measuring the output postural responses to known input conditions, we were able to characterize and interpret the postural control system.

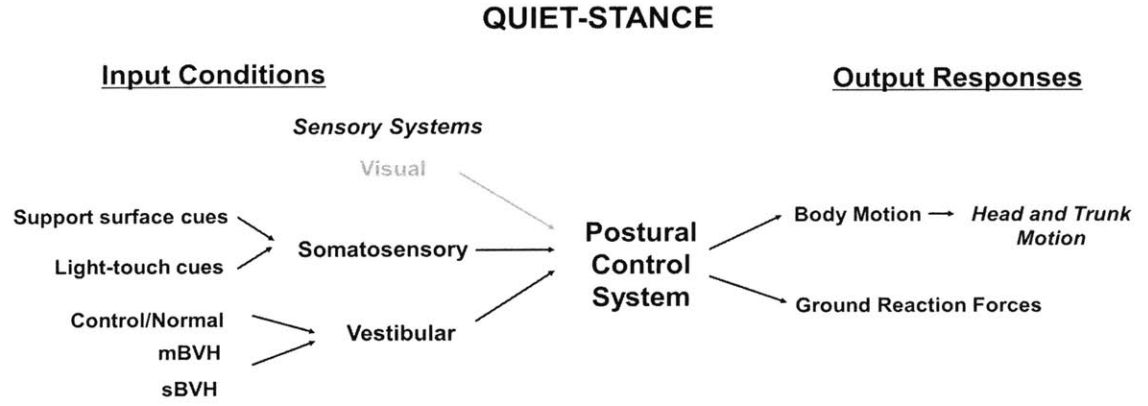

Figure 2.4 Overview schematic of the quiet -stance input conditions and measured output responses. Visual contribution (gray text) was limited.

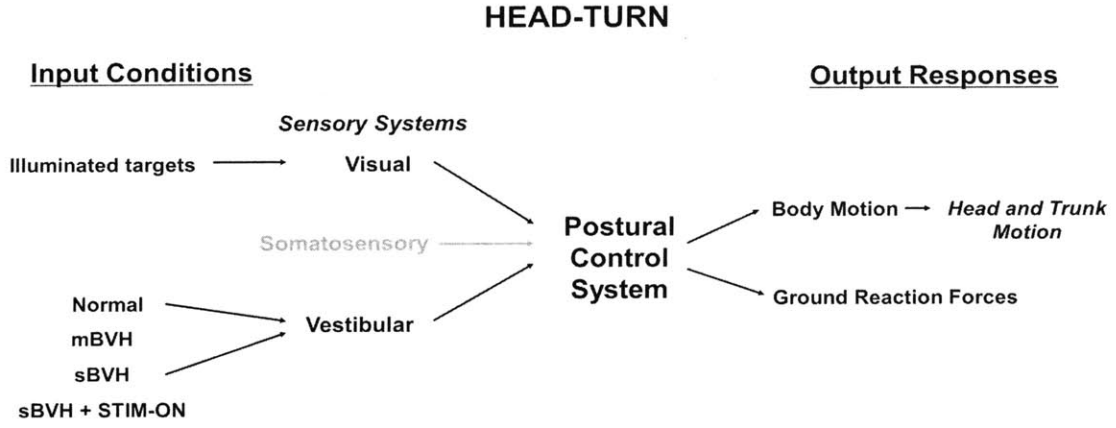

Figure 2.5 Overview schematic of the head-turn input conditions and measured output response. Somatosensory contribution (gray text) remained unaltered.

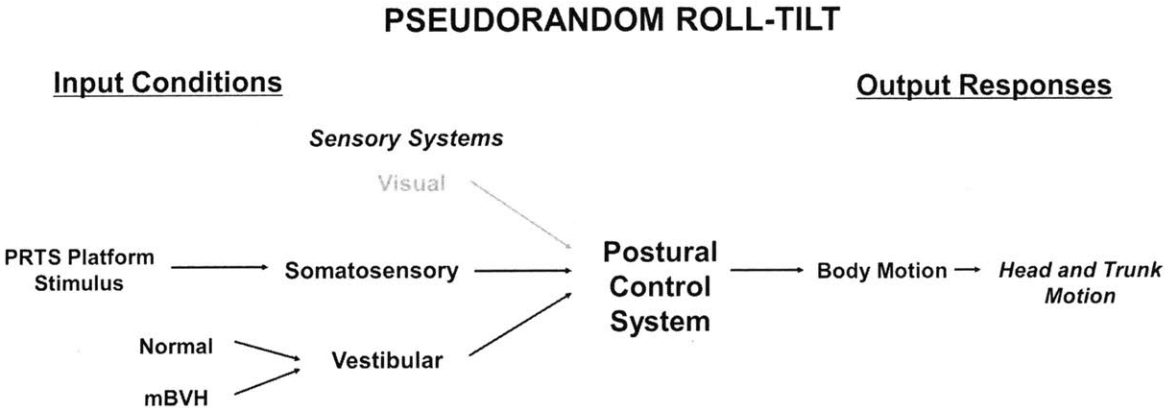

Figure 2.6 Overview schematic of the pseudorandom roll-tilt input conditions and measured output responses. Visual contribution (gray text) was limited.

Figures 2.4, 2.5, and 2.6 provide an overview of the experimental conditions used in this thesis with the input cues/conditions diagrammed on the left side of each diagram and grouped by sensory system (visual, somatosensory, and vestibular). The right side of each diagram shows the (measured) output responses.

In Figures 2.4, left (for quiet-stance) and 2.6, left (for the pseudorandom roll-tilt), note that no cues are listed for the visual system. By using dim lighting and surrounding the monkey and balance platform with a black tarp, these cues were limited. The dim lighting and tarp surround were also used in the head-turn set-up (Figure 2.5) but visual cues (i.e., illuminated targets) were presented to evoke head-turns.

For the quiet-stance condition (Figure 2.4, left), somatosensory cues (e.g., footplate cues and light-touch cues) were varied. Footplate cues were varied by using either a hard gum rubber (stronger cue) or a compliant foam surface (weaker cue). Also, the light-touch cue was either present (earth-mounted dispenser) or absent (head-mounted dispenser). For the head-turn experimental condition (Figure 2.5, left) footplate (somatosensory) cues were held constant (i.e., a hard gum footplate surface was provided). For the PRTS experimental condition (Figure 2.6, left) a PRTS platform tilt stimulus was supplied to the platform.

The vestibular cues available to the animal's postural control system were varied by testing the animal in different states of vestibular function: normal, mBVH, sBVH, and sBVH + STIM-ON. The details of the normal, control, mBVH and sBVH states listed on the left of Figure 2.4 are described in Chapter III (Section 3.3.1) of this thesis. For quiet-stance (Figure 2.4, left), R2 was studied in the normal and mBVH sensory states and monkey R1 was studied in the control and sBVH sensory states. For the head-

turn experimental condition (Figure 2.5, left), R2 was studied in the normal and mBVH states and R1 was studied in the sBVH and sBVH + STIM-ON sensory states. For the PRTS tilt condition (Figure 2.6, left), R2 was studied in the normal and mBVH states.

For all experimental conditions (Figures 2.4, 2.5, and 2.6 right), body motion (e.g., head and trunk motion) was measured.

2.5.1 Quiet-Stance

Figure 2.4 is a schematic representation of the quiet-stance stimulus condition. This is the simplest stimulus condition used to evaluate the effects of the three main sensory systems (i.e., visual, somatosensory and vestibular systems) on postural control by measuring ground reaction forces and head and trunk motion while the animal attempted to stand still.

As previously stated, the controlled variations in somatosensory cues included the stationary balance platform's surface characteristics and presence/absence and character of light-touch cues. The surface characteristics were varied to produce four test levels of increasing task difficulty level (1 being the "easiest" and 4 being the "hardest") were utilized to test the rhesus monkey's quiet-stance posture (Table 2.1). The gum-wide condition (Level 1) provided a hard support surface (i.e., strong footplate cues) and wide (18 cm) stance width that yielded a large base-of-support, while the foam-narrow condition (Level 4) provided a complaint foam support surface (i.e., weak footplate cues) and narrow (9 cm) stance width that yielded a small base-of-support.

Table 2.1 The four support surface test conditions.

Level	Description
1	Gum-wide
2	Gum-narrow
3	Foam-wide
4	Foam-narrow

Two juice reward configurations were used for quiet-stance: 1) an earth-mounted (EM) juice reward configuration that provided a light-touch cue and a stationary reference (Figure 2.3, left), and 2) a head-mounted (HM) juice reward configuration in which the head was free to move and the stationary reference was unavailable (Figure 2.3, middle).

The quiet-stance experimental conditions also allowed us to further develop a quiet-stance feedback controller model originally implemented in humans (Maurer and Peterka 2005), but had not been used to interpret and characterize the postural control mechanisms of non-humans with different degrees of vestibular function. The model was modified and used in conjunction with the animal's sway (trunk roll) in response to the quiet-stance condition. This allowed us to explore the affects of long-latency or intrinsic/short-latency posture control mechanisms on postural control. These mechanisms were explored for the normal, mBVH, and sBVH sensory states.

2.5.2 Head-Turns to Illuminated Targets

In this research, we investigated the effects of four different levels of head-in-space (vestibular) information (i.e., normal, mBVH, sBVH, and sBVH + STIM-ON) while the animal turned its head toward illuminated targets (Figure 2.5, left). As previously stated, R2 was studied in the normal and mBVH sensory states, and R1 was

studied in the sBVH, and sBVH + STIM-ON sensory states. For R2, targets were placed counter-clockwise in yaw (at 0 (or straight ahead), 40, 60, 90°), and for R1, the animal implanted with the right-posterior canal prosthesis, targets were straight ahead, and ~40° oblique (i.e., in the plane of the right-posterior canal). Measured output responses were the body movements of the animal and ground reaction forces (Figure 2.5, right).

The purpose of the head-turn experimental condition was to determine how high-velocity head rotations to illuminated targets affected posture (e.g., trunk position and velocity) in animals with various levels of vestibular information.

2.5.3 Pseudorandom Roll-Tilt Stimulus

Pseudorandom stimuli are beneficial in that they: 1) are white noise approximated stimuli that are unpredictable to the test subject, 2) excite a bandwidth of frequencies (as opposed to one discrete frequency) at approximately equal power, and 3) allow for determination of the impulse response, or the system transfer function, which completely characterizes the linear approximated system.

A white noise approximated signal (e.g. pseudorandom ternary sequence (PRTS) stimulus), has been used as an input perturbation stimulus for human normal and vestibular-loss subjects (e.g., Goodworth and Peterka 2010; Peterka 2002). However, previous posture studies in animals, other than humans, have not utilized pseudorandom roll-tilt stimuli. Such stimuli are valuable in characterizing an animal's posture in that they are unpredictable to the animal, their duration can be customized to accommodate attention/behavioral focus in animals, and also allow a bandwidth of frequencies to be tested simultaneously. Thus, implementation of the PRTS (platform) roll-tilts was a unique opportunity to characterize the normal and mBVH sensory states (Figure 2.6, left)

by measuring output trunk response (Figure 2.6, right). From the measured trunk responses, the frequency response (or system transfer function), as well as trunk orientation as a function of stimulus amplitude (i.e., foretrunk and hindtrunk stimulus-response curves) could be determined. Furthermore, transfer functions derived from the measured data were used in conjunction with a sensorimotor integration model to test for sensory reweighting in the normal and vestibular impaired states.

2.5.4 Criteria for Determining Usable Data

In order to select usable segments of measured data for analysis within each experimental stimulus condition, a unified method for identifying and excluding outliers from the analyses presented here was developed and applied to the measurements made in R1 and R2. The logic behind the development of the criteria is described below.

For one of the animals, R2, video was used to record each test session, so that human handling could be identified and those measured data sections excluded. However, for R1 (tested prior to R2) test sessions were not video recorded, therefore human handling artifacts could not be identified. We aimed to capture "natural" head movements of the animal but to exclude head motions caused by inattention of the animal that were not relevant to the experiment (e.g., the animal turning completely around while on the platform to look at the surroundings). Also, the animals' head motion could vary depending on the level of vestibular dysfunction, and we did not want to exclude useful information about what the trunk was doing relative to the head. Therefore, we did not constrain data to be within a specific head motion criterion for the quiet-stance and PRTS stimulus experimental conditions. We were mainly concerned with trunk motion where most of the body mass resides and hence the COM was located and capturing

characteristics of the trunk that were representative of the test sessions, experimental conditions, and sensory states of the animal.

We used: 1) consistent criteria that could be applied to the measured data of both animals (R1 and R2) and 2) a criterion that has been documented as a method for excluding outliers (e.g., Tukey 1977). Usable data were defined as those segments in which body or head movements fell within a specific movement criterion. For test segments (e.g., quiet-stance trials, PRTS cycles, or head-turn segments) within a given test session, we pooled the segments and computed the sample minimum, lower quartile (Q1), median (Q2), upper quartile (Q3), and sample maximum based on the trunk motion (for the quiet-stance and PRTS experimental conditions) or head motion (for the head-turn experimental condition). Outlier sections were defined as those sections with trunk (or head) motion less than or greater than Q1-1.5*(Q3-Q1) and Q3+1.5*(Q3-Q1), respectively (as in Tukey 1977). All outlier sections were excluded from the analyzed results.

Figure 2.7 displays a plot of foretrunk RMS roll for each trial of a typical quiet-stance test session (for R2). It shows that out of 37 trials, only a 3 were unusable. Overall, a relatively small fraction of all trials were excluded (e.g., R1: ~86% of trials were usable for earth-mounted and ~83% of trials were usable for head-mounted quiet-stance; R2: ~92% of trials were usable for earth-mounted and ~89% of trials were usable for head-mounted quiet-stance)

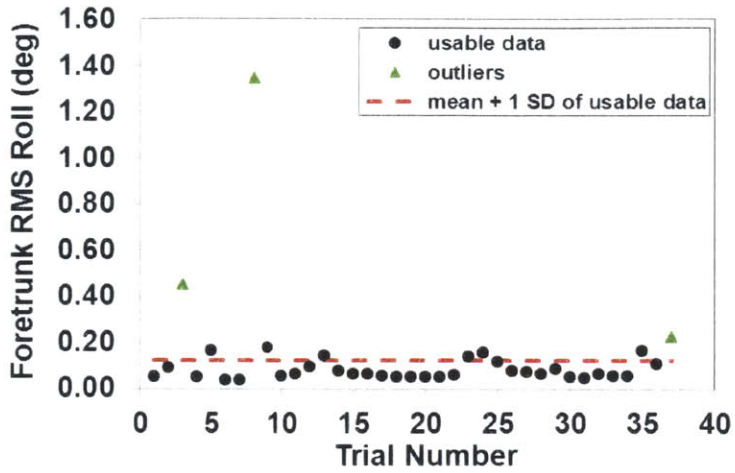

Figure 2.7 Quiet-stance foretrunk RMS roll for each (15 s) trial. Usable data (black) and outliers (green) are shown. The dashed-line (red) represents the mean of the usable data + 1 SD.

2.6 Model Development

The development of models used to explore the characteristics of both the motor and sensory components associated with posture employed control theory techniques. A few of these models are described below.

2.6.1 Previous human models for standing posture

While biped stance is complex with several degrees of freedom, simplified mathematical models have been used to elucidate some of the basic aspects of control processes associated with standing. For the stationary platform (e.g., quiet-stance) or small perturbations of the support surface (e.g., PRTS roll-tilts), the human biped has been often approximated to rotate the body about the ankle joint (ankle strategy) and sway as an inverted pendulum (e.g., McGhee and Kuhner 1970). Because the single-link inverted pendulum model assumes that pivoting only occurs at the ankle of the subject, it disregards movements about the knee and hip joints. Although for large perturbations this may not be the case, for small body deviations from upright, humans utilize the ankle

strategy. Therefore, the single-link model can be a good approximation for quiet standing. In particular, Maurer and Peterka (2005) have shown that a human simple inverted pendulum feedback controller model predicts quiet-stance sway measures (described in Prieto et al. 1996) that were in good agreement with measured experimental data from young and elderly adults (i.e., within 1 SD of the measured results). The inverted pendulum model is the simplest physical model of human posture and greatly reduces the analysis of postural control to manageable proportions, while still allowing approximate predictions of trunk sway. However, because of its simplicity, other models have attempted to account for body movements about joints other than the ankle.

Koozekanani et al. (1980) utilized a multi-segmented inverted pendulum to account for movement at joints other than the ankle while modeling human posture. Stockwell et al. (1981) reviewed and extended the model shown in Koozekanani et al. 1980 and described a five-link model of the human body including the head, torso, thigh, shank, and foot. Movements were measured in test subjects about the ankle, knee, hip, and neck to determine whether four degrees-of-freedom (DOF) was necessary or if a simpler model was adequate to describe human sway. Using this video-computer monitoring system, they attempted to determine whether a four-degrees-of-freedom model was necessary or a simpler model would be adequate to describe human postural sway. Stockwell et al. (1980) developed a method for estimating joint movements using pin lights monitored at 1/30-second intervals by a pair of video cameras. The pin lights were attached to the human subject at the forehead, mastoid, hip and knee. The position of the ankle was measured at the beginning of the observation period and assumed constant. From the measured data, they determined the amplitude spectra from the

measured joint angles of 10 normal subjects during three minutes of quiet standing. These joint angle spectra were described in terms of degrees as a function of frequency. If a single-link model were adequate, significant movement would be present in only one joint, the ankle joint. For a two-link model, movement would only be at two joints (e.g., at the ankle and at the hip). Instead, significant movement was seen in all body joints measured. The authors concluded that a model with at least four degrees of freedom is required to adequately describe human body sway.

In order to obtain accurate measurements of quiet-stance, very high-resolution cameras are needed. However, even with the right equipment, there can still be a high degree of error (e.g., associated with marker placement and human measurement error). In Stockwell et al. (1980), no measurement error was given for the measured data and camera resolution was not provided. However, the camera was described in the paper as "ordinary". Since the magnitude of joint movements for quiet-stance were small it is likely that the level of measurement error was greater than the magnitude of the joint movements. Also, one obvious implication to having a 4 DOF model is higher model complexity and more position measurements needed at the joints. The methodology proposed within the study above may have been more relevant for modeling gait (where joint movements could be much larger than quiet-stance). However, the expense of adding a higher level of model complexity may not be compensated for by the amount of accuracy added to quantify quiet standing. Instead, a simpler model should be used to capture the approximate postural behavior for quiet standing or for small perturbations (e.g., roll-tilts) in stance. Furthermore, a simpler model (i.e., with fewer model

parameters) can yield greater confidence in model-estimated parameter values during optimization routines (e.g., Pintelon and Schoukens 2001).

Nashner (1970) carried the control theory description of postural mechanisms a step further (than modeling purely body dynamics) by conducting a set of experiments with human subjects to formulate a basis for a multi-loop control model. This control model was successful in describing the way in which a human utilizes multiple feedback sensors to control orientation during quiet-stance. A human posture model proposed by Kuo (2005) utilized both state feedback control and optimal state estimation to describe both the body dynamics and sensors associated with postural control. For this model, human body dynamics were modeled as a two-segmented inverted pendulum model that allowed for both ankle strategy (i.e., pivoting from the ankle) and hip strategy (i.e., counter-rotating from the hip). Linear models of the proprioceptive, vestibular, and visual systems were used in combination with the body dynamics. The system that was a combination of these models was controlled by state feedback and optimal control. Measurements made in healthy young subjects, older adult subjects, and bilateral vestibular-loss subjects performing standard sensory organization testing $(SOT)^3$ on a balance platform were comparable to model-predicted COP results. Parameter variations revealed that the model is robust for normal sensory conditions, but not when two or more sensors are unreliable. Removal of the model's vestibular sensor (by decreasing signal-to-noise) led to similar instabilities measured in bilateral vestibular-loss subjects (i.e., instability for test conditions with unavailable or unreliable visual and support surface cues). In contrast to the previous models mentioned, the utility of this model is

that it incorporated both body dynamics and physiological sensor contributions to posture.

A variety of posture models exist (not limited to those discussed here). However, those mentioned above were used exclusively to describe human postural control.

2.6.2 Rhesus monkey feedback controller model

Implementing feedback controller models to describe rhesus monkey posture for normal and vestibular impaired sensory states is novel. The goal of the models used in this research were to adapt and build on models previously applied to human posture while identifying the simplest model that still was able to capture the characteristics (via physiologic model parameter estimates) of rhesus monkey posture. Thus, while multiple segments and links allow for more complex motions and analysis of joint torques, they also lead to higher model complexity. The application of the single-link inverted pendulum analysis served as a first ever approach to modeling rhesus monkey posture in two different sensory states. In this research, we modified inverted pendulum human feedback controller models (Peterka 2002; Maurer and Peterka 2005) to describe the mechanisms associated with rhesus monkey's (foretrunk or hindtrunk) posture for the PRTS and quiet-stance experimental conditions. Through model-estimated parameters, we characterized rhesus monkey posture for the animals in normal and vestibular loss sensory states.

A simple feedback control model was used here in conjunction with experimental transfer functions to investigate model parameter changes between sensory states and to examine sensory reweighting of proprioceptive and graviceptive cues across support surface stimulus amplitudes (Chapter IV).

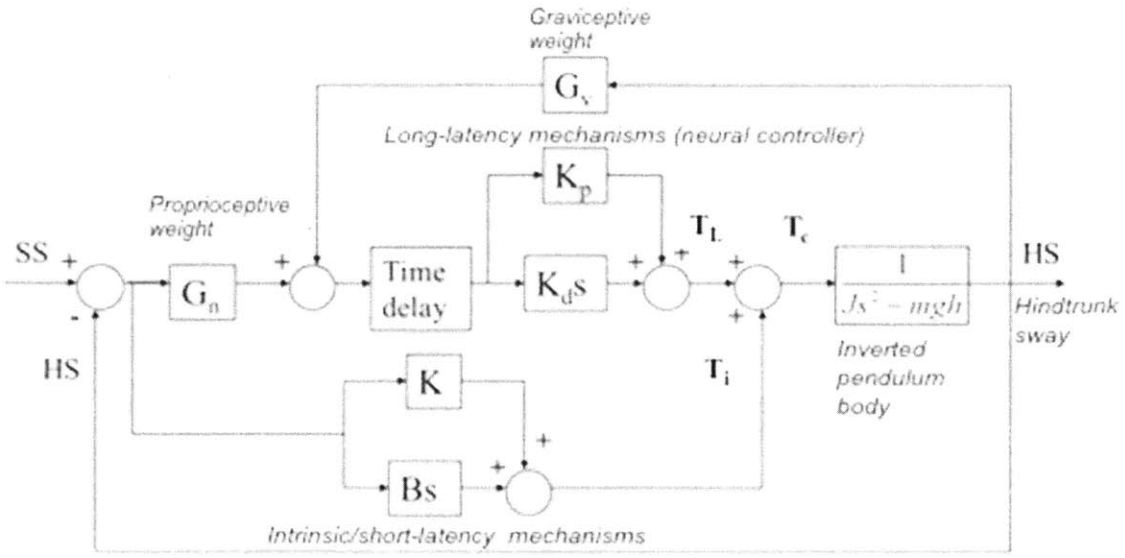

Figure 2.8 PRTS feedback controller model implemented for rhesus monkey posture.

Figure 2.8 displays the feedback controller model that was implemented for the pseudorandom experimental stimulus condition (described in Chapter IV). For a pseudorandom roll-tilt input, the support surface input (SS) is the roll-tilt waveform itself. And the monkey's hindtrunk sway (HS) is the output response. As previously stated, for quiet-stance or small platform motions some models of bipedal human stance have treated the human as a single-link inverted pendulum that is inherently unstable. Because the platform was either stationary or underwent only small perturbations, we modeled the rhesus monkey's trunk as an inverted pendulum. When there is deviation from upright stance, a corrective torque (Tc) comprised of the summation of a torque (T_L), generated by mechanisms with long-latency neural time delay, and an intrinsic/short-latency torque (T_i), generated by mechanisms without time delay (or with short time delay). The torque (T_i), is generated by: 1) the inherent mechanical characteristics of the muscles, joints, ligaments, and musculoskeletal system (time delay = 0) and 2) the short-latency reflexes

(< 25 ms). The intrinsic/short-latency mechanisms consist of stiffness and damping (K and B, respectively). To stabilize the pendulum body, a long-latency (~ 200 ms), torque (T_L) requires a corrective torque equal to the angular deviation times the long-latency stiffness represented by Kp, where "p" indicates proportional feedback, and another component that is the time derivative of the angular deviation times the long-latency damping represented by Kd, where "d" indicates derivative feedback. The incorporation of integral control (Ki) that drives steady-state error of the output to zero has led to better fits to human data but is not necessary to stabilize the pendulum itself (Johansson and Magnusson 1991).

In order to characterize changes in control strategies between sensory states (e.g., effects of increased muscle stiffening on trunk sway) for the animal in quiet-stance (Chapter III), a similar, but slightly modified model, was implemented for the quiet-stance experimental condition and is described in Chapter III. In quiet-stance, the support surface input to the platform (SS) is zero. Although animals attempt to stand stationary, the spontaneous trunk sway is not zero and is measurable. The overall noise in human postural control likely stems from the sensory organs (e.g., van der Kooij et al. 2001), however, we chose to model this as a single noise source. Spontaneous sway was modeled as an input disturbance torque (Td) generated by the low-pass filtered, white noise (as in Maurer and Peterka 2005). This quiet-stance model was used to interpret changes in postural strategy (e.g., muscle "stiffening").

The goal of the model used in this thesis research was to implement a simple model that aided in both interpretation of the results and prediction of physiologic model parameters for the normal and vestibular-lesioned rhesus monkey postural responses. For

quiet standing and relatively small platform perturbations, the application of single-link inverted pendulum analysis served as a first pass approach. Although future models may utilize multiple segments and links which allow for more complex motions and analysis of joint torques, the model used within this thesis allowed us the ability to investigate, and account for, the postural mechanisms associated with our measured results in the normal and vestibular impaired states.

2.7 Conclusion

An innovative approach was implemented to characterize the rhesus monkey postural response (i.e., postural orientation and equilibrium) to the experimental conditions for various levels of vestibular function. Quiet-stance, head-turn, and roll-tilt experimental conditions were used in conjunction with a balance platform to quantify postural control. Compared to previous animal studies, the rhesus monkey balance platform and experiments were novel and unique for the following reasons: 1) capability to evaluate the effects of hard versus compliant footplate surfaces, in combination with the allowing for the alteration of mediolateral stance width, 2) utilization of a motorized platform to provide a continuous and dynamic, pseudorandom roll-tilt input stimulus (something not previously investigated in animals other than humans), 3) characterization and interpretation of rhesus monkey posture through use of control theory techniques (e.g., feedback controller models and transfer function analysis), and 4) comparison of different levels of vestibular function, including prosthetic stimulation, on posture.

Acknowledgements

This section acknowledges the several people involved in developing and conducting the methods described in this chapter. While this may not be an extensive

list, it attempts to acknowledge the time and effort put forth by those involved in motivating and carrying out the sets of experiments discussed in this research. There was a massive effort put forth by the principal investigator, researchers, engineers, and technicians, as well as myself, within the Jenks Vestibular Diagnostic Laboratory and the Jenks Vestibular Physiology Laboratory (JVPL) of the Massachusetts Eye and Ear Infirmary (MEEI).

The principal investigator, Dr. Richard F. Lewis, wrote the grant through which this research was made possible. His extensive knowledge and experience with the species used (the rhesus monkey) aided in formulating the sets of experiments, performing the experiments, and also the interpretation.

Within the Jenks Vestibular Diagnostic Laboratory, there were researchers who aided in the early stages of the research development. Dr. Conrad Wall III aided in formulating and developing the experimental balance conditions used, as well as technical insights. David Balkwill also gave technical insights, in particular, with regards to the PRTS platform programming and trouble-shooting.

Within JVPL, there were technicians and researchers that made the collection of these unique data sets possible. The animal care technicians and researchers, Saori Fukuda Charleton, Fauzia Amuda, and Dr. Csilla Haburcakova, were those responsible for the care and training of the animals. Their role was critical in training the animals to do the experiments that allowed us to obtain these unique sets of data. Furthermore, Dr. Haburcakova added insight regarding the interpretation of animal behaviors, trouble shooting, and wore many hats. Dr. Faisal Karmali aided in ordering of equipment, setup, and trouble-shooting. More specifically, Dr. Karmali was the lead in organizing balance

platform construction and motor selection (to allow the platform to roll-tilt) and installation, installation of force sensors, setup of (miniBird) position sensors, as well as other items. Also, Robert Grimes aided in implementing the appropriate data acquisition software and data acquisition trouble shooting. The JVPL lab director, Dr. Daniel Merfeld gave direction and input and insights wherever necessary.

My main role within the project was the development of the analysis techniques, their application to the measured data and the interpretation of the analysis results.

---

[1]Eye movements and perception were also assessed but are not discussed in detail within this thesis.
[2] Chapter III (Section 3.3.1) describes the differences between the two baseline states (i.e., "normal" and "control") for R1 and R2.
[3]Sensory organization testing (SOT) is used in clinical practice to test the contributions of the visual, vestibular, and proprioceptive systems. The six SOT tests are performed on a computerized dynamic posturography platform that allows alteration of cues from the visual surround and support surface.

III. The severity of vestibular dysfunction influences postural compensation in the rhesus monkey

3.1 Abstract

Previous studies of the effects of vestibular function on human and animal postural responses and control mechanisms have focused predominantly on either normal vestibular function or severe vestibular dysfunction. However, in clinical practice there exists a broad range of vestibular deficits among patients suffering from vestibular loss. In order to characterize the effects of different levels of vestibular function (i.e., normal, mild vestibular hypofunction (mBVH), and severe vestibular hypofunction (sBVH)) on rhesus monkey posture, two experimental conditions (quiet-stance and head-turns) were conducted using a stationary balance platform. Surprisingly, we found that mild bilateral vestibular hypofunction (mBVH) led to decreased trunk roll compared to normal values. In order to compensate for its mild vestibular loss, we hypothesized that the animal, R2, used muscle stiffening (via long-latency and/or intrinsic/short-latency mechanisms). The measured data showed that in order to resist movement of the trunk, footplate forces and roll torque magnitude were increased in the mildly-impaired animal. In order to test the hypothesis that increased intrinsic/short-latency stiffness caused decreases in trunk sway for the animal in the mBVH state, a quiet-stance feedback controller model was implemented. Consistent with the experimental (measured) results, the model-simulated trunk roll decreased when intrinsic/short-latency stiffness was increased from the normal value. Normal and mBVH simulated trunk roll were validated by comparing model-simulated sway measures to those derived from the measured results. The feedback controller model was also used to predict trunk roll in a severely-impaired (sBVH)

animal, R1. The animal in the sBVH sensory state showed increased sway compared to the control state.

The measured and quiet-stance model results were consistent with the following interpretations: 1) in contrast to the normal state of R2, R2 in the mBVH state was able to increase intrinsic/short-latency muscle stiffness and increase trunk stability and 2) for the severe loss of vestibular function (the sBVH state), R1 became unstable and utilized long-latency mechanisms (as opposed to increased intrinsic/short-latency muscle stiffening) due to the larger trunk sways.

3.2 Introduction

Sudden bilateral or unilateral vestibular-loss patients experience ataxia and severe postural instability (Horak 2010). It has been shown that bilateral destruction of the vestibular apparatus leads to broad-based stance, ataxic gait, uncontrolled head movements, and impaired gaze stabilization. After weeks and months following vestibular loss, postural stability may improve by increased reliance on the remaining sensory information. Although the levels and types of compensation associated with vestibular loss may vary across individuals, the behavioral goal of the postural control system remains the same: to maintain postural orientation and postural equilibrium.

Postural orientation is the relative positioning of body segments with respect to one another. Because the trunk determines the positioning of limbs relative to objects with which one may wish to interact, it is one of the most important controlled variables of postural orientation. Postural equilibrium is the balance of the net forces acting on the body. One of the main goals of postural equilibrium is the control of position and velocity of the trunk, where most of the body mass resides. The center-of-mass (COM) is

the point at which the entire mass of the body is balanced. Destabilizing influences, such as gravity, produce external forces on the body's COM. In order to control the position of the COM and maintain equilibrium, internal body forces attempt to counteract destabilizing external forces. The musculoskeletal system has a large number of degrees of freedom and thus the transformation of muscle contraction to forces to movement of the COM is mechanically complex. Although there is not a simple relationship between the muscle contractions and forces generated at the joints, the overall "goal" is to move the COM into the region of stability by applying the appropriate forces (under the animal's feet) to the support surface. The static support surface then exerts an equal but opposite force (or ground reaction force) back on the animal's feet.

For human and non-human subjects suffering from equilibrium disorders of peripheral vestibular origin, maintaining balance may prove to be challenging for situations involving limited visual or somatosensory cues (Horak et al. 1990), decreased base-of-support (e.g., Horak and Macpherson 1996), and large amplitude head-turns (Stapley et al. 2006). In this chapter, we report the results of experiments focused on the trunk position and forces of the normal/control and vestibular-loss rhesus monkeys while standing on a stationary support surface.

Quiet-stance has been used to evaluate posture in both human and animal studies (e.g., Macpherson 1994; Thomson et al. 1991; Winter 1995). Some human studies have shown that vestibular loss has had little effect on the ability to maintain quiet-stance. More specifically, as long as a bilateral vestibular-loss subject is still receiving visual and somatosensory cues they can exhibit normal postural sway (Black and Nashner 1984). Similarly, previous quadruped (cat) posture experiments have shown that vestibular input

has an effect on balance for some test conditions but not others. For instance, in quiet-stance vestibular-lesioned cats had similar sway patterns compared to normal (Thomson et al. 1991). However, narrowing stance width and providing only weak support surface cues may have revealed residual instability. Furthermore, only center-of-pressure (COP) derived from ground reaction force measurements and not body position measurements (e.g. trunk position) were studied. In order to move beyond the limitations of previous quiet-stance cat studies, we did the following: 1) varied somatosensory cues by providing relatively strong or weak surface cues (i.e., thin, hard rubber surface or a thick, compliant foam surface, respectively), 2) varied mediolateral stance width to provide either a large (18 cm) or small (9 cm) base-of-support, 3) measured the animal's head and trunk movements (via position sensors), as well as ground reaction forces (via platform tri-directional force sensors). Unlike human and animal studies that focused on either normal subjects or subjects with severe vestibular deficits, we addressed the effects of various levels of vestibular function (i.e., normal, mild vestibular loss, and severe vestibular loss) on the animals' postural responses to the quiet-stance experimental condition. We also employed an additional stationary platform experimental condition that is more challenging than quiet-stance: head-turns while standing.

When well-compensated bilateral vestibular-loss humans turn their heads while walking, they exhibit difficulty balancing and ataxic gait (Herdman 1994). Stapley et al. (2006) investigated posture in normal and severe vestibular-loss cats undergoing rapid, large-amplitude head-turns. The labyrinthectomized cats produced an unexpected burst in extensors of the limbs contralateral to the direction of the head-turn that thrust the body toward the side of the head-turn. This led to imbalance and falls. It was

hypothesized that this postural "error" arose from the misperception that the trunk was rolling contralaterally (e.g., Mergner et al. 1997). More specifically, vestibular-lesioned cats did not receive the appropriate vestibular (head-in-space) signals to counteract the neck proprioceptive (head-on-trunk) signals, therefore the estimation of trunk position (trunk-in-space) was erroneous.

Previous studies focused on the effects of severe bilateral vestibular-lesioned animals (e.g., via bilateral labyrinthectomy). We introduced a condition of mild vestibular hypofunction (mBVH) to test whether the impaired animal could compensate for the reduced head-in-space (vestibular) signal by altering footplate torques and/or changing relative positioning of body segments in order to stabilize its trunk.

We hypothesized that the rhesus monkey, R2, in the mild bilateral vestibular hypofunction (mBVH) state would be able to compensate (e.g., have the same or decreased sway compared to control) by increasing intrinsic/short-latency stiffness. Based on existing literature (e.g., Horak et al. 1990), we also hypothesized that the rhesus monkey, R1, with severe bilateral vestibular hypofunction (sBVH) would be unable to compensate for its deficit and show increased sway.

3.3 Methods

3.3.1 Subjects and Sensory States

Experiments were conducted with the approval of the Massachusetts Eye and Ear Infirmary (MEEI) Institutional Animal Care Committee and were in accordance with USDA guidelines. For these sets of experiments, two adult female rhesus monkeys, R1 and R2, (R1: 7 yrs, 7.9 kg and R2: 5 yrs, 6.7 kg) were used. In order to study the effects of vestibular loss, two rhesus monkeys (R1 and R2) were studied under two different

sensory states. R2 was studied in the normal and mild bilateral vestibular hypofunction (mBVH) sensory states and R1 was studied in the control and severe bilateral vestibular hypofunction (sBVH) states (described in detail below).

The animal, R1, underwent prosthesis surgery for its right posterior semicircular canal using similar surgical procedures as described in Merfeld et al. (2007) for squirrel monkeys and Lewis et al. (2010) for rhesus monkeys. The sensory state in which R1 was implanted with the prosthesis, but not treated with ototoxic drugs, defined the baseline, or "control", sensory state. In order to quantify sensory state, the rhesus monkey's angular vestibuloocular reflex (VOR), a simple eye movement reflex used to measure semicircular canal function, was tested at discrete frequencies. After quantifying the control state, the monkey then underwent a series of ototoxic treatments that targeted the vestibular hair cells while preserving eighth nerve function. The purpose of these treatments was to target and kill the vestibular hair cells while preserving a functioning eighth nerve. Intratympanic gentamicin (IT gent) specifically targets and kills vestibular hair cells and has been used to treat vertigo in Meniere's patients (e.g., Minor 1999). Initial surgery was conducted under anesthesia (ketamine (10 mL/kg) pre anesthesia and isoflurane (2 - 5% saturation with oxygen)) and consisted of tympanic membrane perforation and gentamicin injection to each ear (i.e., 40 mg/mL in each ear). Peak damage was estimated to be approximately 2 weeks post-administration of the drug (i.e., 1 cycle of IT gent treatment = administration, then 2 week waiting period). R1 underwent a set of 3 cycles of IT gent treatments. In order to cause further vestibular damage, the set of gentamicin treatments was followed by intramuscular streptomycin (IM strep) treatments (350 mg/mL per day for 21 days x 2). At the conclusion of these

treatments, this defined the sBVH state of R1. Figure 3.1 (left) is a plot of the percentage decrease in VOR gain (relative to control) for R1 in the sBVH state.

Unlike R1, R2 did not undergo prosthesis implantation and the normal (or base-line) sensory state of R2 was quantified (in terms of VOR gain) prior to ototoxic treatments. R2 underwent a series of ototoxic treatments under similar procedures to that of R1 (i.e., 5 IT gent cycles and 3 IM strep treatments). The state of the R2 following the ototoxic treatments was defined as mBVH. Figure 3.1 (right) is a plot of the percentage decrease in VOR gain (relative to normal) for R2 in the mBVH state.

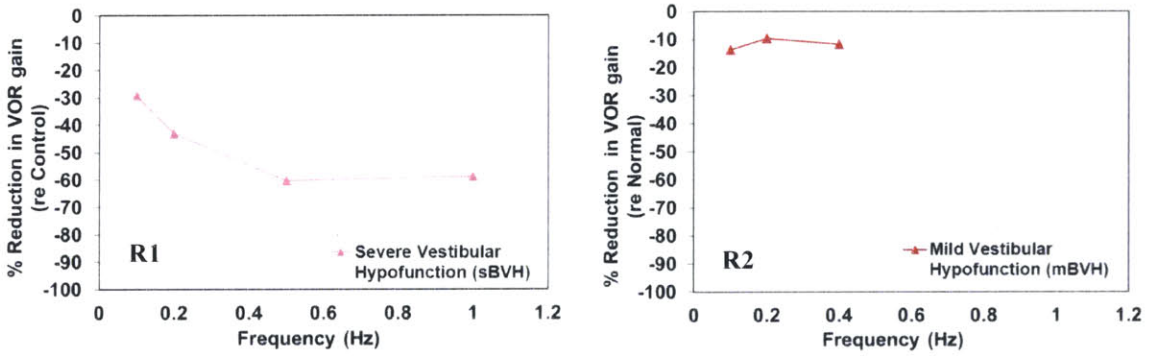

Figure 3.1 Reduction of VOR gain from baseline measurement as a function of frequency measured in R1 (left) and R2 (right).

3.3.2 Equipment

The animals were trained[1] to stand on a stationary balance platform. Each of the four platform footplates was equipped with tri-directional force sensors to quantify ground reaction forces that were equal and opposite the forces exerted by animal on the footplates. Force data were sampled at 200 Hz for quiet-stance and head-turn experiments using LabVIEW (National Instruments Corporation, Austin, TX). The motion of the head, foretrunk, and hindtrunk were measured using three, six degree of freedom sensors (miniBIRD, Ascension Technology Corporation, Milton, VT) with the outputs sampled at 100 Hz for quiet-stance and head-turn experimental conditions.

Sensors were affixed to the head, to the base of the scapula to measure the bulk "foretrunk" motion, and just aft of the iliac crest, but forward of the monkey's tail to measure the bulk "hindtrunk" motion (Figure 3.2).

In order to minimize visual cues, all test sessions were conducted in dim lighting with a black-tarp surround. In order to observe animal behaviors, and identify human handling artifacts within a given test session, cameras were positioned in front of and to the side of the animal. Two infrared illuminators (48-led Illuminator Light Cctv Ir Infrared Night Vision) were used in conjunction with a pair of Kodak cameras with infrared lenses.

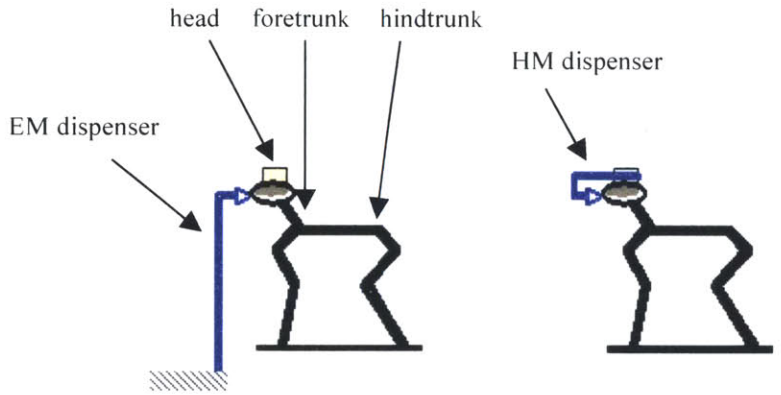

Figure 3.2 Schematic of the juice reward configurations. Earth-mounted, EM, dispenser (left) and head-mounted, HM, dispenser (right).

3.3.3 Quiet-stance experimental condition

In order to observe and quantify rhesus monkey quiet-stance, a stationary balance platform was used. The balance platform allowed for alteration of footplate somatosensory cues via a hard gum rubber surface (more cues) or a thick, compliant foam surface (fewer cues). Also, mediolateral stance width was varied for either wide stance (18 cm footplate separation) or narrow stance (9 cm footplate separation). Four

test conditions of increasing task difficulty level were utilized to evaluate the rhesus monkey's quiet-stance posture: gum-wide, gum-narrow, foam-wide, and foam-narrow.

The monkey was trained to stand on the balance platform, with each foot on the appropriate footplate, while receiving a juice reward from an earth-mounted (EM) juice dispenser or head-mounted (HM) dispenser (Figure 3.2).[1] When the animal was able to stand on the platform free of human constraint with each foot on the appropriate footplate, data were collected. Table 3.1 summarizes the sensory states of the reward configurations used for R1 and R2.

Table 3.1 Quiet-stance reward configurations and sensory states of the animals R1 and R2.

	Quiet-stance	
	Head-mounted dispenser	**Earth-mounted dispenser**
R1	N/A	control
	sBVH	sBVH
R2	normal	normal
	mBVH	mBVH

3.3.4 Head-turn experimental condition

The purpose of investigating the effect of head-turns on rhesus monkey posture was to determine the impact varying levels of head-in-space (vestibular) information have on trunk-in-space (trunk position). During the head-turns, the platform was set to the narrow-gum condition and a head-mounted juice reward (as in Figure 3.2, right) was used to allow free motion of the head. The animal, R2, stood on the stationary platform and light-emitting diodes (LEDs) were positioned on the dark surround at 0 (straight-ahead) at 37, and 60, and 90° counter-clockwise in yaw. A manual switch was pressed by the experimenter to illuminate the targets in the different positions. When the monkey

fixated on the appropriate target, it received juice as a reward. Head-turn data were collected for R2 in the normal and mBVH sensory states.[2]

3.3.5 Data analysis

3.3.5.1 Quiet-stance

For quiet-stance, the main parameters of interest were the roll of the trunk (e.g., foretrunk and hindtrunk RMS roll) and ground reaction forces. In a given test session, data were then broken down into 15 s trials. In order to remove the offset for a given trial, the mean was computed and then subtracted from each data point within the trial. The root-mean-square (RMS) trunk roll was then computed. Usable trials were defined as those sections that fell within specific movement criteria[3]: 1) foretrunk RMS roll from all trials were pooled and the sample minimum, lower quartile (Q1), median (Q2), upper quartile (Q3), and sample maximum were determined, and 2) the outlier trials were defined as those with foretrunk RMS roll less than or greater than Q1-1.5*(Q3-Q1) and Q3+1.5*(Q3-Q1), respectively (as in Tukey 1977). After outlier sections were excluded, computations in the following sections were determined for the usable data.

3.3.5.2 Quiet-stance feedback controller model

The feedback controller model, described briefly in Chapter II, was used to aid in interpreting and predicting control mechanisms associated with the different sensory states.

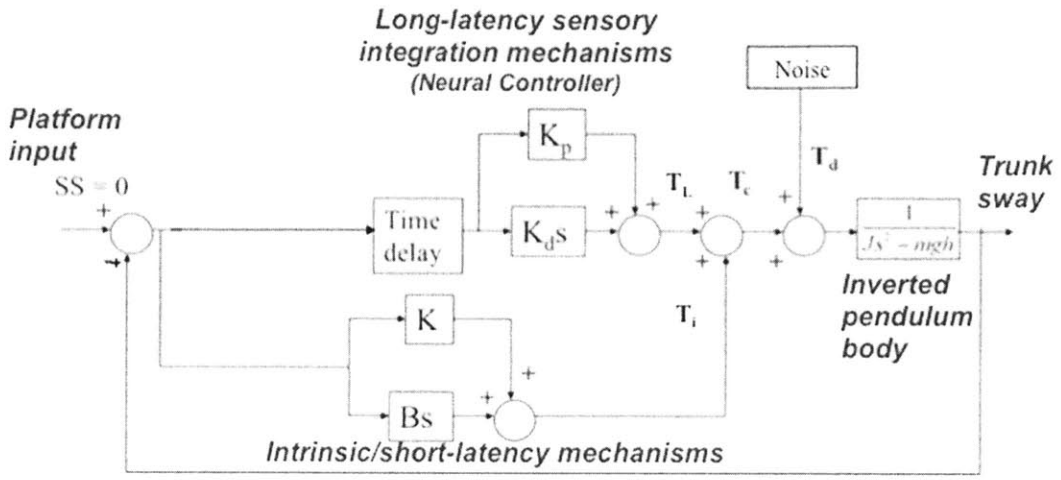

Figure 3.3 Feedback controller model implemented for rhesus monkey posture.

For quiet-stance or small platform motions, some models of bipedal human stance have treated the human as a single-link inverted pendulum that is inherently unstable. We modified the model shown by Maurer and Peterka (2005) for the rhesus monkey foretrunk (Figure 3.3). In quiet-stance, the support surface input to the platform (SS) is zero. Although the animal attempted to stand stationary, we measured spontaneous trunk sway. The mechanism underlying this spontaneous sway was modeled as a disturbance torque (Td) generated by a low-pass filtered, white-noise disturbance input. In order to remain upright, the subject exerts a corrective torque (Tc) comprised of the summation of a torque (T_L), generated by mechanisms with long-latency neural time delay, and/or an intrinsic/short-latency torque (T_i), generated by mechanisms without time delay (or with short time delay). The torque (T_i), is generated by: 1) the inherent mechanical characteristics of the muscles, joints, ligaments, and musculoskeletal system and 2) the short-latency reflexes. The intrinsic/short-latency mechanisms consist of stiffness and

damping (K and B, respectively). In order to stabilize the pendulum body, a long-latency (~ 200 ms), torque (T_L) requires a corrective torque equal to the angular deviation times the long-latency stiffness represented by Kp, where "p" indicates proportional feedback, and another component that is the time derivative of the angular deviation times the long-latency damping represented by Kd, where "d" indicates derivative feedback.

Figure 3.3 shows the feedback controller model that was used to investigate effects of changing intrinsic/short-latency mechanisms (i.e., intrinsic stiffness (K) and intrinsic damping (B)) and long-latency neurally-mediated sensory integration mechanisms (i.e., long-latency stiffness (Kp) and long-latency damping (Kd)) on rhesus monkey trunk sway. In this thesis, intrinsic and short-latency mechanisms are defined as all mechanisms having a latency < 25 ms (e.g., passive muscuoloskeletal, spinal feedback loops), while long-latency mechanisms are defined as those having a latency ~ 200 ms (e.g., visual, somatosensory, and vestibular pathways) (e.g., Goodworth and Peterka 2009). A model of human posture, Goodworth and Peterka (2009), has accounted for differences between long, medium, and short-latency reflexes, as well as those mechanisms inherent to the musculoskeletal system that act without neural time delay. Instead, here we chose to only differentiate between long-latency mechanisms and short-latency reflexes/intrinsic mechanisms that act with little or no time delay. The quiet-stance model (Maurer and Peterka 2005) used a similar approach and described control mechanisms for human quiet-stance either as "active" (i.e., long-latency neural time delays associated with sensory integration mechanisms) or "passive" (i.e. short or no neural time delay).

3.3.5.3 Foretrunk sway measures

Quiet-stance sway measures, previously used to characterize human COP data (Maurer and Peterka 2005; Prieto et al. 1996), were used here to quantify the displacement, velocity, and frequency characteristics for both the experimental and the model-simulated trunk roll (Equations 3.1 to 3.5). Displacement measures included root-mean-square (RMS), or trunk deviation, and maximum distance (MAXD), or peak-to peak-range of displacement. The root-mean-square velocity (RMSV) of trunk roll was also computed. Frequency measures included the centroid frequency (CFREQ), or the frequency where the spectral mass was concentrated, and frequency dispersion (FREQD), which ranged from 0 to 1 (e.g., a perfect sinusoid would have a frequency dispersion of 0).

Root-mean-square displacement (RMS):

$$RMS = \sqrt{\frac{1}{N}\sum_{i=1}^{N}[x(i)]^2} \qquad (3.1)$$

where x(i) is position data for the trunk for sample number "i"
N = number of samples

Maximum distance (MAXD):

$$MAXD = \max(x(i)) - \min(x(i)) \qquad (3.2)$$

where x(i) is position data for the trunk for sample number "i"

Root-mean-square velocity (RMSV):

$$RMSV = \sqrt{\frac{1}{N-1}\sum_{i=1}^{N-1}[\dot{x}(i)]^2} \qquad (3.3)$$

where $\dot{x}(i)$ is derivative of the position data for the trunk for sample number "i"
N = number of samples

Centroid Frequency (CFREQ):

$$CFREQ = \sqrt{\frac{\mu_2}{\mu_0}} \qquad (3.4)$$

where μ_0 and μ_2 are the zeroth and second spectral moments, respectively

Frequency Dispersion (FREQD):

$$FREQD = \sqrt{1 - \frac{\mu_1^2}{\mu_0 \times \mu_2}} \qquad (3.5)$$

where spectral moments μ_0, μ_1, μ_2 are calculated for k = 0, 1, 2, respectively in Equation 3.6

$$\mu_k = \sum_{i=1}^{m} (i \times \Delta f)^k \times G(i \times \Delta f) \quad (3.6)$$

and Δf is the frequency increment (computed as 1/time increment between samples)
G(i x Δf) = discrete Fourier transform of the trunk position trace where "i is the sample number
m = number of discrete power spectral density estimates

3.3.5.4 Mediolateral center-of-pressure (ML COP)

A common measure used to describe the movement of the vertical ground reaction force is the variation in the COP. The COP is derived from ground reaction vertical force data. Since the stance width was smaller in the mediolateral direction than in the anterior-posterior direction, we expected greater instability in mediolateral direction. Thus, we were most interested in mediolateral (ML) shifts in COP (Equation 3.7).

$$MLCOP = \frac{(F_{RFz} + F_{RHz}) - (F_{LFz} + F_{LHz})}{(F_{RFz} + F_{RHz} + F_{LFz} + F_{LHz})} \frac{w}{2} \qquad (3.7)$$

w = mediolateral distance between footplates
F_{LFz} = vertical force on left front footplate
F_{RFz} = vertical force vector on right front footplate
F_{LHz} = vertical force vector on left back footplate

F_{RHz} = vertical force vector on right back footplate

3.3.5.5 Head-turn

For the head-turn experimental condition, a manual switch was pressed by the experimenter to illuminate a target in a specified position. The digital output of the illuminated target had a value of zero or one indicating that the light was on or off, respectively. This allowed us to distinguish head-turns made by the animal to look at the specified target. Each head-turn within the measured data was then marked just before and just after the head-turn. The parameters of interest were the maximum displacement, or range of motion, (MAXD) and the maximum velocity (MAXV) in yaw and roll of the head, foretrunk, and hindtrunk (Equations 3.8 and 3.9). After all head-turns to the target were identified in the measured data, outliers based on MAXD head yaw and were excluded from usable data. In order to normalize the data based on head motion, percentage movement of foretrunk or hindtrunk roll or yaw relative to head yaw were also computed (Equations 3.10 and 3.11).

$$MAXD = \max(x(i)) - \min(x(i)) \tag{3.8}$$

where x(i) is position data for either the head or foretrunk within a given head turn section for sample number "i"

$$MAXV = \max(\dot{x}(i)) - \min(\dot{x}(i)) \tag{3.9}$$

where $\dot{x}(i)$ is derivative of the position data for either the head or foretrunk within a given head turn section for sample number "i"

$$\text{nMAXD trunk roll} = \left| \frac{MAXD_{trunkroll}}{MAXD_{headyaw}} \right| 100\% \tag{3.10}$$

$$\text{nMAXD trunk yaw} = \left| \frac{MAXD_{trunkyaw}}{MAXD_{headyaw}} \right| 100\% \qquad (3.11)$$

3.3.5.6 Torque about projected COM

The moment of a force is the turning tendency, or "torque", about an axis passing through a specific point. In this case, the moment was determined about a point "P" which was located halfway (0.5w) transversely between the footplates and 0.4L towards the front footplates longitudinally (Figure 3.4). Moments were computed about this location because it was the ground projection of the approximate location of the animal's COM. Since the animal exerted ~55-60% weight on the front footplates in quiet-stance and head-turn experiments, the COM was more towards the front footplates. Furthermore, previous studies have shown the rhesus monkey trunk COM to be ~ 40% towards the proximal joint center (Vilenksy 1978). Since the animal had a more narrowed mediolateral stance than anterior-posterior, greater imbalance was expected in roll. Thus, the rolling moment was determined for both quiet-stance and head-turn experiments.

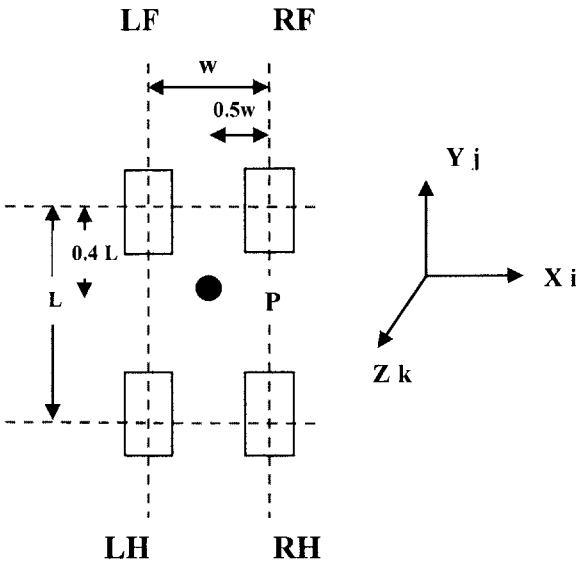

Figure 3.4 Schematic of the top view of platform for moment calculation.

The moment was calculated by computing the cross product of the respective moment arm with the footplate force vectors ("$\overline{M} = \bar{r} \times \overline{F}$") and is shown in the equations below. The torque in roll is shown in Equation 3.14B.

$$\overline{M}_p = \bar{r} \times \overline{F} \quad (3.12)$$

where r = distance vector
F = force vector
P = point from which moments were calculated

or in expanded form

$$\begin{aligned}\overline{M}_p = &\left(0.4L\bar{j} - 0.5w\bar{i}\right) \times \left(F_{LF}\bar{i} + F_{LF}\bar{j} + F_{LF}\bar{k}\right) + \left(0.4L\bar{j} + 0.5w\bar{i}\right) \times \left(F_{RF}\bar{i} + F_{RF}\bar{j} + F_{RF}\bar{k}\right) + \ldots \\ &\left(-0.6L\bar{j} - 0.5w\bar{i}\right) \times \left(F_{LH}\bar{i} + F_{LH}\bar{j} + F_{LH}\bar{k}\right) + \left(-0.6L\bar{j} + 0.5w\bar{i}\right) \times \left(F_{RH}\bar{i} + F_{RH}\bar{j} + F_{RH}\bar{k}\right)\end{aligned} \quad (3.13)$$

where L = anterior-posterior distance between footplate centers
w = mediolateral distance between footplate centers
$\bar{i}$ = unit vector in the x-direction
$\bar{j}$ = unit vector in the y-direction
$\bar{k}$ = unit vector in the z-direction
$\overline{F}_{LF}$ = force vector on left front footplate
$\overline{F}_{RF}$ = force vector on right front footplate
$\overline{F}_{LH}$ = force vector on left back footplate

$\bar{F}_{RH}$ = force vector on right back footplate

Moment in roll:

$$(M_p)_{roll} = M_p\bar{j} = (-0.5w\bar{i} \times F_{LF}\bar{k}) + (0.5w\bar{i} \times F_{RF}\bar{k}) + (-0.5w\bar{i} \times F_{LH}\bar{k}) + (0.5w\bar{i} \times F_{RH}\bar{k}) \quad (3.14A)$$

or in scalar form

$$(M_p)_{roll} = (+0.5w(F_{LF})_z) + (-0.5w(F_{RF})_z) + (+0.5w(F_{LH})_z) + (-0.5w(F_{RH})_z) \quad (3.14B)$$

where "z" denotes vertical

3.3.5.7 Anchoring Indices

Anchoring indices (Amblard et al.1997) have been used as a means of describing the relative angular deviations of a body segment relative to an inferior body segment (e.g. head relative to trunk) and is shown in Equation 3.15.

$$AI = \frac{\sigma_r - \sigma_a}{\sigma_r + \sigma_a} \quad (3.15)$$

where
AI = anchoring index
σ_r = standard deviation of the relative angular distribution (with respect to axes linked to inferior anatomical segment)
σ_a = standard deviation of absolute angular distribution of segment considered

Anchoring index (AI) was utilized to determine the movement of one body segment relative to an inferior body segment for control and vestibular-lesioned states. An AI < 0 would, in theory, indicate that the body segment was more stable relative to the inferior body segment than in space (i.e., en bloc motion), an AI > 0 would indicate that the body segment was more stable in space than relative to the inferior body segment, and an AI = 0 would indicate that the body segment was neither more stable in space nor relative to the inferior body segment. For both normal and mBVH sensory

states of R2, head to foretrunk (or head-foretrunk AI) and foretrunk to hindtrunk (or foretrunk-hindtrunk AI) were determined in roll.

In regards to comparison of results, for the above analyses a student's t-test (assuming unequal variance, unequal sample size) was used in order to determine significance.

3.4 Results

3.4.1 Quiet-stance experimental condition

Quiet-stance posture with head-mounted (HM) juice dispenser was studied in the normal and mild vestibular-loss (mBVH) rhesus monkey, R2, and was quantified by measuring both foretrunk (Figure 3.5, top left) and hindtrunk roll (Figure 3.5, top right). In the normal state, changing stance distance for either gum or foam surfaces had no significant effect on foretrunk roll, however changing from the gum to the foam surface led to an increase in RMS foretrunk roll ($df = 83$, $t = 2.80$, $p < 0.01$). For R2 in the mBVH state, foretrunk RMS roll was not significantly different for the gum conditions but was significantly decreased from normal values for both the foam-wide condition ($df = 74$, $t = -3.03$, $p < 0.01$) and the foam-narrow condition ($df = 70$, $t = -3.9$, $p < 0.001$). Initially, the decreased RMS roll for R2 in the mBVH state may seem counterintuitive and is addressed in the discussion section. For the "most difficult" quiet-stance test condition (foam-narrow), increases were seen in RMS ML COP ($df = 99$, $t = 11.10$, $p <$

0.001) for the mBVH state compared to the normal state (Figure 3.5, bottom).

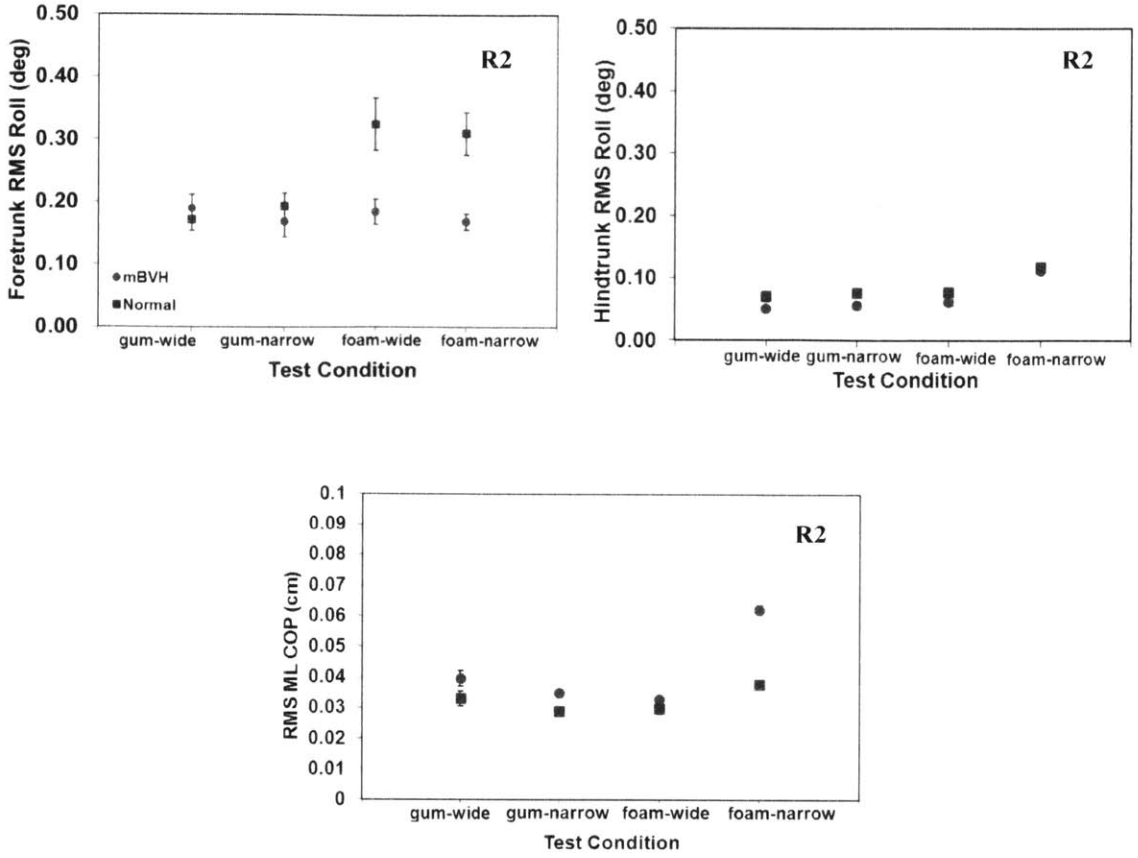

Figure 3.5 R2 quiet-stance head-mounted juice reward configuration results for foretrunk (top left) and hindtrunk (top right) RMS roll as well as RMS ML COP (bottom) as a function of test condition, with standard error bars shown.

Quiet-stance posture, for the earth-mounted juice configuration, was studied in R2 in the normal and mild vestibular loss (mBVH) sensory state and in R1 for the control and severe vestibular loss (sBVH) sensory state.

During the quiet-stance experiments, there were several factors that could have led to the sBVH animal, R1, performing worse that were not relevant to postural control (e.g., behavioral issues, change in temperament, and inattention of the animal due to its severe impairment). For these reasons, we compared R1's best quartile performance (RMS values in the lowest 25% bracket) to R2's best quartile performance (Figure 3.6).

Severely-impaired (sBVH) R1 showed an increase in sway in comparison to control values, while mildly-impaired (mBVH) R2 showed a decrease in sway compared to normal values except for the foam-narrow test condition (Figure 3.6).

In the normal state, R2 exhibited non-monotonic RMS roll for increased task difficulty in that there was an increase in RMS roll between gum-wide and gum-narrow ($df = 20$, $t = 4.75$, $p < 0.001$), no significant difference between gum-narrow and foam-wide, and a decrease between foam-wide and foam-narrow ($df = 13$, $t = -3.65$, $p < 0.01$). In the mBVH state, R2 showed a significant increase ($df = 5$, $t = 11.18$, $p < 0.001$) in RMS roll between gum-wide and gum-narrow, and no significant difference between gum-narrow and foam-wide, and between foam-wide and foam-narrow. In comparing mBVH sensory state to the normal state, foretrunk RMS roll decreased for all quiet-stance test conditions (e.g., gum-narrow: $df = 14$, $t = -6.77$, $p < 0.001$) except for the foam-narrow condition (Figure 3.6, right).

In the control state, R1 did not exhibit the characteristics seen in the normal state of R2 (Figure 3.6, left). This difference between R1 and R2 could be accounted for by the fact that R1 in the control state may have sustained some level of vestibular damage caused by the surgical prosthetic implantation unlike the unimplanted R2. For control R1, there was a slight increase in RMS roll between gum-wide and gum-narrow. Between gum-wide and foam-narrow, there was a large significant increase ($df = 8$, $t = 10.59$, $p < 0.001$). This response was opposite that of R2's response. R2 consistently placed a greater percentage of weight (~ 55-60 %) on the forelimbs, and therefore was able to brake her COM more effectively. Figure 3.6 shows that R1 in the sBVH sensory state had increased RMS roll when compared to the control state values except for the

foam-narrow condition. Severely-impaired R1 may have used an alternate strategy in the foam-narrow condition: crouching to lower its COM. This could have effectively allowed the animal to become more stable. When comparing sBVH to the control sensory state for R1, there was a significant increase in RMS roll for gum-wide, gum-narrow, and foam-wide test conditions ($df = 3$, $t = 4.39$, $p < 0.05$; $df = 4$, $t = 10.54$, $p < 0.001$; $df = 3$, $t = 20.14$, $p < 0.001$, respectively) and an insignificant difference for the foam-narrow condition.

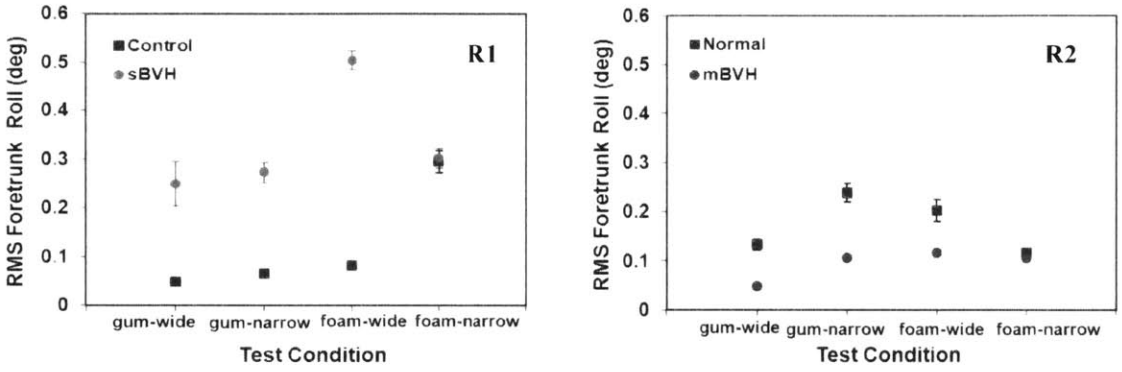

Figure 3.6 Best quartile foretrunk RMS roll as a function of test condition, with standard error bars shown.

3.4.2 Head-turn experimental condition

R2 performed the head-turn experiment in both the normal and the mBVH sensory states. For peak (MAXD) head yaw, both normal and mBVH states show that MAXD yaw increased with increasing target amplitude (Figure 3.7, left). However, for all head-turn amplitudes, for both sensory states, the animal undershot the actual target position (i.e., the animal turned its head part of the way and then likely used eye movements to fixate on the target). In comparing peak head movements for 60 and 90° targets there were no significant difference between normal and mBVH states. However, MAXD for mBVH was significantly less than normal ($df = 71$, $t = -5.68$, $p < 0.001$) for

the 37° target. The mBVH animal possibly used its eye movements to fixate on the small-amplitude target rather than turning its head.

Although the MAXD yaw of the head was insignificantly different for the 60 and 90° target amplitudes when comparing the normal and mBVH states, there were differences detected in roll (Figure 3.7, right). For the 37° target amplitude, there were insignificant differences in peak head roll between normal and mBVH. However, the roll of the head in the mBVH sensory state was significantly greater than normal for the 60 and 90° targets ($df = 181$, $t = 5.70$, $p < 0.001$ and $df = 91$, $t = 2.57$, $p < 0.02$, respectively).

In both the normal and mBVH sensory states, the animal's foretrunk and head yaws were in the same direction (towards the target). MAXD foretrunk yaw was normalized by MAXD head yaw ("nMAXD foretrunk yaw") and is expressed as an absolute percentage (Figure 3.8, left). For the normal state, nMAXD foretrunk yaw increased with increasing target amplitude. For the mBVH state, nMAXD foretrunk yaw was not significantly different for the 37° target amplitude. For the 60° and the 90° amplitudes, the animal's mBVH nMAXD foretrunk yaw and the MAXD foretrunk roll normalized by MAXD head yaw ("nMAXD foretrunk roll" shown in Figure 3.8, right) were significantly less than normal ($df = 223$, $t = -9.09$, $p < 0.001$ and $df = 96$, $t = -5.16$, $p < 0.001$). For the mBVH state, nMAXD foretrunk roll decreased for increased target amplitude.

In both the normal and mBVH states, hindtrunk motion in yaw was opposing head and foretrunk motion in yaw. Hindtrunk yaw was normalized by head yaw input and was described as an absolute percentage of the peak head yaw, or "nMAXD hindtrunk yaw" (Figure 3.9, left). For the mBVH animal, nMAXD hindtrunk yaw was the not

significantly different from the normal value for the 37° amplitude. However, at the 60 and 90° amplitudes, nMAXD hindtrunk yaw for the mBVH state was significantly less than the normal state (e.g., $df = 172$, $t = -2.50$, $p < 0.05$ for the 90° amplitude). Similarly, mBVH nMAXD hindtrunk roll (Figure 3.9, right) was significantly less than the normal values for the two highest target amplitudes (e.g., $df = 172$, $t = -9.10$, $p < 0.001$ for the 90° amplitude). Although only peak displacements are only shown here, peak velocities were also computed and showed similar trends (i.e., decreased velocity for the mBVH sensory state in comparison to normal values).

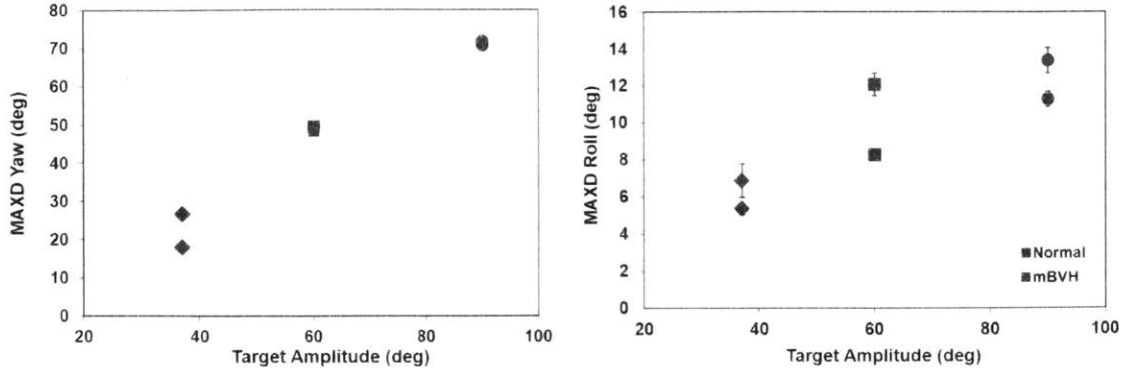

Figure 3.7 MAXD Head yaw (left) and roll (right) as a function of target amplitude. Standard error bars are shown.

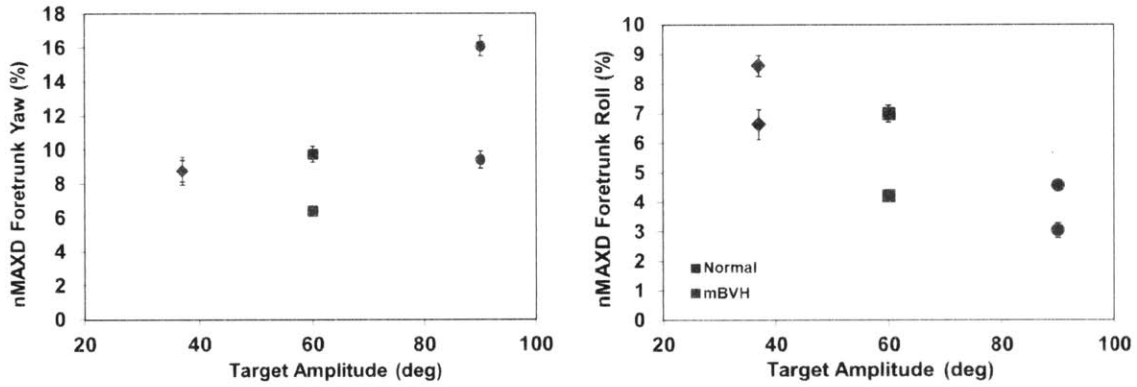

Figure 3.8 nMAXD foretrunk yaw (left) and nMAXD foretrunk roll (right) as a function of target amplitude. Standard error bars are shown.

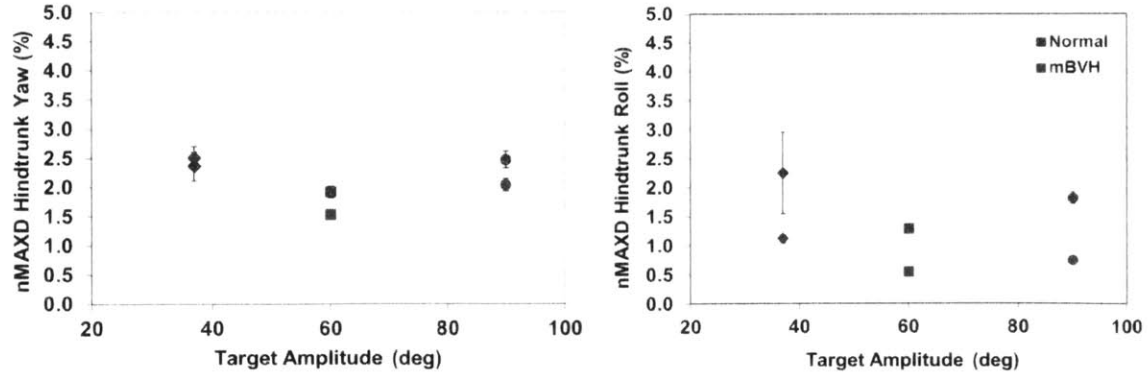

Figure 3.9 nMAXD hindtrunk yaw (left) and nMAXD hindtrunk roll (right), as a function of target amplitude. Standard error bars are shown.

3.4.3 Moments in roll and horizontal forces

One of the behavioral goals of the postural response is to control the COM. Since most of the rhesus monkey's body mass resides in the trunk, trunk position and stability are directly related to stabilizing the COM. When the animal exerted the appropriate forces on the platform to oppose external forces acting on the body, COM stability was achieved.

Figure 3.10 displays the mean roll moments about an approximate COM projection, for quiet-stance test conditions (Figure 3.10, left) and head-turn amplitudes (Figure 3.10, right). Roll torques were computed calculating the cross product of the moment arm vector (from the approximate COM projection to the center of each footplate) and the vertical ground reaction force vectors that were equal and opposite of the forces that animal was exerting on the balance platform footplates.

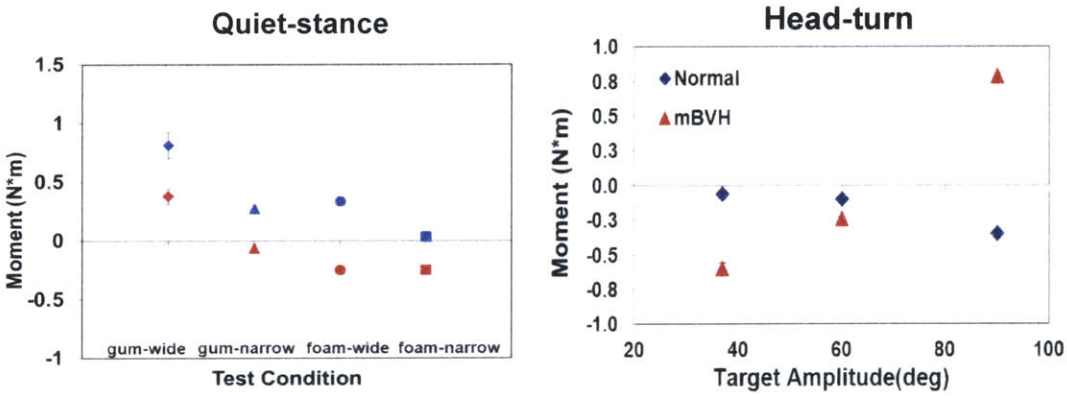

Figure 3.10 Mean roll moments, with standard error bars, about the approximate center-of-mass projection for quiet-stance (head-mounted dispenser) (left) and head-turn (right).

Positive roll torque is rolling to the right and negative roll torque indicates rolling to the left. Increases in magnitude, or absolute value, mean that the animal is becoming more resistant to motion in roll. In the quiet-stance gum test conditions, the animal had a smaller magnitude roll moment in the mBVH sensory state than normal, indictating that

the animal was excerting less torque on the platform in the mBVH state (Figure 3.10, left). However, in the mBVH state animal going from the gum-wide to foam-wide, resulted in a change in direction of the torque (i.e., the torque became < 0) indicating a possible change in strategy from normal. For the foam conditions, the mBVH torque remained < 0. In the mBVH state, the animal exerted a torque equal in magnitude but opposite in direction to the normal animal in the foam-wide condition. For the foam-narrow condition, the normal animal exerted ~ 0 torque, however, for the mBVH state it exerted a torque < 0. This torque helped the animal to remain rigid in the roll plane (i.e., reduced RMS trunk roll) even though the test condition (foam-narrow) was difficult. This strategy is consistent with increased ML COP, and decreased RMS foretrunk roll seen in Figure 3.5 for the foam-narrow condition.

For the head-turn experimental condition, the normal animal showed torques slightly < 0. However, the for mBVH state the animal showed increasing torque magnitude (or absolute value of torque) for increasing target amplitude. This result is consistent with: 1) the animal using different strategies during head-turns in the normal and mBVH states and 2) the animal exerting greater torque to reduce its body roll in the mBVH state. This increased torque exerted by the animal in the mBVH sensory state allowed it to "stiffen" (i.e., reduce its trunk body sway) compared to the normal state. This increased "stiffness" is consistent with previous results that show body or head displacements in bilateral vestibular-loss humans and cats leads to higher levels of tonic activity in the neck, trunk, and legs (Horak et al. 1994).

Horizontal ground reaction forces are shown for both the normal and mBVH states in the quiet-stance gum-wide and gum-narrow test conditions (Figure 3.11). As

has been shown previously in normal cats (Macpherson 1994), the normal horizontal ground reaction forces were diagonal. Consistent with previous findings, when mediolateral stance width was changed from wide to narrow, the horizontal force vectors rotated medially, towards the centerline.

However, when the rhesus monkey was mildly impaired, forces typically rotated (and even reversed directions), as well as increased in magnitude. In particular, the forelimb forces that were acting to stabilize the foretrunk became much larger in magnitude than the normal values, indicative that the animal was resistant to movement (i.e., becoming more "stiff"). The animal exerted a greater percentage weight on the forelimbs (~55- 60%) than the hindlimbs, so its COM was closer to the foretrunk than the hindtrunk for all conditions. This application of forces seen in the forelimbs indicated that the animal in the mBVH state applied a much larger force than in the normal state in order to stabilize its COM (Tables 3.2 and 3.3). In terms of body movements, the exertion of larger forces led to either no difference or decreased trunk roll (as seen in Figure 3.5). In the mBVH state, the change in force pattern seen between wide and narrow was possibly a way for the animal to counteract unwanted bending of the trunk. More specifically, the force couple seen at the narrowed stance width (Figure 3.11, right) were a means of resisting the bending moments of the animals' vertebral column that had resulted from standing in the narrowed platform configuration.

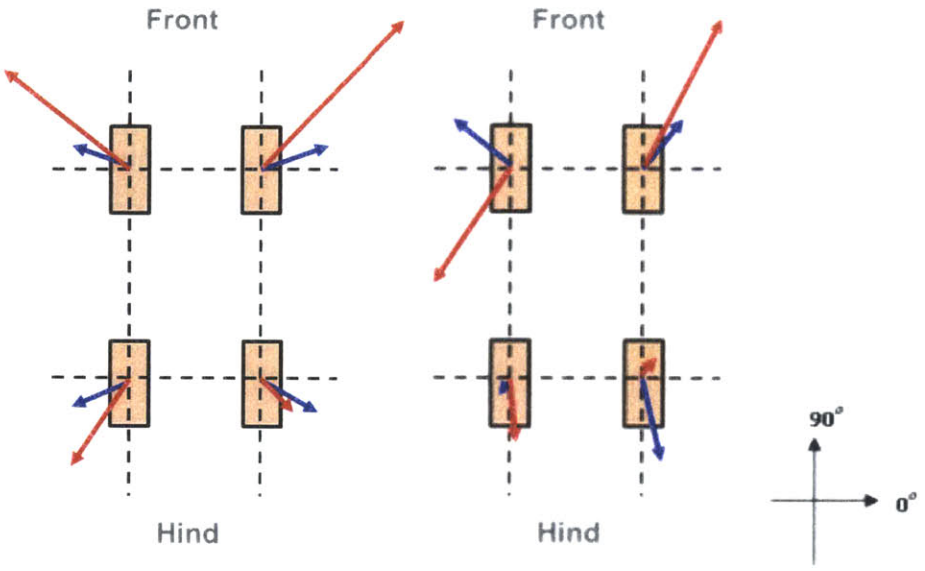

Figure 3.11 Schematic of quiet-stance mean (averaged) horizontal forces for all gum-wide (left) and gum-narrow (right) usable trials. Normal (blue) and mBVH (red).

Table 3.2 Quiet-stance gum-wide horizontal forces magnitude (top) and direction (bottom) for normal and mBVH states.

	MAGNITUDE			
	Left Front (N)	Right Front (N)	Left Hind (N)	Right Hind (N)
Control	1.62 +/- 0.12	1.76 +/- 0.13	1.19 +/- 0.07	1.90 +/- 0.17
mBVH	3.97 +/- 0.12	4.46 +/- 0.17	2.48 +/- 0.04	1.77 +/- 0.04

	DIRECTION			
	Left Front (deg)	Right Front (deg)	Left Hind (deg)	Right Hind (deg)
Control	171.43 +/- 43.65	29.36 +/- 56.56	187.99 +/- 55.84	323.42 +/- 83.37
mBVH	158.91 +/- 25.16	37.33 +/- 57.04	246.75 +/- 44.54	316.91 +/- 67.26

Table 3.3 Quiet-stance gum-narrow horizontal forces magnitude (top) and direction (bottom) for normal and mBVH states.

	MAGNITUDE			
	Left Front (N)	Right Front (N)	Left Hind (N)	Right Hind (N)
Control	1.09 +/- 0.07	1.06 +/- 0.06	0.09 +/- 0.04	2.51 +/- 0.08
mBVH	2.97 +/- 0.08	2.98 +/- 0.03	1.08 +/- 0.06	0.30 +/- 0.04

	DIRECTION			
	Left Front (deg)	Right Front (deg)	Left Hind (deg)	Right Hind (deg)
Control	125.10 +/- 80.79	53.91 +/- 60.26	266.01 +/- 67.17	283.08 +/- 70.60
mBVH	244.83 +/- 60.31	60.40 +/- 43.91	274.12 +/- 67.74	86.66 +/- 45.25

3.4.4 Relative motion of body segments for normal and mBVH sensory states

3.4.4.1 Anchoring Indices (in roll)

Anchoring indices were used to characterize the relative motion of a superior (e.g., the head) to inferior body segment (e.g., foretrunk) for R2 in the normal and mBVH sensory states (Figure 3.12). For the quiet-stance experiment, in comparing each test condition for the normal and mBVH sensory states, head-foretrunk roll AI were not significantly different from each other. However, head-foretrunk AI was significantly < 0 for all test conditions for both sensory states (i.e., the head was more stable relative to the foretrunk than in space). In comparing the normal and mBVH foretrunk-hindtrunk roll AI, there was no significant difference for the gum conditions, however, there were significant differences seen in the two foam conditions. More specifically, foam-wide mBVH AI signficantly increased compared to normal ($df = 75$, $t = 3.93$, $p < 0.001$) and foam-narrow mBVH AI significantly decreased compared to normal ($df = 100$, $t = -2.12$, $p < 0.02$). For the foam-wide condition, the animal in the mBVH state had a foretrunk-hindtrunk AI that was not significantly different than 0 indicating that the foretrunk was neither more stable in space nor relative to the hindtrunk. However, for the foam-narrow condition the animal in the the mBVH state showed a foretrunk-hindtrunk roll AI that was less than normal and significantly < 0 meaning that the foretrunk was more stable relative to the hindtrunk than in space (i.e., en bloc motion possibly indicative of increased stiffening).

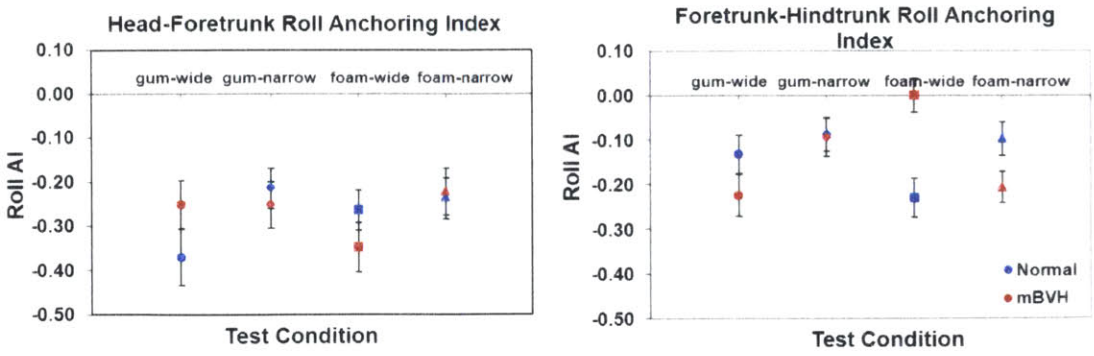

Figure 3.12 Quiet-stance experimental conditions (head-mounted dispenser): head-foretrunk (left) and foretrunk-hindtrunk (right) roll AI with standard error bars.

For the head-turn experiments, head-foretrunk AI was < 0 but increased with target amplitude in both the normal and mBVH states (Figure 3.13). An AI < 0 indicated that the head was more stable relative to the foretrunk than in space. The decrease in AI seen in going from normal to mBVH states was due to the animal compensating by changing postural strategy. More specifically, in the mBVH state the animal may have adopted a head fixed to trunk strategy to compensate for its mild vestibular loss. This strategy has been seen in human vestibular-loss subjects (Herdman 1994). In both the normal and mBVH sensory state, foretrunk-hindtrunk AI decreased with an increase in target amplitude (i.e., the animal's body motion shifted towards en bloc foretrunk-hindtrunk motion with the two segments being "carried" together when the animal turns its head towards the target), however, the results were not significantly different between the two sensory states.

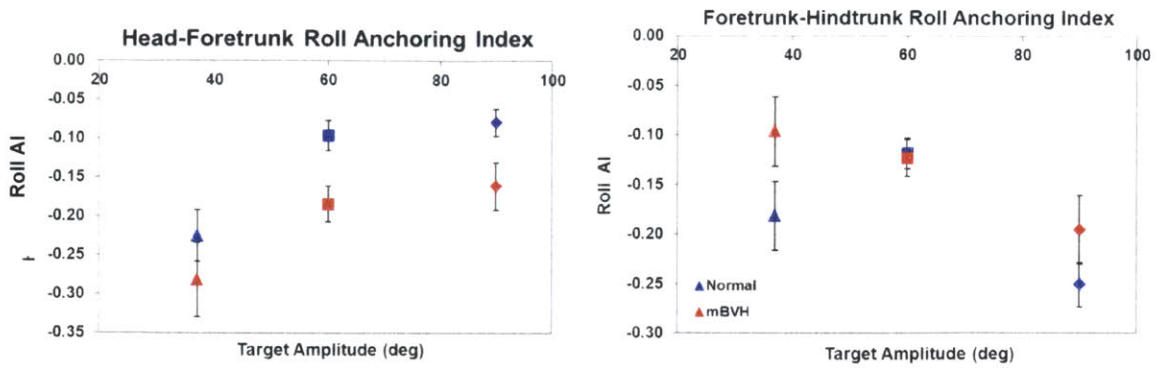

Figure 3.13 Head-turn experimental condition: head-foretrunk (left) and foretrunk-hindtrunk (right) roll AI with standard error bars.

3.5 Discussion

The purpose of this study was to determine the effects of degrees of vestibular dysfunction on the rhesus monkey postural response to stationary support surface experimental conditions. The principal findings were that for a mildly impaired (mBVH) sensory state there was reduced body sway (RMS roll) compared to the normal state, however, for a severely impaired (sBVH) sensory state there was increased body sway compared to control state. Further investigation of mBVH measurements showed increased moments and increased (horizontal) footplate force application (Figures 3.10 and 3.11). This, in conjunction with the decrease in trunk roll of the mildly-impaired state compared to normal values (as shown in Figures 3.5 and 3.8), led to the notion of "stiffening" compensation. We hypothesized that increased intrinsic/short-latency stiffness was utilized as a postural compensation mechanism for the animal in the mBVH state, R2, for quiet-stance, and possibly head-turns, in that it reduced body roll from normal values. However, it was hypothesized that increased intrinsic/short-latency stiffness was an insufficient postural compensation mechanism in the animal in the sBVH

state, R1, and that an alternate strategy was used. Hypotheses involving mBVH and sBVH states were explored utilizing a quiet-stance feedback controller model.

3.5.1 The role of long-latency and intrinsic/short-latency mechanisms for postural control on a stationary platform

Based on previous findings in humans and animals with severe bilateral vestibular hypofunction, it was originally hypothesized that the animal in the mBVH sensory state would exhibit increased trunk sway in the more challenging quiet-stance test condition (foam-narrow) and head-turn experimental conditions due its vestibular loss. However, for the quiet-stance and head-turn experiments, we measured either no significant difference or decreased roll compared to the normal values. It has been proposed that in vestibular-loss subjects perceived threat (e.g., fear of falling at height) alters the postural control mechanisms used such that subjects became tense, more rigid, and therefore able to maintain sway ranges comparable to controls (e.g., Carpenter et al. 2001). Thus, one possible explanation is that in the mBVH sensory state, the animal compensates for the partial impairment by becoming more rigid, thereby reducing its trunk roll. We hypothesized that the animal may have been able to compensate for the mild impairment by increasing muscle "stiffness" (via intrinsic/short-latency and/or long-latency mechanisms), in particular for the foretrunk region, therefore causing a decreased trunk roll.

Upright stance involves the use of both long-latency and intrinsic/short-latency mechanisms to generate corrective torques (e.g., gravity acting on the body generates a torque that drives the body away from vertical, thus a corrective torque must be generated in order to correct for this torque and remain upright). We describe long-latency (~ 200

ms) mechanisms as those that are mediated by the three main sensory systems used for upright posture. The vestibular, visual, and proprioceptive systems are used to provide long-latency neural feedback control of upright balance (e.g., vestibular system senses head motion and orientation in space, proprioception detects orientation of one body segment relative to another, and vision detects head orientation and motion in space). In order to extract overall information of body orientation in space and elicit the appropriate postural response, the information from each sensory system is integrated. Short-latency reflexes that act with "short" (< 25 ms) neural time delay, and intrinsic mechanisms are derived from the inherent mechanical properties of muscles and tendons around the joints that act with no time delay. Intrinsic/short-latency stiffness provides a force that counteracts gravity analogous to the way a spring generates a counter force when it is displaced from equilibrium. In regards to previous studies of upright stance in humans, the effective role of long-latency (commonly called "active") versus intrinsic/short-latency (commonly called "passive") mechanisms is still a controversial topic of debate and some studies even fail to differentiate between the two.

Peterka (2002), and others, described a view that intrinsic/short-latency ankle stiffness (i.e., stiffness without neural modulation) is very low (i.e., < 10-15% mgh, where mgh is equal to body mass x gravity x vertical COM height, is the "load stiffness") but that long-latency (neural controller) stiffness plays a dominant role in postural response. Low intrinsic values are supported by transfer function fits to human experimental data for pseudorandom platform (pitch) tilts for stimuli ranging between 0.5 to 8^{o} peak-to-peak (Peterka 2002). Another study that describes long-latency ("active") dominance was (Qu and Nussbaum 2009). This study held the view that long-latency

neural controller mechanisms dominated quiet-stance posture and that intrinsic/short-latency (e.g., "passive") mechanisms were typically < 10% of long-latency torques.

In an alternate view, it has been proposed that intrinsic/short-latency ankle torque (i.e., torques not attributed to long-latency neural feedback) generate a large proportion of corrective torque necessary to counteract the torque produced by gravity. Previous studies (e.g., Gurfinkel et al. 1975; Nashner 1976), advocated that intrinsic/short-latency stiffness in activated calf muscles is sufficient to stabilize the human inverted pendulum. Loram and Lakie (2002) and Casadio et al. (2005) reported that although intrinsic/short-latency stiffness values are < 100% (i.e., 91 and 65% of mgh, respectively), they are large enough to make a significant contribution to postural stabilization. Furthermore, although there is no differentiation between intrinsic or sensory modulated mechanisms, Kearney and Hunter (1982) have shown that ankle stiffness increases as stretch size decreases.

The extent that intrinsic/short-latency mechanisms and long-latency mechanisms contribute to quiet-stance and dynamic torque remains controversial. However, Loram et al. (2007) showed that intrinsic/short-latency stiffness is substantial for small, slow ankle rotations but that intrinsic/short-latency stiffness decreases as the size of the ankle rotation increased. (Long-latency) muscle response was recorded by use of electromyography (EMG). For short stretches (i.e., for 0.4 and 0.15 deg rotations), the 'without EMG' and 'with EMG' models showed stiffness coefficients that were not significantly different: 'without EMG': 3 +/- 1 and 3.6 +/- 0.9 Nm/deg for 0.4 and 0.15 deg rotations and 'with EMG': 3 +/- 0.9 and 3.6 +/- 0.8 Nm/deg. That is, stiffness for small rotations reflect mechanical (e.g., intrinsic) and not long-latency modulation of

ankle torque, therefore implying that muscle activity makes little difference to "short-range" stiffness. However, for long stretches (e.g., 7° rotations), short-range stiffness decreases. Short-range stiffness is high (101% mgh) at 0.03° and decreases drastically to 19% mgh for 7° rotations. This finding is in good agreement with previous work (Peterka 2002), in that (long range) intrinsic/short-latency stiffness is low (e.g., 13% mgh) during perturbed stance..

Other findings (Cenciarini et al. 2010) have shown that increases in long-latency (commonly called "active") stiffness with corresponding increases in long-latency damping are a means of compensation in elderly adults (i.e., long-latency stiffness and damping are significantly larger in the older subject group than in the young adult subjects) in response to a pseudorandom roll-tilt stimuli supplied to the support surface. Peterka (2002) also found that long-latency stiffness values are higher for bilateral vestibular-loss subjects than normal subjects, suggesting that the vestibular-loss subjects use this as a mechanism to compensate. Furthermore, it was determined that intrinsic/short-latency (also commonly called "passive") mechanisms are small relative to long-latency mechanisms for support surface tilts.

Based on the findings within the reported literature and this thesis, we have hypothesized that in quiet-stance for normal and mBVH sensory states (i.e., with short ankle stretch and stationary platform surface), that intrinsic/short-latency mechanisms dominate (e.g., in the forelimbs of the animal). For large platform rotations (e.g., pseudorandom roll-tilts) and possibly for larger sways while standing on stationary platform (e.g., quiet-stance performance of the animal in the sBVH sensory state) long-latency (neural controller) mechanisms dominate. In this chapter we investigate the

hypothesis that in the mBVH sensory state, the animal, R2, uses increased intrinsic/short-latency stiffness to compensate for situations where the platform surface is stationary. In the sBVH sensory state, the animal, R1, was unable to compensate and exhibits large sway. Although the platform was stationary in quiet-stance the animal's body sway in the sBVH state was much larger than in the control state. Thus, we hypothesize that R1's utilization of intrinsic/short-latency mechanisms had decreased due to large sways (and therefore large ankle stretch), and that sway was substantial enough that neural feedback control was involved in the response. As previously stated, long-latency neural feedback is necessary for large ankle stretch (e.g., during large platform rotations) as shown in Peterka (2002).

In future work, direct measurement of muscle activity via EMG in the rhesus monkey would aid in elucidating the role of long-latency mechanisms (acting with long neural time delay) versus intrinsic/short-latency mechanisms (acting with little or no time delay). Chronic invasive implantable EMG electrodes have been used in cats (e.g., Macpherson 1988b) and in rhesus monkeys (Hodgson et al. 2001). However, this method requires intensive surgery that would involve subcutaneous implantation of the electrode in the belly of each specific muscle. In the current study, non-invasive methods, like reaction forces, body measurement data and a simple model (Section 3.5.2), were used as a first step to gain insights into the roles of long-latency and intrinsic/short-latency control mechanisms in the rhesus monkeys with varied levels of vestibular function.

3.5.2 Quiet-stance control model

The quiet-stance controller model implemented below shows proof-of-concept that increased intrinsic/short-latency stiffening from normal, as proposed for the mBVH

sensory state, can decrease body sway, and in the severe vestibular loss sensory state, sBVH, the animal used different control mechanisms but was unable to compensate or maintain stability.

For quiet-stance, the human biped is often approximated to sway as a single-link inverted pendulum, rotating rigidly about the ankle joint (ankle strategy). Models of bipedal, human stance have treated the human as a single-link inverted pendulum that is inherently unstable and requires feedback control to stabilize. When there is deviation from upright stance, a corrective torque, Tc, comprised of the summation of an long-latency (neural controller) torque, T_L, and intrinsic/short-latency torque, T_i, is generated. Neural controller torque, T_L, is generated with stabilization requiring one component of corrective torque proportional to the angular deviation, Kp, another component that is the time derivative of the angular deviation, Kd, and also a third component, the integral of the angular deviation, Ki, has allowed for an even better explanation of human posture data but is not necessary to stabilize the pendulum (Johansson and Magnusson 1991). This proportional-integral-derivative "PID" controller has been used to model the neural controller involved with stabilizing the human, inverted pendulum. A simple PID feedback control model can be used in conjunction with experimental quiet-stance COP (Maurer and Peterka 2005) or COM data traces.

As opposed to a full-body, complex biomechanical model, the simple inverted pendulum model is implemented here to model the foretrunk in order to display proof-of-concept that increased stiffening can decrease trunk roll.

Figure 3.3 shows the quiet-stance proportional-derivative (PD) feedback control model for the rhesus monkey foretrunk that was implemented using Simulink

(MATLAB, Mathworks, Natick, MA, version 2008b). Since integral gain, Ki, was not necessary to stabilize the pendulum, we set this term to zero. Although the monkey attempted to stand stationary, there was measurable spontaneous sway present that was modeled as a low-pass, white noise disturbance input. The moment of inertia of the foretrunk was J ~ 0.09 kgm^2 and mgh ~ 2.5 kgm^2/s^2 were determined using anthropometric measurements derived from cadaveric rhesus monkeys (Vilensky 1979). Noise gain, Kn was set to 462 Nm and Tn, to 100 s (as in Maurer and Peterka 2005). The white-noise input creates a disturbance torque, Td, and outputs are the angular deviation of the trunk in roll. Visual, vestibular, and proprioceptive gains are assumed to sum to one (i.e. total sensory system gain = 1). Human mean intrinsic/short-latency stiffness (~ 4 Nm/deg) and intrinsic/short-latency damping (~ 0.7 Nms/deg) values for small ankle stretch (0.15°) were used as initial values for the controller model and long-latency mechanisms were assumed to play minimal a role and set to ~ 0 (Loram et al. 2007) for normal and mBVH quiet standing.

Simulink (MATLAB, Mathworks, Natick, MA) model simulations were run for 600 s. The 600 s simulation was then segmented into forty, 15 s trials. For each trial, the mean was computed and subtracted from each data point within the given trial. The trials were then pooled and the means and standard errors for each of the sway measures were computed. These simulated sway measures were then compared to experimental sway measures computed for the foam-wide head-mounted test condition for R2 in the normal and mBVH sensory states and R1 in the sBVH sensory state. This test condition was selected because it was where changes in sway were seen in mBVH R2 and sBVH R1 compared to their baseline (i.e., normal or control) states.

3.5.2.1 Normal and mBVH model-simulated sway

Head-mounted control and mBVH data from R2 were used in conjunction with the model. Control intrinsic/short-latency stiffness, K, affected displacement sway measures and intrinsic/short-latency damping, B, affected velocity and frequency sway measures. The human values of K = 4 Nm/deg and B = 0.7 Nms/deg (Loram et al. 2007) were used as initial values. The experimental mean values for the sway parameters RMS and RMSV were compared to the RMS and RMSV obtained by model-simulated roll resulting from various K and B values. The optimal values for K and B occurred when the model-predicted sway parameters for RMS and RMSV intersected the experimental values for RMS and RMSV. However, in order for the model-predicted sway measures to better match the other sway measures (MAXD, CFREQ, and FREQD) within ~ 10 % error from the experimental values, K and B values were then adjusted. Thus, the final normal-fitted values for the animal were K = 8 Nm/deg and 0.62 = Nms/deg. This increase in stiffness for the normal animal, compared to the human, could be accounted for due to physiological and anatomical (e.g., rhesus monkeys have high strength-to-weight, and strength-to-height, ratios), and structural differences (e.g, quadrupedal as opposed to bipedal stance) between the rhesus monkey and human.

Using a similar procedure described above, for the mBVH sensory state K and B were determined to be 12.5 Nm/deg and 1.47 Nms/deg, respectively. Figure 3.14 shows that as K is increased from the normal value (8 Nm/deg) to the mBVH value (12.5 Nm/deg), and the simulated roll decreased. Experimental (measured) and model-predicted sway measures were closely matched and are shown for normal and mBVH in Figure 3.15.

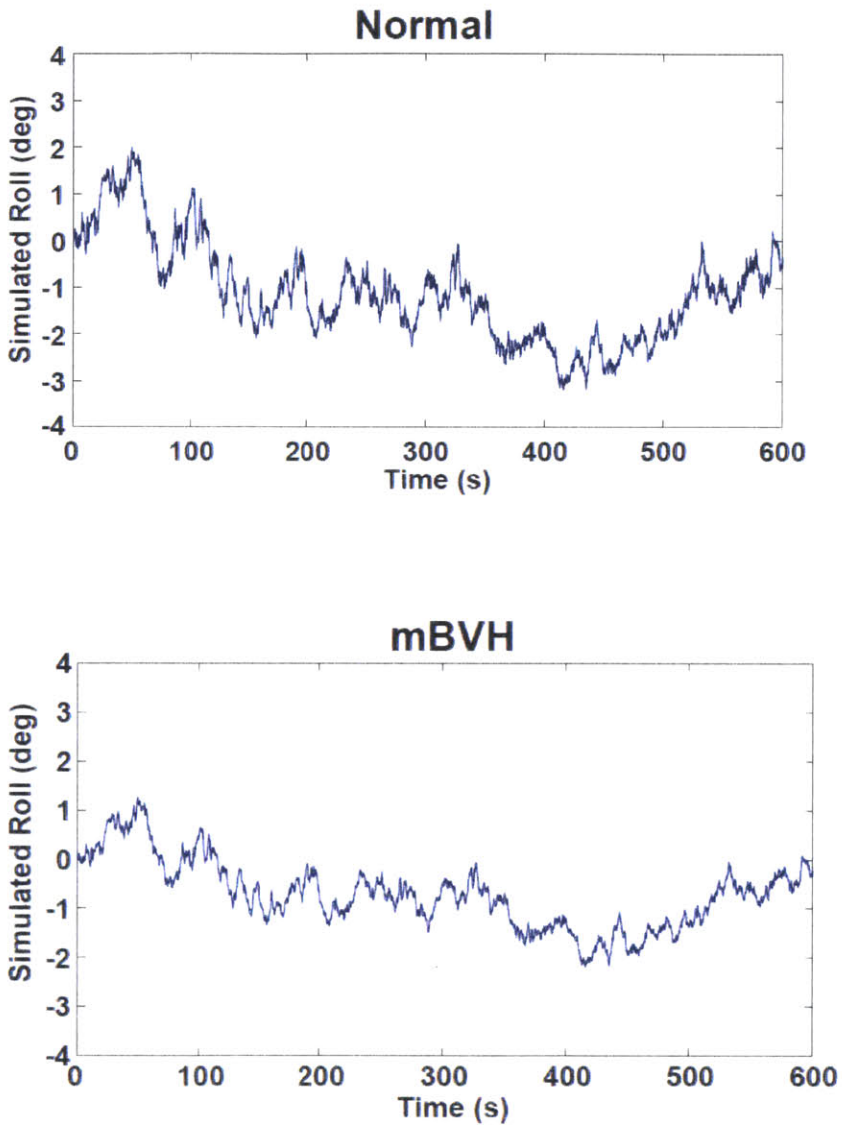

Figure 3.14 Model-predicted foretrunk roll for normal (top) and mBVH sensory states (bottom).

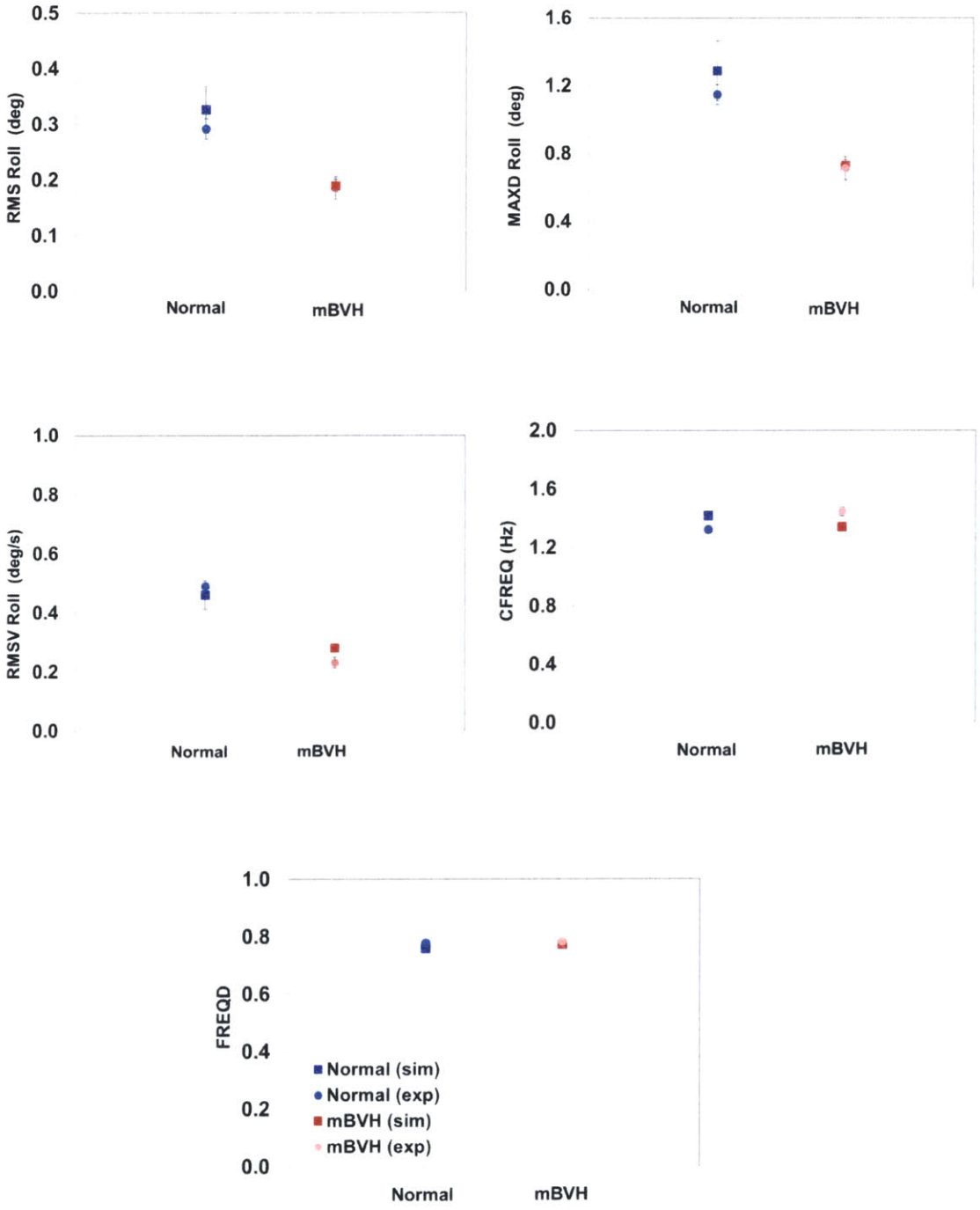

Figure 3.15 Foretrunk roll sway measure values for normal (blue) and mBVH (red) sensory states: model-predicted (square) and measured data (circle). Bars represent standard error.

3.5.2.2 sBVH model-simulated sway

In the sBVH experimental results (Figure 3.6), increases from control were seen. Three possible hypotheses were posed to account for this: 1) there was a large increase in intrinsic/short-latency stiffness (e.g., the animal attempted to apply a similar, but more exaggerated strategy than in the mBVH state) without a corresponding increase in damping thus leading to oscillatory behavior and increased sway (e.g., a severely underdamped system), 2) there was very small intrinsic/short-latency stiffness and damping due to the animal having an *opposite* postural response compared to normal and thus the animal was unable to compensate and increased roll resulted, or 3) the animal utilized an alternate strategy than in the normal and mBVH sensory states by activating neural feedback mechanisms, such as long-latency stiffness and damping, due to the larger sways (and larger ankle stretch) in the sBVH sensory state.

The first scenario seems the least likely because very large increases in intrinsic/short-latency stiffness would be unlikely to yield a drastic decrease in intrinsic/short-latency damping. Furthermore, increases in natural frequency (oscillatory behavior) of trunk sway associated with this increases in stiffness for low damping values is not physiologic. For example, for R2 in the normal and mBVH sensory states, experimental values for CFREQ (normal: 1.415 +/- .021 Hz and mBVH: 1.445 +/-.031 Hz) were not significantly different and therefore were possibly independent of the sensory state of the animal. The second scenario seems more likely in that sBVH animals (as in Macpherson et al. 2007) exhibit opposite postural strategies when compared to control. However, the third hypothesis is most aligned with the previous discussion on small versus large (ankle) rotations (Section 3.5.1). More specifically, due to the large

ankle rotation in the sBVH state, and hence large body sway, the animal was likely utilizing long-latency mechanisms. Decreases in intrinsic/short-latency stiffness were shown for increased ankle rotations (Loram et al. 2007), but the relationship of intrinsic/short-latency damping to amplitude of rotation is less clear. Although the animal is applying neural feedback control mechanisms, it is severely impaired and therefore is not generating a large enough long-latency mediated corrective torque to compensate for its loss.

A head-mounted set of quiet-stance sBVH foretrunk data from R1 (not shown) was used to estimate model parameters. Simulated foretrunk roll is shown in Figure 3.16. Kp and Kd were determined to predict simulated sway measures within the ~10% sway measure error criterion. Kp was determined to be 0.7 Nm/deg and Kd = 0.02 Nms/deg. In order to allow better velocity fits, intrinsic/short-latency damping was held at 0.4 Nms/deg. Simulated roll sway measures were closely matched to experimental sway measures and are shown in Figure 3.17.

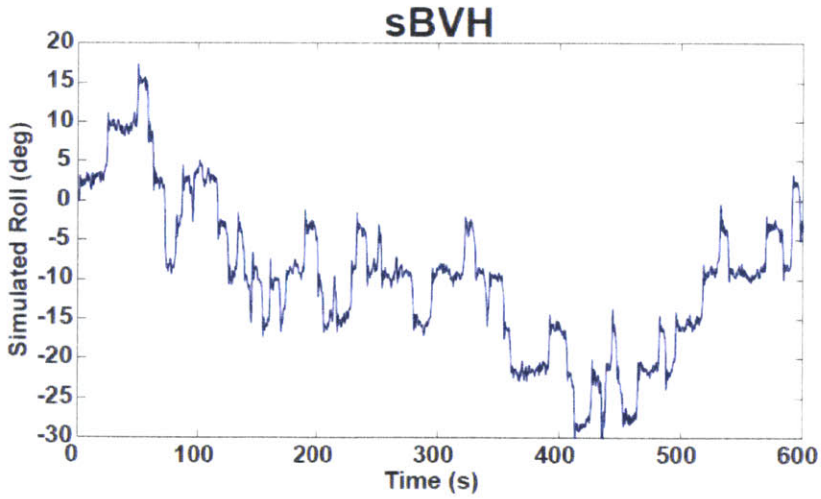

Figure 3.16 Model-predicted foretrunk roll for sBVH sensory state.

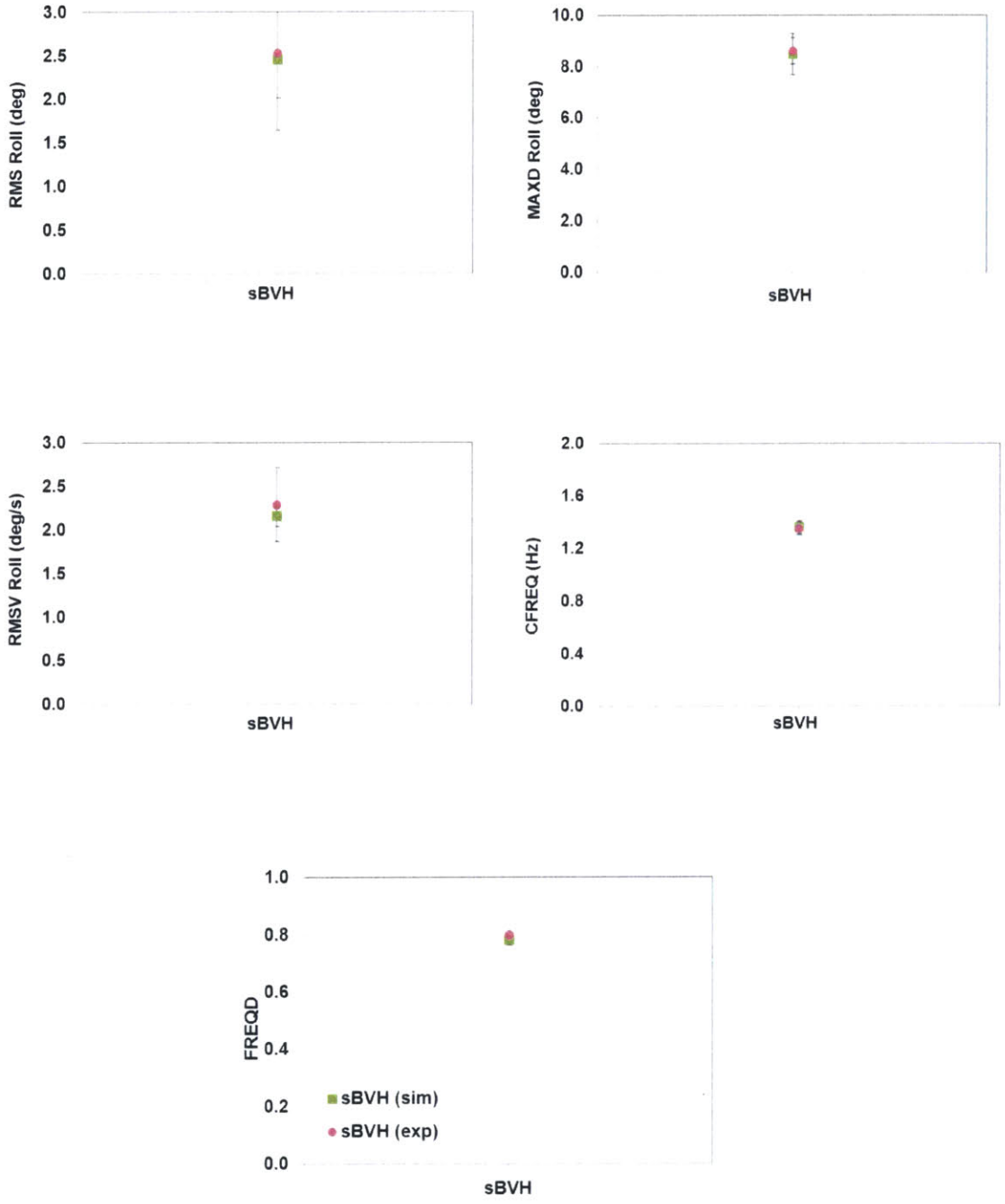

Figure 3.17 Foretrunk roll sway measure values for the sBVH state: model-predicted (green-square) and measured data (pink circle). Bars represent standard error.

3.6 Conclusions

Previous studies of normal and severe bilateral vestibular-loss (e.g., labyrinthectomized) animals and humans have not addressed postural responses as a function of the degree of bilateral vestibular impairment. This chapter demonstrated that the rhesus monkey can compensate for a mild degree of vestibular loss by: 1) altering the forces exerted on the support surface and 2) increasing intrinsic muscle stiffness and becoming more rigid (e.g., increasing intrinsic/short-latency muscle stiffening). However, with a severe degree of vestibular loss, the animal was unable to compensate using the same mechanisms as normal or mBVH states and thus an increase in trunk sway was seen. Predictions of a feedback controller model were consistent with the general hypothesis that the degree of vestibular function has an influence on the postural control mechanisms used.

---

[1]Chapter II (Section 2.4.2) addresses animal training.
[2]Chapter VI addresses head-turn experimental results for a severely-impaired (sBVH) animal with partially restored vestibular cues (via vestibular prosthesis). Head-turn data was collected for R1 in the sBVH and sBVH aided by a vestibular prosthesis (sBVH +STIM-ON) sensory states.
[3]Chapter II (Section 2.5.4) justifies the logic behind the outlier criteria used.

IV. Sensory reweighting in the rhesus monkey postural response

4.1 Abstract

Do rhesus monkeys with normal or mild vestibular loss have the ability to modulate their reliance on sensory feedback for postural responses? Can sensory reweighting explain differences between animals with normal vestibular function and those with vestibular dysfunction? To answer these questions, a dynamic, pseudorandom ternary sequence (PRTS) roll-tilt input stimulus was applied at several amplitudes to a balance platform and rhesus monkey trunk roll was measured. Similar to normal human responses, the normal rhesus monkey exhibits a nonlinear saturating increase in hindtrunk root-mean-square (RMS) roll for increases in stimulus amplitude (sway saturation indicative of a change in sensory reliance).. An animal with mild bilateral vestibular hypofunction (mBVH) also exhibited some sway saturation, but in general showed larger sway than normal at the larger stimulus amplitudes. For each stimulus amplitude, a linear approximation of body sway was used to characterize behavior in the form of a system transfer function. Transfer function gain (e.g., hindtrunk roll/input roll) and phase were determined for the animal (R2) in the normal and mBVH sensory states. Transfer function gain of the mild vestibular-lesioned animal increased compared to the normal state. The animal in the mBVH state oriented more with the platform surface compared to the normal state that oriented more with earth-vertical at larger stimulus amplitudes. Transfer function results were used in conjunction with a feedback controller model to test the sensory reweighting hypothesis: the animal "weighs" (or relies upon) graviceptive cues more heavily (i.e., orients more with earth-vertical) as stimulus

amplitude increases. Model predictions were consistent with this hypothesis in that the normal and mild impaired states model results showed increases in graviceptive sensory weight (orientation to earth-vertical) with increases in stimulus amplitude. The model also indicated that differences between the normal and impaired states could be explained by a change in utilization of sensory feedback (as opposed to other neural mechanisms such as long-latency stiffness or time delay). Specifically, the model showed that the monkey in the mBVH state reduced graviceptive sensory weighting and increased proprioceptive sensory weighting compared to the normal state. In conclusions, both experimental (measured) results and model predictions support the hypothesis that sensory reweighting is a balance control mechanism used in both normal and mild vestibular dysfunction sensory states.

4.2 Introduction

Control theory techniques have been used to characterize the postural control system (e.g., Goodworth and Peterka 2012; Peterka 2002). For a system approximated as linear, cross-correlating a random input signal with the system output response yields an impulse response function, or in the frequency domain the system transfer function, that fully characterizes the system. Peterka (2002) studied postural control of normal and severe bilateral vestibular-loss humans. For postural control, transfer function gains exhibited nonlinear (saturating) stimulus-response curves (Peterka 2002). More specifically, a normal human's root-mean-square (RMS) center-of-mass (COM) body sway saturated for the larger platform tilt amplitudes (sway saturation). Saturation of the normal subjects' response was attributed to the normal test subject's ability to increase reliance, or weight, on graviceptive (e.g., vestibular cues) as stimulus amplitude

increased. This prevented them from falling off the platform. However, human subjects with severe bilateral vestibular loss did not exhibit the same sway saturation in that the stimulus-response curves remained linear with increases in stimulus amplitude. More specifically, even at the larger stimulus amplitudes the severe vestibular-loss subjects continued to orient towards the platform surface and therefore could not maintain stability. Characteristics that were seen in the RMS stimulus-response curves could also be seen in the gain relationships of the system transfer functions. For larger stimulus amplitudes, normal humans' COM was increasingly more stable relative to earth-vertical (i.e., gain = body tilt /stimulus tilt was decreasing away from 1) than to the platform. However, bilateral vestibular-loss subjects' COM was more stable relative to the platform (i.e., gain = body tilt /stimulus tilt > or = 1) than to earth-vertical.

Previous posture studies in quadrupedal animals have not utilized pseudorandom tilts. Instead, ramp and hold rotations (Macpherson et al. 2007) and discrete sinusoidal inputs (e.g., Beloozerova et al. 2003; Brookhart et al. 1965) were used. Ramp and hold, pitch and roll rotations (for 6^{o} peak) of the support surface have been used to study normal and bilateral labyrinthectomized cats (Macpherson et al. 2007). In the normal animals, there was activation of the extensors of the "uphill" (away from the direction of platform rotation) limbs and inhibition of extensors in the "downhill" (with the direction of platform rotation) limbs. However, following labyrinthectomy there was an opposite postural response: excitation of the uphill limbs and inhibition of the downhill limbs. This postural response accelerated the body's COM with the downhill rotation, or in the same direction as, the platform surface leading to imbalance and falls. This result was consistent with Peterka's (2002) finding in severe bilateral vestibular-loss humans that

showed large body sway in response to larger stimulus amplitudes. This finding suggested that muscle activation patterns were opposite those of the normal subjects (i.e., abnormal response magnifies body sway leading to destabilization).

Postural response gain (ratio of the limb axis angle to the platform angle) was determined for the cat. Similar to the human studies, gain = 1 signified that the limb axis was tilted at the same amplitude as platform rotation. For normal cats, peak gains in roll were approximately 0.5. However, after labyrinthectomy, the limb axis peak gains were > 1 (angle of limb > angle of platform). A gain approaching 0 (e.g., a gain decreasing away from 1), signified that the limb axis was becoming more stable relative to earth-vertical and less stable relative to the platform. Thus, due to missing or unreliable vestibular information the vestibular-lesioned cats tried to align their limb axis with the platform surface as opposed to earth-vertical. When the severe vestibular-lesioned animals aligned with the platform surface, the body was accelerated in the same direction as the platform rotation. This response to platform motion contributed to imbalance and falls. However, the normal intact animals were capable of aligning with earth-vertical and therefore were able to restore their balance when the platform was tilted.

We hypothesize that the rhesus monkey exhibits sway characteristics consistent in pattern to those seen in normal and severe vestibular-loss human and cat subjects. As opposed to previous studies that have focused on normal vestibular function or severe vestibular dysfunction, we examined the effects of mild vestibular dysfunction, or mBVH, on the animal's posture. The main goals of this study were: 1) to determine if the rhesus monkey stimulus–response curves exhibited sway saturation for normal and/or mBVH sensory states (indicative of sensory reweighting), 2) to describe the rhesus

monkey postural control system in terms of system transfer functions, 3) to determine if a feedback control model based on human postural feedback studies could be applied to understand monkey postural responses, and 4) if a feedback control model could be utilized, to test the sensory reweighting hypothesis for the animal in the normal and mBVH states

4.3 Methods

Experiments were conducted with the approval of the Massachusetts Eye and Ear Infirmary (MEEI) Institutional Animal Care Committee and were in accordance with USDA guidelines. One adult, female rhesus monkey (R2: 5 yrs, ~6.7 kg) was used for these sets of experiments.

The animal was trained to stand free of restraint on the platform to receive a juice reward. Once the animal was able to stand on the moving platform, normal data were collected. After the normal experiments were conducted, the monkey underwent a series of ototoxic treatments. The purpose of these treatments was to target and kill the vestibular hair cells while preserving a functioning eighth nerve.

Intratympanic gentamicin (IT gent) kills vestibular hair cells and has been used to treat vertigo in Meniere's patients (e.g., Minor 1999). Initial surgery was conducted under anesthesia (ketamine (10 mL/kg) pre anesthesia and isoflurane (2 - 5% saturation with oxygen)) and consisted of tympanic membrane perforation and gentamicin injection into each ear (i.e., 40 mg/mL in each ear). Maximum damage was estimated to be approximately 2 weeks post-administration of the drug (1 cycle of IT gent treatment = administration + 2 week waiting period). The animal underwent 5 cycles of IT gent treatments. The gentamicin treatments were followed by intramuscular streptomycin (IM

strep) treatments (350 mg/mL per day for 21 days x 2) that were injected into the animal's muscle.

The degree of vestibular impairment was quantified in terms of the angular vestibuloocular reflex (VOR) gain (-eye velocity/head velocity). The angular VOR, a simple eye movement reflex used to measure semicircular canal function, was tested at discrete frequencies. Final VOR gain (post ablative procedures) was 15% reduction from normal (for 0.1 to 0.4 Hz). This level of vestibular dysfunction defined the mBVH sensory state.

4.3.1 Training and data collection

The monkey stood in its natural quadrupedal stance on the balance platform with 9 cm footplate separation in the transverse plane and 31 cm footplate separation in the longitudinal plane. A platform-mounted juice reward system with a flexible mouthpiece was used to motivate the animal to stand on the moving platform (Figure 4.1).[1] Because the reward system was mounted to the platform, its orientation relative to the moving platform did not provide the animal an earth-vertical stationary reference.

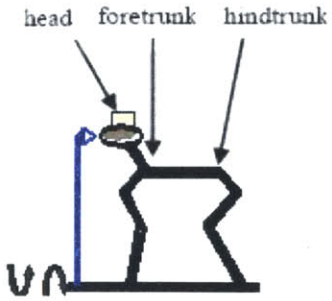

Figure 4.1 Schematic of the juice reward configuration.

In order to limit visual cues, a black tarp surround and dim lighting were used. To measure the motion of the head, foretrunk, and hindtrunk, the output of tri-directional angular position and linear position sensors were sampled at a rate of 150 Hz (miniBIRD, Ascension Technology Corporation, Milton, VT). In the transverse (mediolateral) dimension, the stance width was smaller (9 cm) than in the longitudinal (anterior-posterior) direction (31 cm). Thus, maintaining balance in the mediolateral direction was a more demanding postural task than in the anterior-posterior direction. As such, the platform was made to move along the roll-axis (Figure 4.1). In both the training and testing of the animal, roll-tilt amplitudes of 0.5, 1, 2, 4, 6, 8 $^{\circ}$ peak-to-peak (or "pp") were used. The pseudorandom stimulus that was used is described below. During testing, each stimulus cycle was presented 8 times before moving on to the next amplitude. The stimulus presentation continued until the monkey stopped attending to the task (e.g., the animal was no longer motivated by the juice reward and hopped off the platform).

4.3.2 Pseudorandom ternary sequence (PRTS) roll-tilt stimulus

A white noise approximated stimulus (pseudorandom sequence) was used as an input stimulus to control the platform support surface. In the frequency-domain, white noise has a constant power spectrum for all frequencies much greater than the bandwidth of the system, however, in the time-domain white noise is an impulse. By cross-correlating the input, x(t), with the system output response, y(t), an impulse response function can be obtained, or in the frequency domain H(s), also known as the system transfer function (Figure 4.2). For a linear system, the transfer function fully characterizes the system.

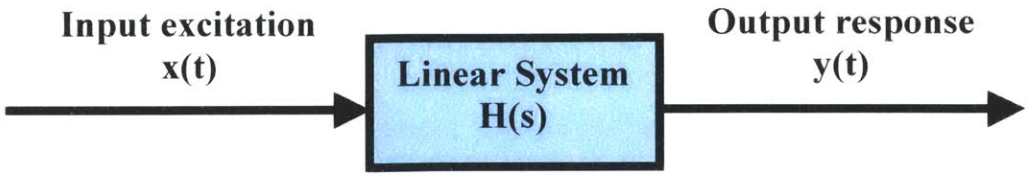

Figure 4.2 System schematic.

$$H(s) = \frac{L[y(t)]}{L[x(t)]} = \frac{Y(s)}{X(s)} = \text{transfer function} \qquad (4.1)$$

where

L = Laplace operator
s = complex variable
x(t) = the input (as a function of time, t)
X(s) = the Laplace transform of x(t)
y(t) = the output (as a function of time, t)
Y(s) = the Laplace transform of y(t)

The advantages to using a white noise input are the following: 1) constant power input for all frequencies, 2) the experiment can be performed while the system is functioning in normal mode, 3) measurements are immune to unwanted noise provided it is independent of (uncorrelated with) the input white noise source, and 4) presence of stored energy does not affect the impulse response. However, one disadvantage of using white noise as an input is that it takes a very long time to obtain an accurate estimate of the cross-correlation function. In an ideal case, integration time would be infinite (Davies 1970). The long integration time required for an accurate estimate is overcome by the use of pseudorandom noise. Pseudorandom noise has approximately the same autocorrelation as white noise (an impulse), but repeated each period. Thus, the cross-correlation function may be obtained by integration over only one period of the noise.

Pseudorandom noise signals can have a number of output states (e.g., binary (or 2 output states), ternary (or 3 output states), pentary (or 5 output states)) depending on the

application. A pseudorandom ternary sequence, or PRTS, (depicted in the schematic of Figure 4.3, top) can be generated using a shift register and consists of 3 output states: 0, 1, and 2. The sequence is initialized with a series of logics states. Within the shift register, each stage is cross-connected and simultaneously triggered by a clock pulse, or the shift time (Δt). For each clock pulse, the logic contents of the i^{th} stage are transferred to the $(i+1)^{st}$ stage and a new logic state is introduced to the input of the first stage via the feedback circuit.

The sequence obtained from the shift register depends on where the feedback connection is inserted. A modulo-three gate produces the sum-digit table shown in Table 4.1. For modulo-three addition, the result is the same as regular addition.

Table 4.1 Modulo-three addition. ($A \oplus_3 B$)

A\B	**0**	**1**	**2**
0	0	1	2
1	1	2	0
2	2	0	1

In applying a PRTS input stimulus to the balance platform, 0 corresponded to –v platform velocity, 1 corresponded to zero platform velocity, and 2 corresponded to +v platform velocity, where "v" is a constant (Figure 4.3, middle). Furthermore, integration of this sequence yielded platform position. When the PRTS input roll-tilt stimulus was applied to the platform, output trunk roll was measured (Figure 4.3, bottom).

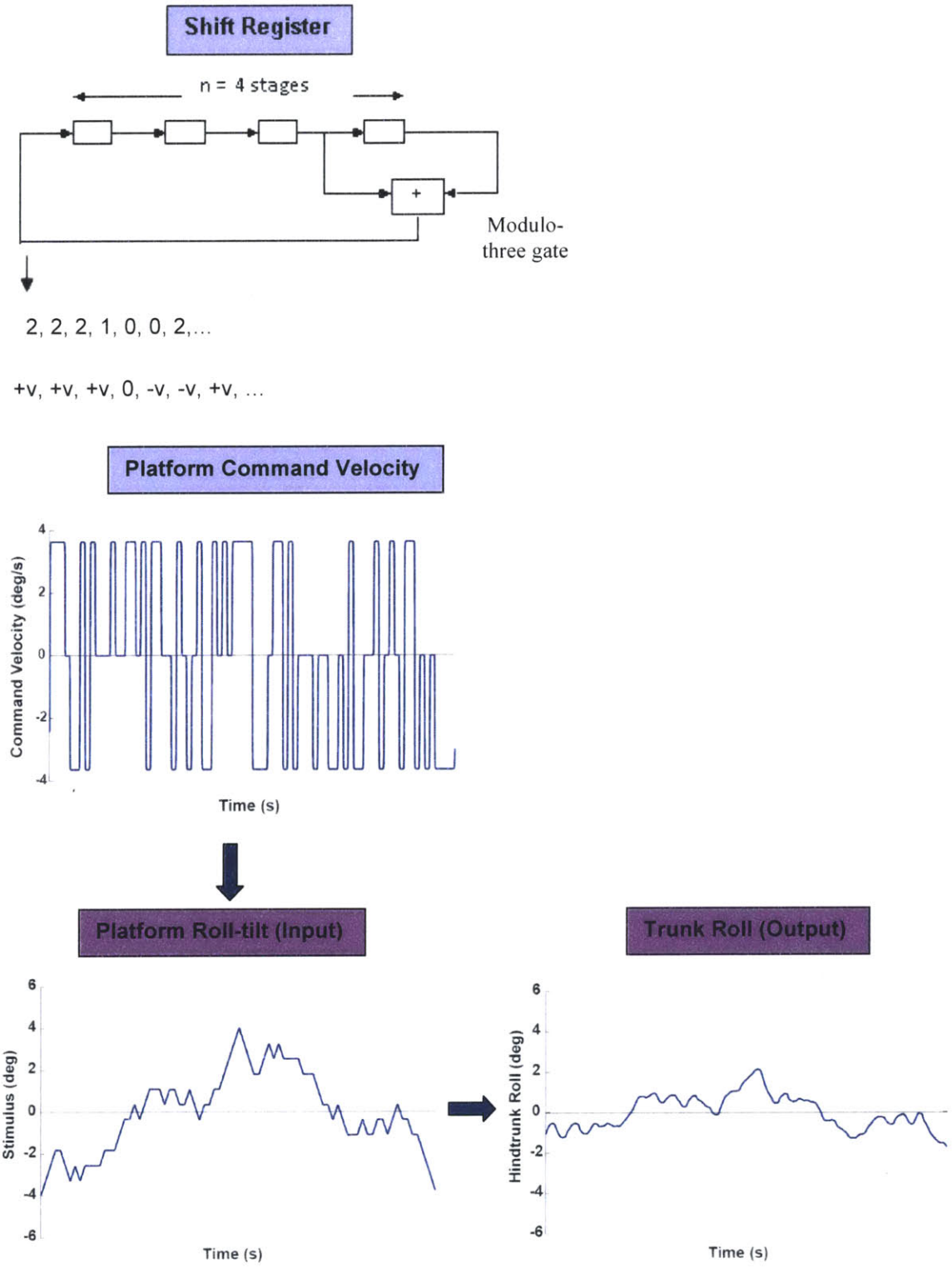

Figure 4.3 Schematic of PRTS generation and application.

A maximum length sequence is one in which the length of the pseudorandom sequence, N, is maximum for the given number of stages within the register, n, before the sequence repeats itself. For a ternary sequence, there is a total of 3^n different states, however occurrence of the state in which the shift register contains 0 logic in each of its stages (meaning all zero sequence) must be prevented. Thus, the largest possible length, N, is:

$$N = 3^n - 1 \qquad (4.2)$$

where
n = number of stages
N = maximum length

The period of the pseudorandom ternary sequence is:

$$T = \Delta t(3^n - 1) \qquad (4.3)$$

where
Δ t = shift time
n = number of stages
T = period

The frequency bandwidth of the sequence is:

$$f_1 = \frac{1}{N\Delta t} \text{ to } \quad f_2 \cong \frac{1}{3\Delta t} \qquad (4.4)$$

where
Δ t = shift time
f_1 = lower frequency bound
f_2 = upper frequency bound

For the set of experiments in this chapter, a PRTS that operated using a 4-stage shift register was used. The PRTS generated an 80 length sequence. The selection of appropriate shift time and period were based on monkey's attention span and on the

frequency bandwidth of interest. Thus, the animal tolerated a shift time of 200 ms that yielded a cycle period of 16 s and a frequency bandwidth of 0.0625 to ~2.33 Hz.

4.3.3 Usable data

In order to identify data sections with human handling artifact, video screening was conducted. Measurements made during PRTS cycles with human handling artifacts and during first cycles of each set of PRTS stimuli were discarded. For all the remaining cycles, offset was removed for each individual cycle. Measurements from remaining cycles for a given stimulus amplitude were pooled and the sample minimum, lower quartile (Q1), median (Q2), upper quartile (Q3), and sample maximum were determined. Outlier sections were defined as those with foretrunk RMS roll less than or greater than Q1-1.5*(Q3-Q1) and Q3+1.5*(Q3-Q1), respectively (Tukey 1977). Outlier cycles were identified and discarded from the analysis.[2] The remaining cycles were marked as "usable". A large number of usable cycles were obtained for the normal and mBVH sensory states (Table 4.2).

Table 4.2 Number of usable cycles for each stimulus amplitude for normal and mBVH sensory states.

	Normal		mBVH	
(°pp)	usable	*unusable*	usable	*unusable*
0.5	18	*4*	20	*4*
1	14	*3*	18	*3*
2	15	*3*	23	*4*
4	7	*3*	20	*4*
6	11	*2*	28	*6*
8	18	*3*	23	*2*

4.3.4 Transfer function analysis

The system transfer function, the relationship between output trunk roll to input platform roll, were computed for the normal and mBVH states.

Power spectra were computed and averaged over the number of usable cycles. A discrete Fourier transform (DFT) was used to decompose the PRTS and measured response to their sinusoidal components. The power spectra computed were the following:

$$G_x(j\omega) = \frac{1}{N}\sum_{i=1}^{N} X_i(j\omega)^* \cdot X_i(j\omega) \qquad (4.5)$$

$$G_y(j\omega) = \frac{1}{N}\sum_{i=1}^{N} Y_i(j\omega)^* \cdot Y_i(j\omega) \qquad (4.6)$$

$$G_{xy}(j\omega) = \frac{1}{N}\sum_{i=1}^{N} X_i(j\omega)^* \cdot Y_i(j\omega) \qquad (4.7)$$

where
N = number of usable cycles
$X_i(j\omega)$ = discrete Fourier transform of the stimulus
$Y_i(j\omega)$ = discrete Fourier transform of the response
$G_x(j\omega)$ = power spectral density of the input stimulus
$G_y(j\omega)$ = power spectral density of the output response
$G_{xy}(j\omega)$ = cross power spectral density

A property of the PRTS stimulus is that all even frequency components have zero amplitude (Davies 1970). These even frequency points were discarded from the analysis leaving 32 odd frequency samples. Spectra were smoothed by averaging the adjacent frequency points as frequency increased (as described in Peterka 2002). Thus, the power spectra were represented by 12 points.

The transfer function was computed from the smoothed (denoted by the subscript "s") odd frequency bands using Equation 4.8.

$$H(j\omega) = \frac{G_{xys}(j\omega)}{G_{xs}(j\omega)} \qquad (4.8)$$

where
$H(j\omega)$ = system transfer function
ω = angular frequency

Equations 4.9, 4.10, and 4.11 show magnitude and phase of the transfer function, as well as coherence, respectively.

$$\left|H(\omega)\right| = \sqrt{H(j\omega)^* \cdot H(j\omega)} \qquad (4.9)$$

$$\angle H(\omega) = \left(\frac{180^\circ}{\pi}\right)\tan^{-1}\left(\frac{\mathrm{Im}(H(j\omega))}{\mathrm{Re}(H(j\omega))}\right) \qquad (4.10)$$

$$\gamma^2(\omega) = \frac{\left|G_{xys}(j\omega)\right|^2}{G_{xs}(\omega)\cdot G_{ys}(\omega)} \qquad (4.11)$$

As described above (Equations 4.9 and 4.10), transfer function gain and phase were computed from the measured trunk roll-tilt and PRTS roll-tilt stimulus. Here we discuss the significance of the gain and phase values. A gain = 0 indicates that the trunk orientation is stable relative to any earth reference (e.g., earth vertical). Thus, if the animal is upright before the stimulus is applied, the trunk tilt is 0° from upright for a given platform tilt. Conversely, if gain = 1 at a particular frequency, this indicates that the trunk orientation is stable relative to the platform surface (i.e., trunk sway equals platform tilt angle) at that particular frequency. If the gain is decreasing away from a value of 1, this indicates that the trunk is increasingly more stable relative to earth-vertical and less stable relative to the tilting platform. If the gain > 1, then the trunk tilt is larger than the platform tilt. A phase = 0 at a particular frequency indicates that the

motion of the trunk is synchronous with the platform tilt stimulus at that particular frequency. However, a phase < 0 or phase > 0 means that the motion of the trunk is either lagging or leading the platform stimulus, respectively.

In order to determine whether the relationship between the stimulus and response is linear, coherence functions were computed. Coherence can vary from 0 to 1, with 1 indicating a perfect linear correlation between stimulus and response and 0 indicating that there is no linear correlation between stimulus and response. In theory, coherence should give an index of the proportion of the output that can be attributed to a linear transformation of the input. All computations were conducted in Matlab (MathWorks, Natick, MA, version 2008b).

4.3.5 Anchoring Indices

Anchoring index (Amblard et al. 1997) has been used to describe the relative angular deviation of a body segment relative to an inferior body segment (e.g., head relative to trunk) and is shown in Equation 4.12.

$$AI = \frac{\sigma_r - \sigma_a}{\sigma_r + \sigma_a} \qquad (4.12)$$

where
AI = anchoring index
σ_r = standard deviation of the relative angular distribution (with respect to axes linked to inferior anatomical segment)
σ_a = standard deviation of absolute angular distribution of segment considered

For normal and vestibular lesioned states, the anchoring index (AI) was utilized to determine the movement of one body segment relative to an inferior body segment. An AI < 0 would, in theory, indicate that the body segment was more stable relative to the inferior body segment than in space (en bloc motion), an AI > 0 would indicate that the

body segment was more stable in space than relative to the inferior body segment, and an AI = 0 would indicate that the body segment was neither more stable in space nor relative to the inferior body segment. Head-to-foretrunk (or head-foretrunk AI) and foretrunk-to-hindtrunk (or foretrunk-hindtrunk AI) were determined in roll.

In regards to comparisons of the measured results, for the above analyses a student's t-test (assuming unequal variance, unequal sample size) was used to determine significance.

4.3.6 Model parameter estimation

Model transfer functions were compared to the experimental transfer functions computed from the measured data. The model transfer function (Equation 4.15) was based on the model described in Figure 4.9. A constrained optimization function ("fmincon", Matlab Optimization Toolbox), was used to adjust the model parameters to minimize the normalized mean square error (NMSE) described in Equation 4.14.

$$E = \frac{tf_{\text{exp}} - tf_{\text{model}}}{|tf_{\text{model}}|} \qquad (4.13)$$

$$NMSE = mean(E \bullet E^{*}) \qquad (4.14)$$

where
E = error
tf_{exp} = transfer function computed from measured roll data
tf_{model} = transfer function computed by model

The error, E, is the difference between the model and experimental transfer functions divided by the magnitude of the model transfer function (Equation 4.13). Normalized mean square error (NMSE) is the mean of the error times the conjugate of the error (Equation 4.14). This definition of E was determined heuristically in previous

human studies (e.g., Goodworth and Peterka 2009; Peterka 2002) to obtain quality model-fits to transfer functions derived from the measured human data.

For the each of the 1, 4, and 8°pp PRTS stimulus amplitudes, a set of optimized model parameters was computed from the measured data (non-simultaneous model parameter estimation). For non-simultaneous model parameter estimation (Section 4.5.2.1), the NMSE was computed as shown in Equation 4.14 for each PRTS amplitude. However, we also estimated model parameters for all stimulus amplitudes together, or "simultaneously", (simultaneous model parameter estimation). As opposed to the non-simultaneous model parameter estimation, the simultaneous model parameter estimation (Section 4.5.2.2) involved: 1) constraint of specific model parameters to be equal across the 1, 4, and 8°pp stimulus amplitudes and 2) a normalized mean square error that was the sum of the error terms for the 1, 4, and 8°pp PRTS stimulus amplitudes. For the simultaneous parameter estimation, we will call the normalized mean square error term "$NMSE_{sim}$" to differentiate from the "NMSE" described for the non-simultaneous model parameter estimations. The motivation behind simultaneous fits is described in Section 4.5.2.2.

4.4 Results

4.4.1 Foretrunk and hindrunk RMS roll versus stimulus amplitude

Foretrunk and hindtrunk RMS roll as a function of stimulus amplitude (stimulus-response curves) are shown in Figure 4.4. In the figure, the dashed-lines represent the foretrunk or hindtrunk RMS roll for the zero stimulus amplitude (or a stationary platform). For the normal animal's foretrunk, the stimulus-response curve was roughly flat for the three lowest and two highest stimulus amplitudes. For roll-tilts < 4° pp the

normal animal's foretrunk was not responding to the stimulus in that RMS roll was comparable to values seen for no platform motion (i.e., quiet-standing). For the normal animal's hindtrunk stimulus-response curve, there was a non-proportional increase in RMS roll, or "sway saturation", at the higher amplitudes that was also seen in normal humans (as shown in Figure 4.22 and Peterka 2002). The types of saturation seen in stimulus-response curves of the foretrunk and hindtrunk were different. There were also differences seen in foretrunk and hindtrunk transfer functions (Figures 4.5 and 4.6). This implied that there were different mechanisms involved in the control of the foretrunk or hindtrunk (discussed in Section 4.5.1).

For the animal in the mBVH state, the hindtrunk stimulus-response curve showed that the RMS roll saturates at the larger stimulus amplitudes but to a lesser extent than in the normal state. When compared to the normal response, the hindtrunk stimulus-response curve for the mBVH state showed a slight decrease or no significant difference at the lowest stimulus amplitudes but was elevated at the larger stimulus amplitudes.

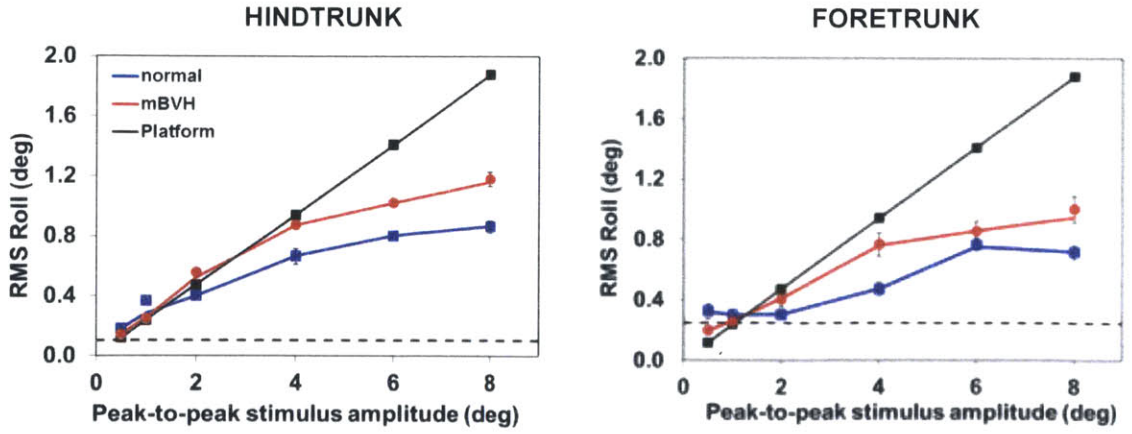

Figure 4.4 RMS roll of hindtrunk (left) and foretrunk (right) as a function of stimulus amplitude with standard error bars. Black-dashed lines represent foretrunk or hindtrunk RMS roll value for stationary platform (i.e., quiet-standing)

4.4.2 Foretrunk and hindtrunk transfer functions

For 1 to 8° pp stimulus amplitudes, normal foretrunk transfer function gain was < 1 and approximately constant across frequency (Figure 4.5, top left). For all stimulus amplitudes, foretrunk phase (Figure 4.5, middle left) had ~ 0 lag (i.e., foretrunk was in phase with the platform) at the lowest frequencies, then increased in phase lag with increasing stimulus frequency. Furthermore, foretrunk coherence (Figure 4.5, bottom left) was low (< ~ 0.6) for all stimulus amplitudes, except for the 6 and 8° pp amplitudes at low frequencies, indicating that, in general, any relationship between the stimulus and the foretrunk roll was weak. The mBVH coherence (Figure 4.5, bottom right) was < ~ 0.6 for all stimulus amplitudes and was the smallest for the lowest stimulus frequency in the 1 and 4° pp responses (i.e., ~ 0 coherence). In the mBVH animal, foretrunk transfer function gain was relatively flat across stimulus amplitudes and frequencies (Figure 4.5, top right) and in some cases less than normal (e.g., at the lowest frequency for the 1 and 4° pp stimuli). The animal in the mBVH state had a slight phase lead for the lowest stimulus frequency (i.e., foretrunk was leading the platform stimulus) compared to the normal animal for the 1 and 4° pp stimuli. Given that the lowest stimulus frequency for the 1 and 4° pp stimuli had an ~ 0 coherence, it was not surprisingly that the gain and phase were very different compared to the other frequencies. As in the normal animal, the mBVH foretrunk response phase lag increases with increasing frequency (Figure 4.5, middle right).

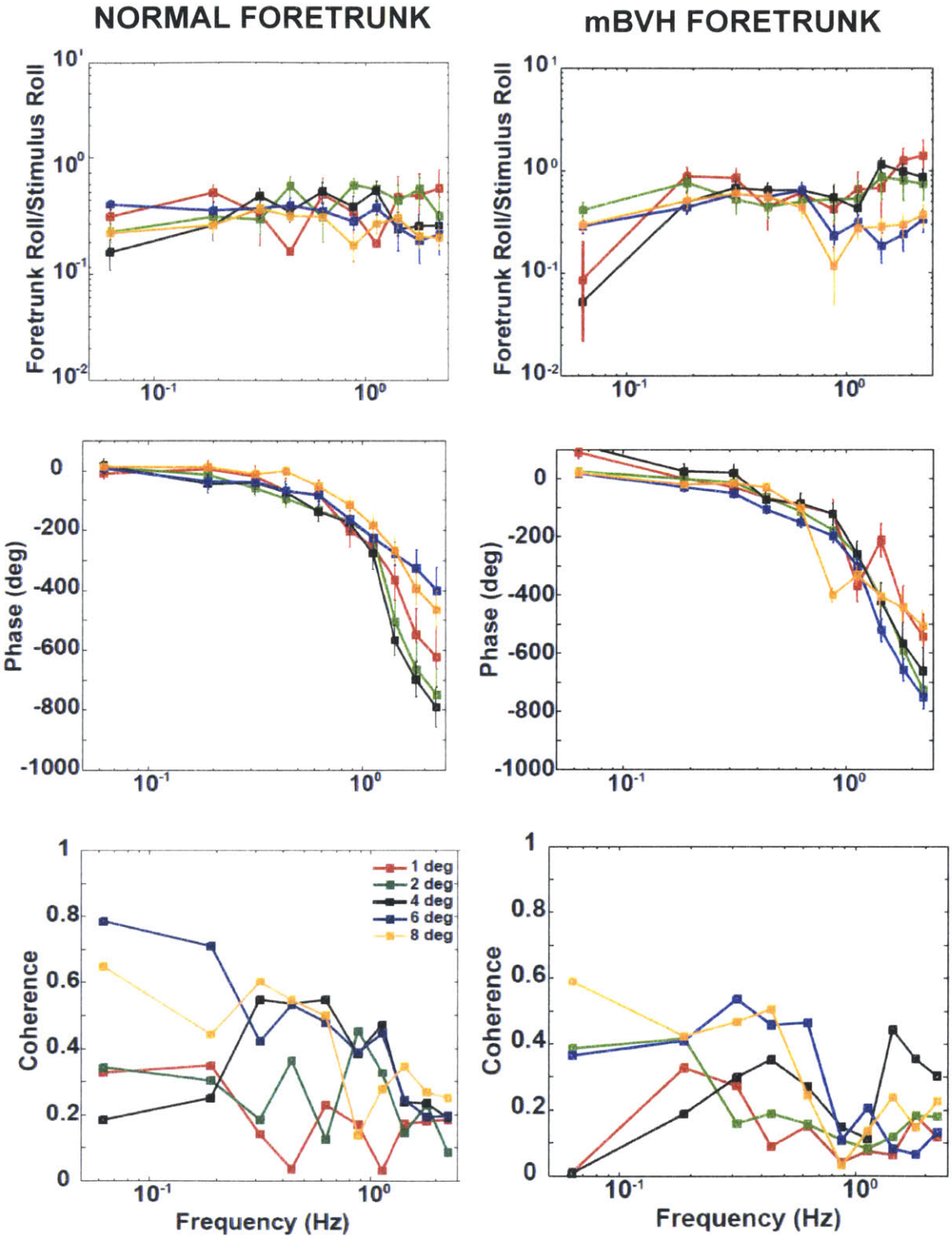

Figure 4.5 Foretrunk transfer function gain (top) and phase (middle), and coherence (bottom) of for normal (left) and mBVH (right) sensory states. Bars shown represent standard error.

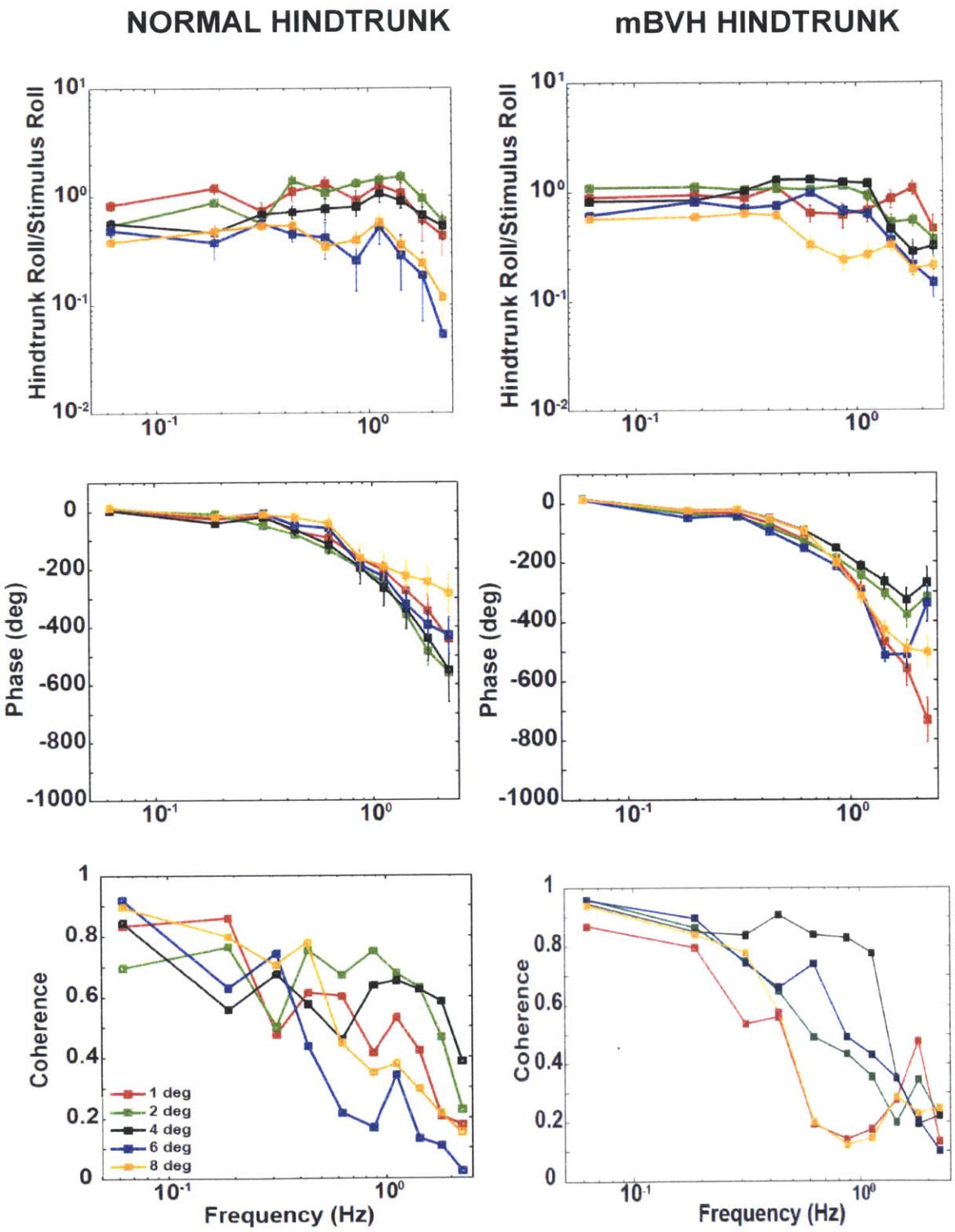

Figure 4.6 Hindtrunk transfer function gain (top) and phase (middle), and coherence (bottom) of for normal (left) and mBVH (right) sensory states. Bars shown represent standard error.

In the normal hindtrunk transfer function gain (Figure 4.6, top left), sway saturation was seen in that the gain tended to decrease away from 1 as stimulus amplitude increased. However, for the lower amplitudes normal hindtrunk gains were ~ 1 indicating that the animal was orienting more with the platform. Hindtrunk gain for lower stimulus amplitudes (i.e., 1 and 2° pp) for frequencies near 1 Hz, were slightly > 1, which means that hindtrunk roll was slightly greater than that of the platform. For larger stimulus amplitudes (i.e., 6 and 8° pp) the gain was < 1 for all frequencies consistent with hindtrunk roll saturating at larger amplitudes (shown in Figure 4.4, left). For neither normal nor mBVH states, were resonant peaks observed. For larger stimulus amplitudes, this shift away from a gain = 1 (toward gain = 0) indicated that the hindtrunk was aligning increasingly more with earth-vertical and less with the platform surface. For all stimulus amplitudes, hindtrunk phase showed ~ 0 lag at the lowest frequencies, and increased phase lag for increased frequency (Figure 4.6, middle left). In general, normal hindtrunk coherence (Figure 4.6, bottom left) was higher than normal foretrunk coherence at the lowest frequencies (Figure 4.6, bottom left) and decreased in coherence as the stimulus frequency increased.

The mBVH hindtrunk transfer function gains (Figure 4.6, top right), most gain functions were elevated relative to the normal gains (Figure 4.6, top left). For example, for the lowest frequency (0.0625 Hz) with the highest coherence, mBVH gain was significantly greater than normal at all amplitudes > than 1° pp (2° pp: $df = 30$, $t = 6.829$, $p < 0.001$; 4° pp: $df = 12$, $t = 3.876$, $p < 0.005$; 6° pp: $df = 18$, $t = 3.239$, $p < 0.005$; 8° pp: $df = 36$, $t = 4.119$, $p < 0.001$). For all stimulus amplitudes, hindtrunk phase (Figure 4.6,

middle right) showed ~ 0 phase lag at the lowest frequencies, then increasing phase lag with increasing stimulus frequency. The mBVH hindtrunk coherence (Figure 4.6, bottom right) was generally higher than mBVH foretrunk coherence for frequencies < 0.3 Hz indicating a more linear relationship between the platform tilt stimulus and hindtrunk response at the lower frequencies. As in the normal hindtrunk response, coherence decreased substantially at higher frequencies.

The transfer function results show that foretrunk responses differed from hindtrunk responses. Foretrunk gains did not change systematically (i.e., were relatively flat across stimulus amplitude and frequency) for both normal and mBVH. Furthermore, foretrunk coherence was relatively low (< ~ 0.6 and in some cases ~ 0) for the two sensory states indicating a weak linear relationship with the stimulus. In contrast, hindtrunk responses showed systematic gain changes (i.e., decreases in gain as stimulus amplitude was increased) for the normal sensory state. For example, Figure 4.6 (top left) which displays the gains for the normal hindtrunk shows that the gain function for the 8^{o} pp stimulus amplitude was less than the gain function for the 1^{o} pp stimulus amplitude. Furthermore, for low frequencies (less than ~ 0.3 Hz) coherence was higher for the hindtrunk than the foretrunk indicating a stronger linear relationship between the hindtrunk response and the input stimulus.

4.4.3 Relative motion of body segments

For the normal and mBVH sensory states, relative motion of the foretrunk and hindtrunk were determined in terms of: 1) gain ratio and phase difference and 2) anchoring indices.

Gain ratio (foretrunk gain/hindtrunk gain) and phase difference (foretrunk phase – hindtrunk phase) were computed. Gain ratio = 1 indicates that the foretrunk roll and hindtrunk roll were equal, whereas a gain ratio ~ 0 indicates that the foretrunk rolled much less than the hindtrunk. Phase difference = 0 means that both the foretrunk and hindtrunk are in perfect phase with each other. Phase difference < 0 indicates that the foretrunk is lagging the hindtrunk and phase differences > 0 indicates that the foretrunk is leading the hindtrunk. Mean gain ratios and mean phase differences are shown in Figure 4.7.

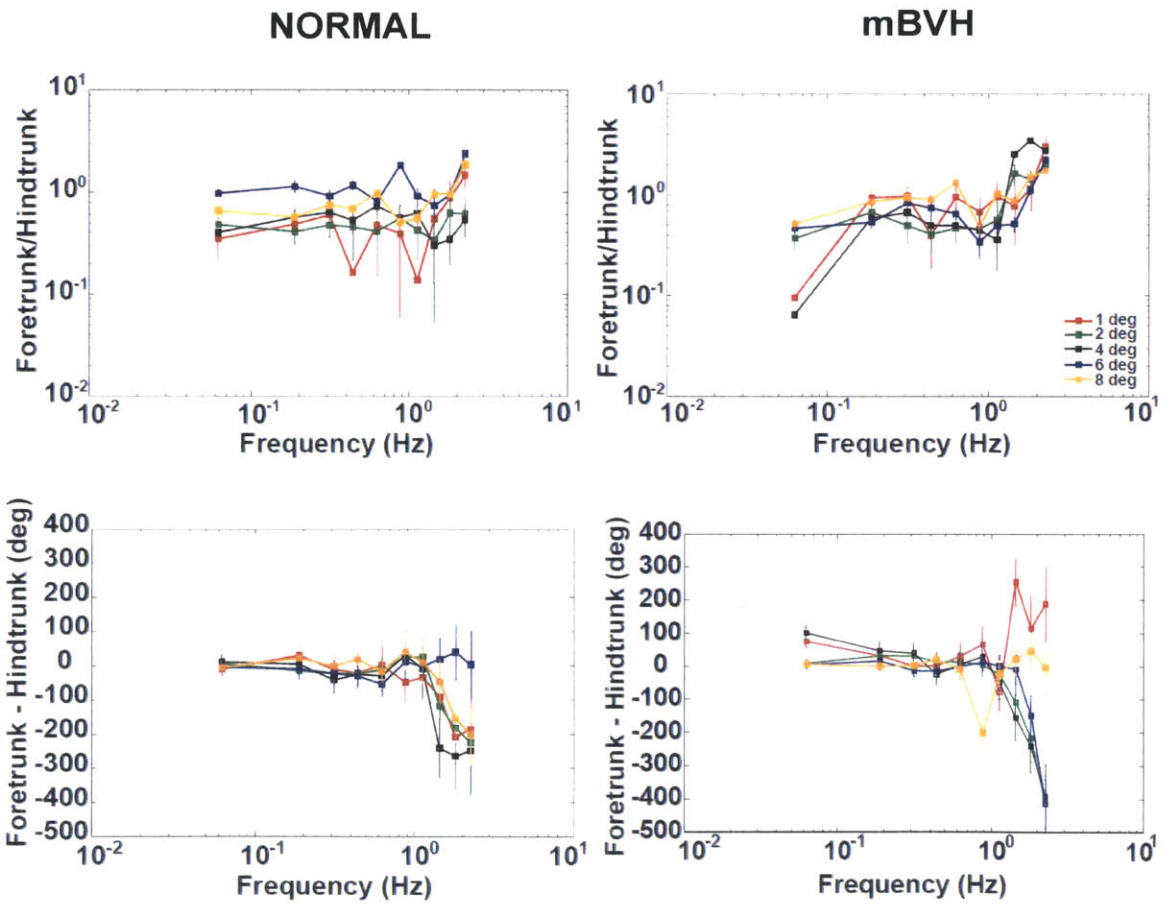

Figure 4.7 Mean foretrunk-hindtrunk gain ratio (top) and phase difference (bottom), with standard error bars, for normal (left) and mBVH (right) sensory states.

In general, the normal animal's foretrunk-hindtrunk gain ratio was close to 1 for the highest stimulus amplitudes (6 and 8° pp) but was < 1 for the lower stimulus amplitudes (e.g., 2 and 4° pp). This indicated that roll of the foretrunk and the hindtrunk were comparable at the higher amplitudes. At the lower amplitudes the foretrunk rolled less than the hindtrunk. Gain ratio fluctuated across frequency, which may have been possibly due to intrasubject variability.

In the normal state, the animal's foretrunk roll was in phase with the hindtrunk for frequencies < 1 Hz and tended to lag the hindtrunk for frequencies > 1 Hz for all stimulus amplitudes except the 6 ° pp. This is analogous to the normal human upper body and lower body response while undergoing a mediolateral pseudorandom tilt stimulus (Goodworth and Peterka 2010).

In the mBVH animal, the foretrunk-hindtrunk gain ratio was < 1 (the foretrunk rolled less than the hindtrunk) for frequencies < 1 Hz for all stimulus amplitudes. However, for frequencies > 1 Hz the gain ratio was > 1 indicating that the foretrunk rolled more than the hindtrunk.

In the mBVH animal, the foretrunk led the hindtrunk for the lowest frequency (0.0625 Hz) for the 1 and 4° pp stimulus amplitudes. However, it is important to note that coherence was ~ 0 for the foretrunk at this frequency for the two amplitudes (Figure 4.5, bottom right). For the intermediate frequencies (0.0625 - 1 Hz) the foretrunk and hindtrunk were in phase. For higher frequencies (> 1 Hz), foretrunk and hindtrunk were out of phase with the foretrunk lagging the hindtrunk for all stimulus amplitudes except for the 1° pp amplitude, where the foretrunk led and the 8 ° pp stimulus where the phase difference remained near zero.

For the PRTS stimulus, normal and mBVH head-foretrunk roll AI's were significantly different ($df = 25$, $t = -2.240$, $p < 0.05$) for only the 4° pp stimulus amplitude (Figure 4.8, left). Normal and mBVH head-foretrunk roll AI's that were not significantly different from 0 or slightly < 0 indicated that the head and foretrunk were neither more stable in space than relative to the foretrunk, or that the head was more stable relative to the foretrunk than in space, respectively.

Normal and mBVH foretrunk-hindtrunk roll AI's were positive (> 0) but not significantly different than 0, and from each other, for the 0.5, 1, 2, and 4° pp amplitudes (Figure 4.8, right). This indicated that the foretrunk was not more stable in space or relative to the hindtrunk for the normal and mBVH sensory states at lower amplitudes. However, at 6° pp mBVH foretrunk-hindtrunk AI was not significantly different than 0, while the normal foretrunk-hindtrunk AI was significantly < 0 ($df = 10$, $t = 4.375$, $p < 0.02$), indicating that the foretrunk was less stable in space than relative to the hindtrunk. This suggested that the animal in the mBVH state changed its postural strategy for the larger amplitudes. However, at the largest stimulus amplitude, 8° pp, both the normal and mBVH foretrunk-hindtrunk roll AI were not significantly different than 0 and not significantly different from each other. At the highest amplitude, the animal's foretrunk in the normal and mBVH states were neither more stable in space or relative to the hindtrunk. Since the level of vestibular impairment was only mild, the animal in the mBVH state was still able to utilize a strategy similar to normal. More drastic differences may be seen in a more severely-impaired animal.

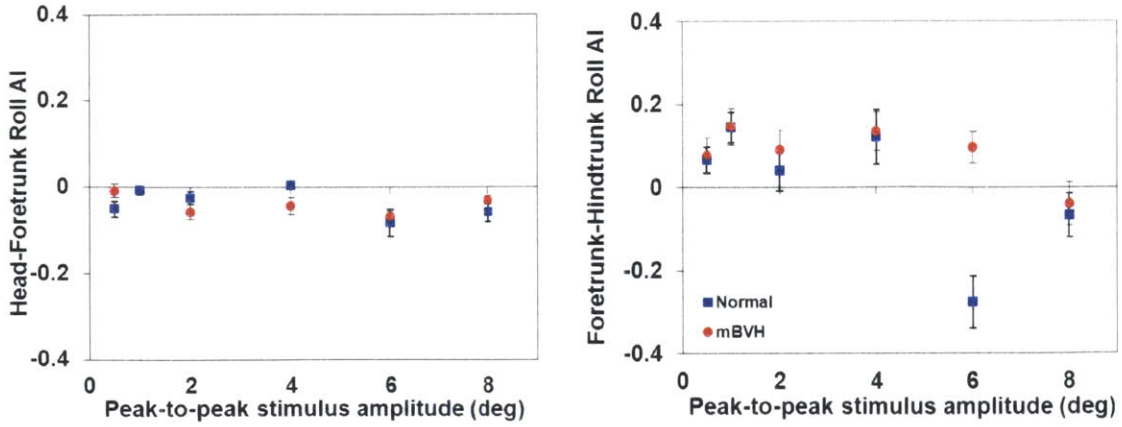

Figure 4.8 Head-foretrunk (left) and foretrunk-hindtrunk (right) roll AI, with standard error bars, as a function of stimulus amplitude.

4.5 Discussion

From the stimulus-response and transfer function results, it was hypothesized that the rhesus monkey "weighted" its graviceptive cues higher for larger stimulus amplitudes (sensory reweighting) to limit the roll of the trunk. In particular, the normal monkey's hindtrunk results showed characteristics similar to those seen in humans (rhesus monkey and human stimulus-response curves shown in Figure 4.22). A human inverted pendulum model (introduced in Chapter II, Section 2.6.1 and described in this chapter in Section 4.5.2) was modified and implemented to test the sensory reweighting hypothesis.

4.5.1 Sensory reweighting seen in hindtrunk but not foretrunk

A previous study conducted in normal humans (Goodworth and Peterka 2012) characterized sensorimotor integration in the frontal plane and described the upper body and lower body utilizing different control mechanisms. The lower body control relied primarily on sensory feedback and control mechanisms across stimulus amplitude that was consistent with sensory reweighting (i.e., amplitude dependent reliance predominantly on proprioceptive or graviceptive cues). In upper body control, sensory

reweighting was not the dominant mechanism, but instead, intrinsic/short-latency musculoskeletal mechanisms along with a relatively fixed reliance on sensory feedback across stimulus amplitudes. The notion that the human upper and lower body is analogous to the foretrunk and hindtrunk of the rhesus monkey is further supported by the similar relative phase characteristics across frequency (Figure 4.7, bottom left).

Based on the differences between the animal's foretrunk and hindtrunk stimulus response curves and transfer function, we proposed that the foretrunk (or "upper body") relied more heavily on intrinsic/short-latency mechanisms that were not mediated by neural feedback as opposed to the hindtrunk ("lower body") that predominantly utilized neural-mediated mechanisms involved with sensory weighting. One reason for this may be due to different mechanical functions of the foretrunk and hindtrunk. It has been proposed that the foretrunk is used primarily to provide stability as struts that stiffen, support, and help steer the animal (Kimura 1985), however, the hindtrunk is used to generate propulsive forces (Courtine 2005) and therefore the postural control mechanisms associated with each are likely to differ. Based on the results (i.e., stimulus-response curves and also transfer functions) shown here for the foretrunk and hindtrunk we propose that: 1) the foretrunk was utilizing a different mechanism for control (i.e., not predominantly utilizing the sensory-mediated mechanisms, such as sensory reweighting) and 2) the hindtrunk was predominantly utilizing sensory feedback, thus leading to a saturating response seen in both the stimulus-response and transfer function gains of the normal and mBVH states. In this chapter, we explored the second point: sensory reweighting in the animal's hindtrunk.

4.5.2 Modeling to describe sensory reweighting

Experimental characteristics associated with sensory reweighting (saturation) were apparent in the normal hindtrunk response to the platform stimulus (Figure 4.6, top left). However, the normal foretrunk data did not show gain saturation characteristics across stimulus amplitude (Figure 4.5, top left). An independent channel model (e.g., Peterka 2002) was used to test the sensory reweighting hypothesis in the hindtrunk only. More specifically, a model was implemented to determine if changes in model parameters (e.g., sensory weights) across stimulus amplitudes and also between normal and mBVH sensory states could predict the measured hindtrunk results. The model implemented is shown in Figure 4.9 and described by Equation 4.15.

For a pseudorandom roll-tilt input, the support surface input (SS) is the roll-tilt waveform itself. And the monkey's hindtrunk sway (HS) is the output response. As previously stated, for quiet-stance or small platform motions some models of bipedal human stance have treated the human as a single-link inverted pendulum that is inherently unstable. Because the platform underwent only small perturbations, we modeled the rhesus monkey's trunk as an inverted pendulum. When there is deviation from upright stance, a corrective torque (Tc) comprised of the summation of a torque (T_L), generated by mechanisms with long-latency neural time delay, and an intrinsic/short-latency torque (T_i), generated by mechanisms without time delay (or with short time delay). The torque (T_i), is generated by: 1) the inherent mechanical characteristics of the muscles, joints, ligaments, and musculoskeletal system (time delay = 0) and 2) the short-latency reflexes (< 25ms). The intrinsic/short-latency mechanisms consist of stiffness and damping (K and B, respectively). In order to stabilize the pendulum body, a long-latency (~ 200 ms), torque (T_L) requires a corrective torque equal

to the angular deviation times the long-latency stiffness represented by Kp, where "p" indicates proportional feedback, and another component that is the time derivative of the angular deviation times the long-latency damping represented by Kd, where "d" indicates derivative feedback.

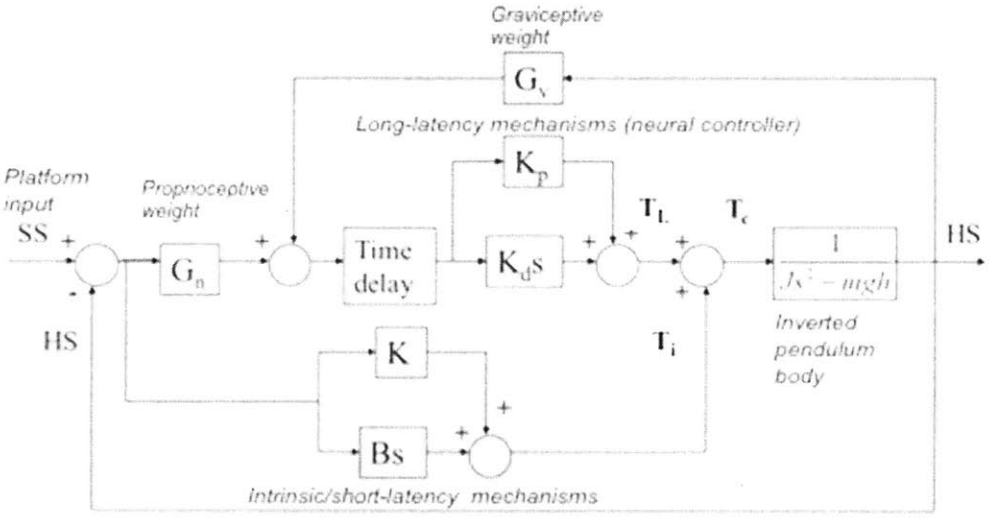

Figure 4.9 Modified "independent channel model" for the rhesus monkey hindtrunk.

In modeling the rhesus hindtrunk, the moment of inertia of the hindtrunk (J = 0.09 kg*m^2) and hindtrunk mass x gravity x hindtrunk COM height (mgh = 2.054 kg*m^2/s^2) were determined using anthropometric measurements derived from cadaveric rhesus monkeys (Vilensky 1979). The weights of sensory channels, proprioceptive (G_n), and graviceptive (G_v), were assumed to sum to unity. Since all experiments were conducted in dim lighting with a black tarp surround to limit visual cues, the visual weight was assumed to be ~ 0.

Transfer functions derived from the experimental results were used in conjunction with transfer functions derived from the modified independent channel model (Equation

4.15) to determine model parameters that minimized the normalized mean square error (described in Equation 4.14).

$$\frac{HS(s)}{SS(s)} = \frac{(Bs+K)+W(K_D s+K_P)e^{-\tau_D s}}{(Bs+K)+Js^2-mgh+(K_D s+K_P)e^{-\tau_D s}} \qquad (4.15)$$

where
HS/SS = transfer function of output hindtrunk roll/input platform tilt
s = complex variable
K_p = Proportional gain or "long-latency stiffness"
K_d = Derivative gain or "long-latency damping"
τ_d = long-latency time delay
G_n = Proprioceptive gain
G_v = Vestibular gain
$W = G_n = 1 - G_v$
$1 = G_n + G_v$
K = intrinsic/short-latency stiffness
B = intrinsic/short-latency damping

Since there was only one test subject, experimental transfer functions were not averaged (smoothed) across test subjects, but instead multiple (7 to 28) PRTS cycles from one animal were used (Table 4.2). Because this was the first attempt ever at modeling sensory-derived monkey postural responses, one goal of the study was to determine if physiologic model parameters could be obtained to account for the experimental behaviors seen. Factors that could impede the use of a human-based feedback control model include: 1) poor resolution of experimental data such that non-linear behavior is evident within each test condition and across repeated cycles; 2) highly variable experimental data resulting in low confidence in model parameters; 3) inadequate similarity between human and monkey postural system such that a similar model structure cannot be shared, resulting in a model that simply cannot account for experimental results without major changes in model structure and parameters included; and 4) inappropriate model structure that results in non-physiological model parameters

(i.e., the model can describe the data, but not with realistic parameter values). We realized these limitations and thus investigated several modeling iterations. Below, I describe how model parameter estimates were determined for the 1, 4, and 8° pp normal and mBVH data using: 1) non-simultaneous model parameter estimation (Section 4.5.2.1) and 2) simultaneous model parameter estimation (Sections 4.5.2.2 and 4.5.2.3).

4.5.2.1 Non-simultaneous model parameter estimation

For non-simultaneous model parameter estimation, we investigated three frequency ranges (0.0625-2.33 Hz, 0.0625-1.125 Hz, and 0.0625- 0.625 Hz) using: 1) a "basic model" that included long-latency (neural controller) stiffness (Kp) and damping (Kd), sensory weight (Gn), and long-latency time delay (τ_d); and 2) the basic model (consisting of Kp, Kd, Gn, and τ_d) with the addition of model parameters for intrinsic/short-latency stiffness (K) and damping (B). The normalized mean square error (NMSE) described in Equation 4.14 was the metric used to assess the degree to which the model-derived transfer functions predicted those computed from measured data.

Good model fits (e.g., NMSE < 0.04) were not possible for the ranges of 0.0625 - 2.33 Hz (the full frequency range) or 0.0625 - 1.125 Hz. This was due to: 1) intrasubject variance and 2) low coherence at the higher frequencies. We restricted the parameter estimation procedure to the lower input spectrum of 0.0625-0.625Hz because coherence was relatively high across this range.

A number of reasons led us to exclude the model parameters K and B. While their inclusion could reduce the NMSE, it led to unrealistic increases and decreases in parameters with no clear pattern across stimulus amplitudes (probably due to too many free parameters). Since relatively large values of intrinsic/short-latency parameters (e.g.,

a relatively large value of intrinsic/short-latency stiffness, K) and proprioceptive weighting, Gn, (e.g., ~1) results in orientation to the platform surface, these two parameters were redundant within the model. Furthermore, inclusion of the intrinsic/short-latency parameters, K and B, led to unrealistically large time delays (τ_d). For example, for the mBVH 8 °pp condition a model-estimated time delay was ~ 0.646 s; much longer than the physiologic time delays of ~ 0.171 s reported for human (Peterka 2002). The non-simultaneous model parameter estimation allowed us to develop the basic model that included only long-latency parameters (i.e. Kp, Kd, Gn, and τ_d). This set of model parameters was used to describe the hindtrunk over the frequency range with highest coherence.

Transfer function gain and phase predicted by the basic model using model parameters derived by the non-simultaneous procedure (see Section 4.3.6) are shown for the normal and mBVH sensory states in Figures 4.10 and 4.11, respectively.

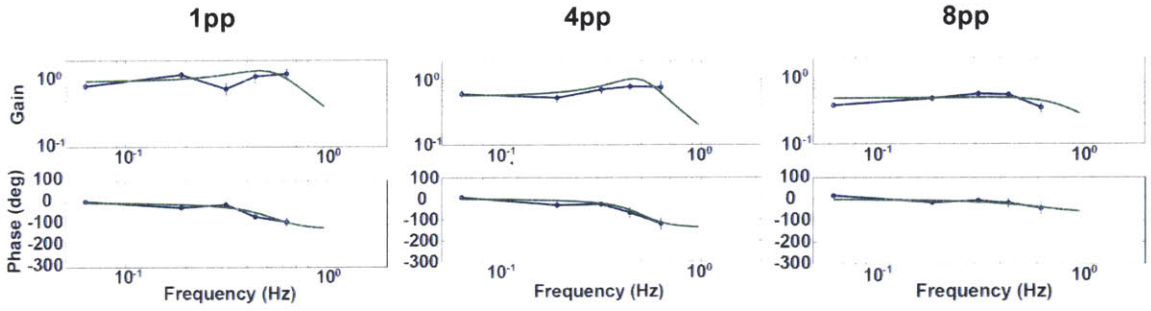

Figure 4.10 Model (green) and measured (blue) hindtrunk transfer functions with standard error bars for the normal sensory state.

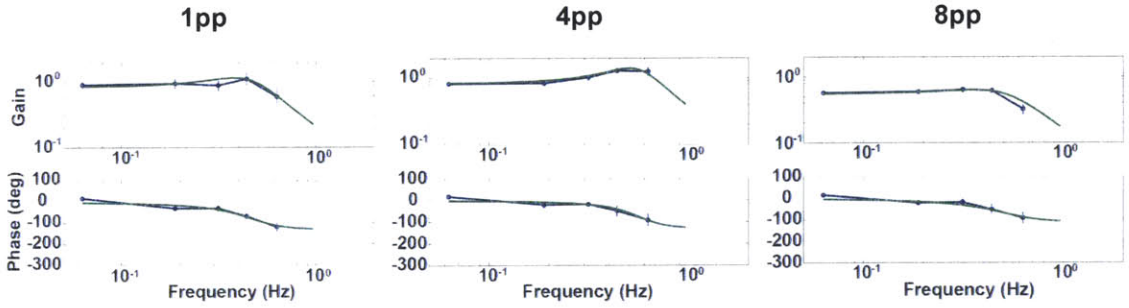

Figure 4.11 Model (green) and measured (blue) hindtrunk transfer functions with standard error bars for the mBVH sensory state.

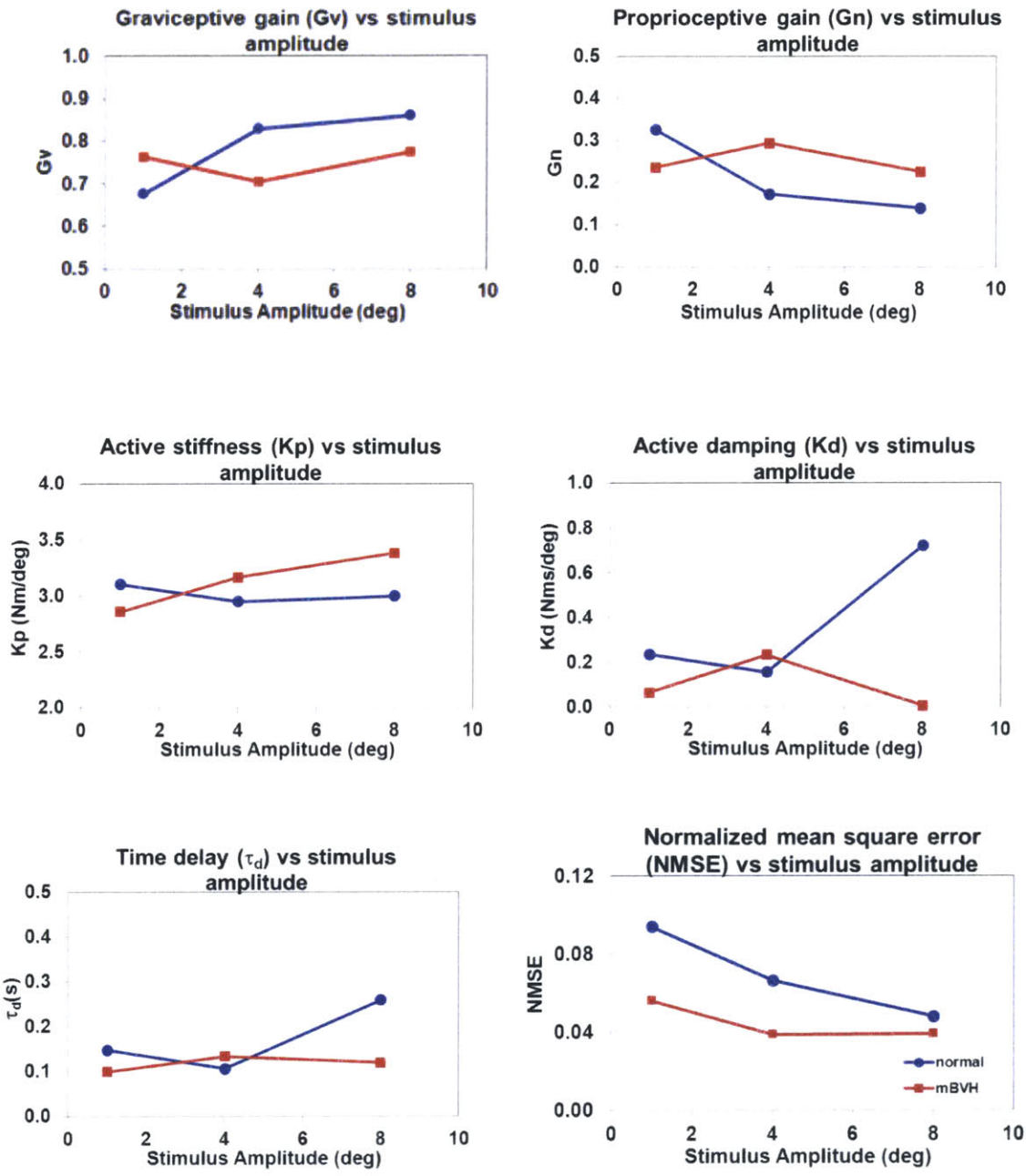

Figure 4.12 Non-simultaneous model parameter estimates and NMSE as a function of stimulus amplitude for the normal and mBVH sensory states.

Figure 4.12 shows the non-simultaneous model parameter estimates computed from the hindtrunk results measured at the 1, 4, and 8° pp stimulus amplitudes. They show that the animal in the normal state weighted graviceptive (e.g., vestibular) cues more heavily than proprioceptive cues at the larger stimulus amplitudes and that the animal in the mBVH state weighted proprioceptive cues more heavily than the graviceptive cues at the larger stimulus amplitudes. This was consistent with the stimulus-response (Figure 4.4) and transfer function (Figures 4.5 and 4.6) results that show that the normal animal oriented its hindtrunk more with earth-vertical than the support surface at the larger stimulus amplitudes, leading to sway saturation, and that the animal in the mBVH state oriented its hindtrunk more with the platform surface than earth-vertical at the higher stimulus amplitudes, leading to increased roll compared to normal. In the normal state, long-latency (neural controller) damping, Kd, increased for the largest stimulus amplitude, however, long-latency (neural controller) stiffness, Kp, showed little change across stimulus amplitudes. Increases in Kd are known to increase the stability of the system, reduce the overshoot, and improve the transient response (Ogata 2003). Here we deduced that the increase seen in Kd in the normal animal for the largest stimulus amplitude caused reduction in the (output) hindtrunk RMS roll (Figure 4.4) and frequency response gain (Figure 4.6). Time delay, τ_d, also increased for the largest stimulus amplitude, however, this may have been due to the correlation (R^2 = .9823) of Kd and τ_d within the model as opposed to physiologic changes in τ_d.

In the mBVH state, Kp increased with stimulus amplitude, whereas in the normal state Kp remained relatively constant. Peterka (2002) showed that some severe bilateral vestibular-loss human subjects had increases in long-latency (neural controller) stiffness

in comparison to normal test subjects and hypothesized that this could serve as a compensation mechanism. Increases in Kp are known to decrease the rise time but increase the overshoot of the response (Ogata 2003). Therefore, increases in stiffness without increases in damping could yield a more oscillatory response and increased gains (e.g., in the mBVH animal, Kp increased with stimulus amplitude).

Non-simultaneous model parameter estimation aided in: 1) development of the basic model, which includes the range of frequency points amenable to modeling and exclusion of intrinsic/short-latency mechanisms, 2) support the sensory reweighting hypothesis across stimulus amplitude, 3) lend insight into other possible neural changes that took place across stimulus amplitude and between sensory states, and 4) suggest that a model based on human postural control could be applied to the monkey to give meaningful insights into neural control

The "unconstrained" fits provided a simple model fitting routine for each test condition, however, for the normal and mBVH non-simultaneous model parameter estimates, non-monotonic changes seen in parameter values across stimulus amplitudes were unlikely physiologic in nature (but possibly due to the quality of the data, with only one test subject available). Therefore, to increase our confidence in the observed parameter trends, the most favorable option would be to test a larger number of subjects. However, for this set of experiments this option was not possible as there was only one test subject available. Instead, we explored the effects of introducing a more complex fitting routine in order to increase confidence in parameter estimates (i.e., constraining the basic model parameters across stimulus amplitude). For simultaneous model parameter estimation, we constrained specific model parameters across stimulus

amplitude, which allowed us to further analyze the model parameters as a function of sensory state and stimulus amplitude.

4.5.2.2 Simultaneous model parameter estimation: Constrained model parameters within the "basic model"

In the previous section, non-simultaneous model parameters were estimated for which the NMSE was computed and minimized separately for individual (1, 4, and 8° pp) stimulus amplitudes. In simultaneous model parameter estimation the error minimized was the sum of the normalized mean square error terms for all amplitudes combined (we call this "$NMSE_{sim}$" to differentiate from the "NMSE" described for the non-simultaneous model parameter estimations). As previously stated (Section 4.3.6), the normalized mean square error ($NMSE_{sim}$) was the sum of the errors for the 1, 4, and 8° pp stimulus amplitudes. The optimal model parameter estimates were determined for the 1, 4, and 8° pp stimulus amplitudes simultaneously by minimizing $NMSE_{sim}$. An advantage of simultaneous model fitting was that it allowed the investigation of the effects (in terms of $NMSE_{sim}$) of constraints placed on the free parameters within the basic model across stimulus amplitude.

Table 4.3 shows the constrained model variation number and description. For the first model variation, no parameters were constrained (the non-simultaneous case). However, for the second model, variation of time delay (τ_d) was constrained to be equal across the 1, 4, and 8° pp stimulus amplitudes, but the other basic parameters were unconstrained. Although the τ_d was constrained to be equal across the 1, 4, and 8° pp stimulus amplitude, the value of τ_d was determined along with the unconstrained model parameters within the optimization based on the minimized $NMSE_{sim}$ criterion. The other constrained model

variations within Table 4.3 followed a similar procedure that allowed estimates of the basic model parameters.

Table 4.3 Simultaneous model parameter estimation: constrained model variations

1	None
2	Time delay (τ_d)
3	Active damping (Kd)
4	Active stiffness (Kp)
5	Proprioceptive Weight (Gn)
6	Active damping (Kd) and time delay (τ_d)
7	Active stiffness(Kp) and time delay (τ_d)
8	Active stiffness(Kp), active damping (Kd), and time delay (τ_d)

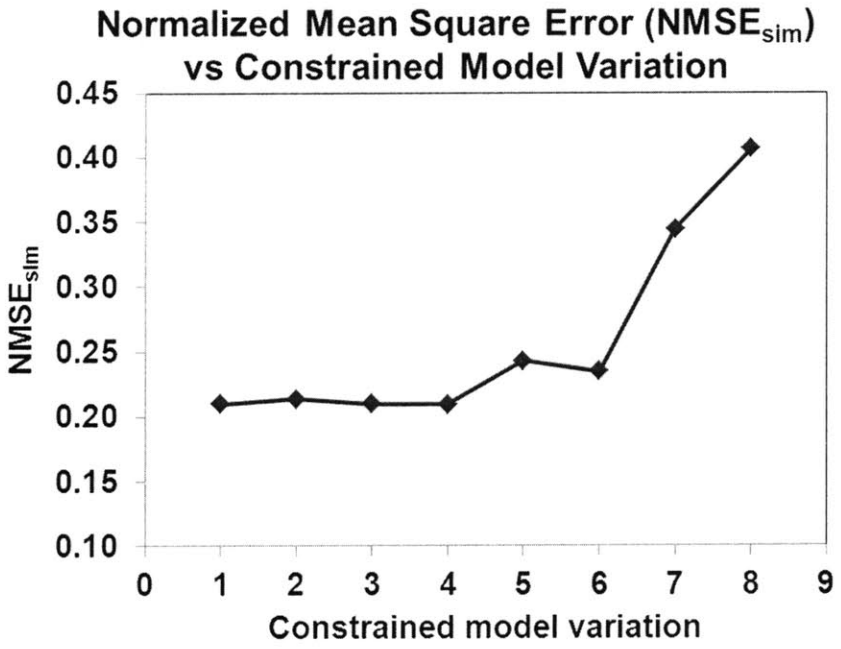

Figure 4.13 Normalized mean square error ($NMSE_{sim}$) for the normal state as a function of constrained model variation.

Figure 4.13 displays the $NMSE_{sim}$ as a function of the constrained model variation (described in Table 4.3) for the normal sensory state. When the individual model

parameters τ_d, Kd, and Kp were constrained across stimulus amplitude, there was little change in $NMSE_{sim}$, suggesting that allowing these parameters to vary added redundancy to the model and that the monkey did not actually modulate these neural parameters across changes in stimulus amplitude. However, when the sensory weight (Gn) was constrained (held constant) across stimulus amplitude (as in variation 5) there was an increase in $NMSE_{sim}$, for the normal sensory state (Figure 4.13), suggesting that changes in the sensory weight were critical for the model to describe the experimental data and that the nervous system may in fact primarily modulate the sensory weight across stimulus amplitude. **This result is consistent with sensory reweighting being present in the normal state.**

Can changes in sensory weight explain the all the changes seen in the 1, 4, and 8° pp normal measured transfer functions? In order to answer this question, we allowed only sensory weight, Gn, to vary across stimulus amplitude and constrained all other model parameters to be equal across stimulus amplitude. The largest $NMSE_{sim}$ was found in variation 8, where all parameters except Gn (i.e., Kp, Kd, and τ_d) were constrained across stimulus amplitude. This led us to conclude that other model parameters needed to vary across stimulus amplitude. In other words, at each stimulus amplitude, the measured transfer function data could not be fully explained by allowing only the sensory weight to vary.

To determine which additional parameter/s needed to be added to account for the experimental results, we systematically allowed the sensory weight plus one more parameter to vary. We observed that "Variation 4" was consistent with very minimal changes in Kp observed in the normal non-simultaneous (unconstrained) model

parameter estimate (Figure 4.12). By constraining Kp, the number of parameters that were allowed to vary were reduced with minimal impact on $NMSE_{sim}$ (Figure 4.13). By constraining parameters that were not changing a large amount across stimulus amplitude, our confidence in changes seen across stimulus amplitude in the remaining model parameters increased.

Figures 4.14 and 4.15 show the model fits for variation 4 and Figure 4.16 shows the model parameter changes across stimulus amplitude, as well as sensory state.

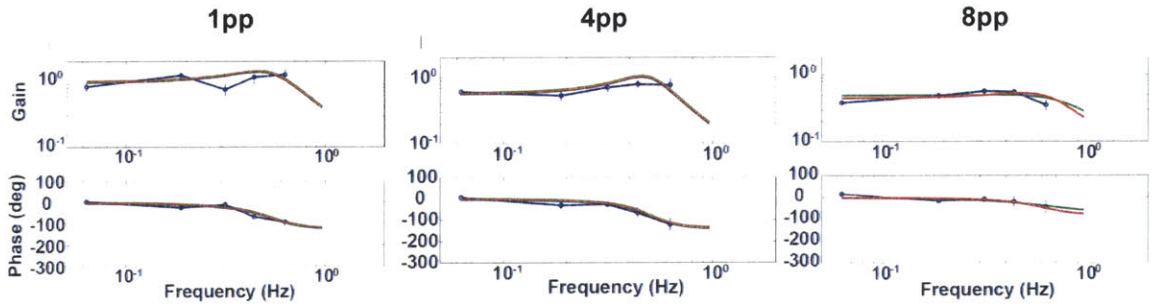

Figure 4.14 Unconstrained, or non-simultaneous case (green), constrained variation 4 (red), and measured (blue) transfer functions with standard error bars for the normal sensory state.

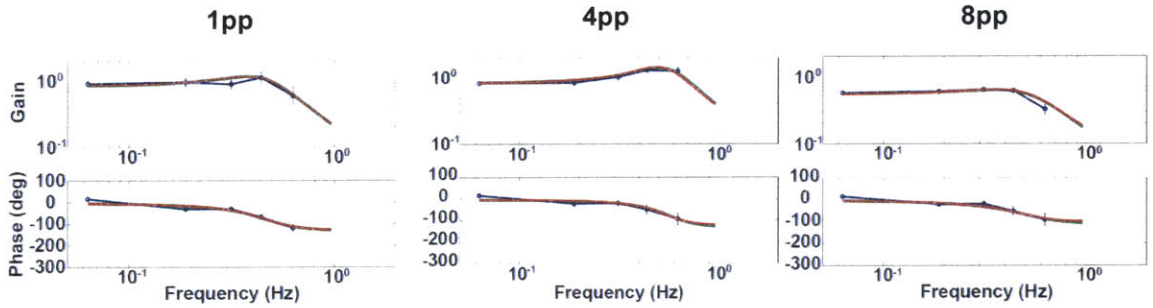

Figure 4.15 Unconstrained, or non-simultaneous case (green), constrained variation 4 (red), and measured (blue) transfer functions with standard error bars for the mBVH sensory state.

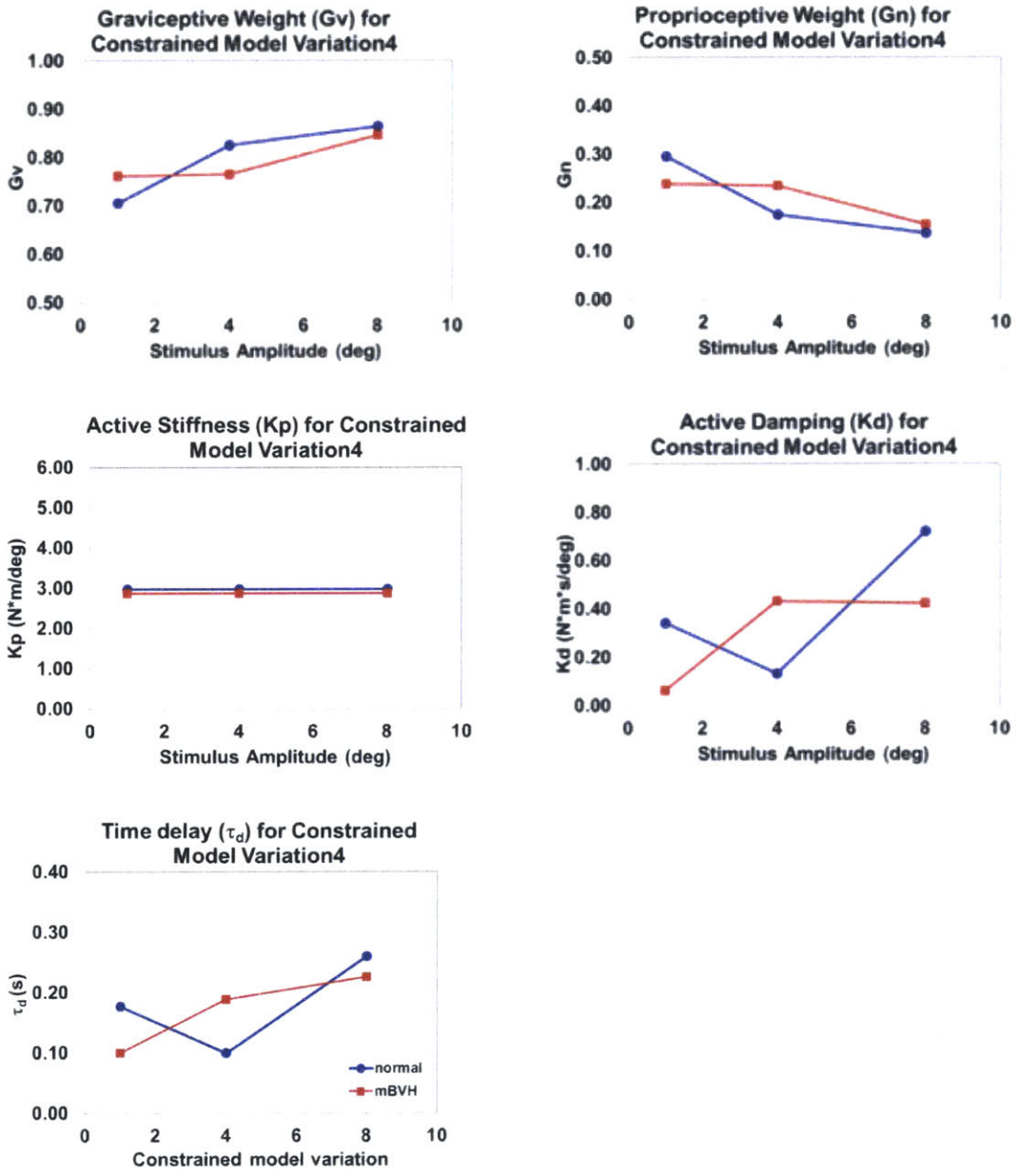

Figure 4.16 Normal and mBVH model parameter estimates computed using the simultaneous procedure as a function of stimulus amplitude for constrained model variation 4.

Because the non-simultaneous model parameter estimation did not predict large changes in normal Kp (Figure 4.12) and the simultaneous model parameter estimation did not show large changes in $NMSE_{sim}$ (Figure 4.13), we investigated constrained variation 4 further (model-predicted transfer functions are shown in Figures 4.14 and 4.15 and model parameter estimates are shown in Figure 4.16). As in the case where model parameters were unconstrained across stimulus amplitude (i.e., the non-simultaneous model parameters shown in Figure 4.12), Kd and τ_d were correlated in constrained variation 4 and still increased for the largest stimulus amplitude. The non-montonic changes in these parameters are likely due to some level of redundancy between them (as evidenced by their correlation) which our model could not tease apart, even using more complex fitting methods. Nonetheless, the constrained variation 4, with fewer model parameters allowed to vary across stimulus amplitude, further supported the sensory reweighting hypothesis in that graviceptive weight increased with increasing stimulus amplitude for the normal and mildly-impaired animal.

4.5.2.3 Simultaneous Model Parameter Estimation: Identification of differences in neural feedback between normal and mBVH states

In both types of fitting routines (unconstrained and constrained), sensory weights indicated that the graviceptive contribution in the mildly-impaired state was slightly higher at the lowest stimulus amplitude and lower at the two higher stimulus amplitudes. To further understand the graviceptive weight at each stimulus amplitude, we used the constrained model variation 4 to isolate and investigate the effects of sensory reweighting in the mBVH state while fixing other parameter values to those determined for the normal state.

Figure 4.17 shows the transfer functions computed from the measured hindtrunk data and from the model prediction based on the "mBVH w/normvals1" model configuration. For this model configuration, the mBVH measured data were estimated by the model with: 1) the normal constrained variation 4 value for Kp, 2) the model parameters Kd and τ_d that were set equal to the normal parameter values for the 1, 4, and 8^o pp stimulus amplitudes, and 3) sensory weight, Gn, that was allowed to vary across stimulus amplitude. Figure 4.18 shows the "mBVH w/normvals2" model configuration. For this model configuration the mBVH measured data was estimated by the model with: 1) the normal constrainced variation 4 value for Kp, 2) the model parameter τ_d that was set equal to the normal parameter for the 1, 4, and 8^o pp stimulus amplitude and 3) Gn and Kd allowed to vary across stimulus amplitude.

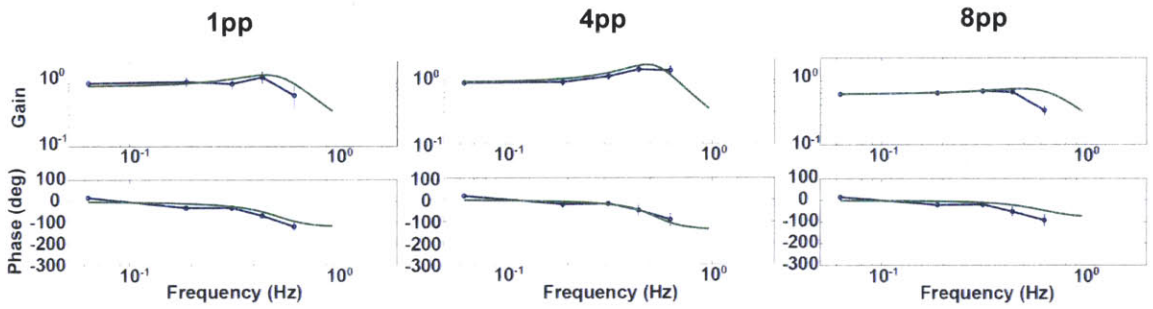

Figure 4.17 "mBVH w/normvals 1" model transfer function (green) and mBVH measured transfer function (blue) with standard error bars.

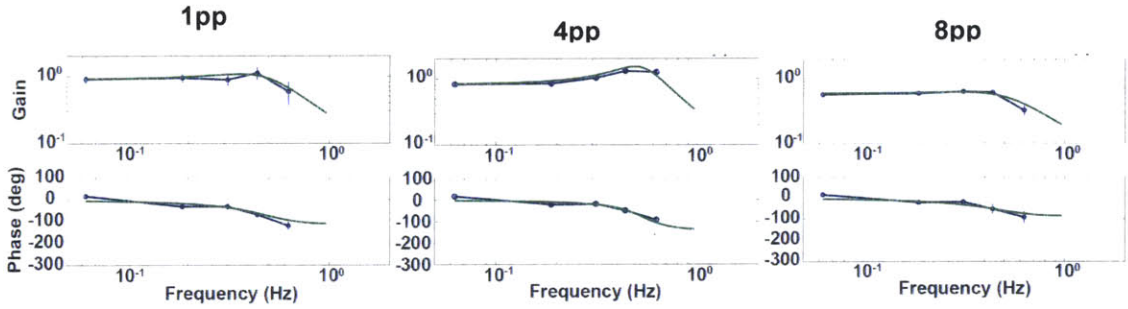

Figure 4.18 "mBVH w/normvals 2" model transfer function (green) and mBVH measured transfer function (blue) with standard error bars.

In comparing normal and mBVH configurations (described above), the sensory reweighting hypothesis was further confirmed. Figure 4.19 shows an overlay plot of the proprioceptive weight (Gn) and graviceptive weight (Gv) for: the normal variation 4, the mBVH w/normvals1 model configuration, and the mBVH w/normvals2 model configuration. For an increase in stimulus amplitude, the normal configuration showed an increase in Gv (or orientation to earth-vertical), and as a consequence decreased Gn (or orientation to the platform surface). Increased weighting of graviceptive cues, enabling the normal animal to saturate its response at larger stimulus amplitudes, is consistent with both the stimulus-response and transfer function results shown in Figures 4.4 and 4.6, respectively. However, for both mBVH model configurations, Gv weighting (or orientation to earth-vertical) decreased with increasing stimulus amplitude, and as a consequence of this, reliance on Gn (or orientation to the platform surface) increased. With mild vestibular impairment, it is not surprising that the mBVH state showed a decreased reliance on graviceptive cues relative to normal. However, the animal in the mBVH state exhibited increased weighting of Gv for increased stimulus amplitude, but the magnitude of this sensory reweighting as not a strong as in the normal state.

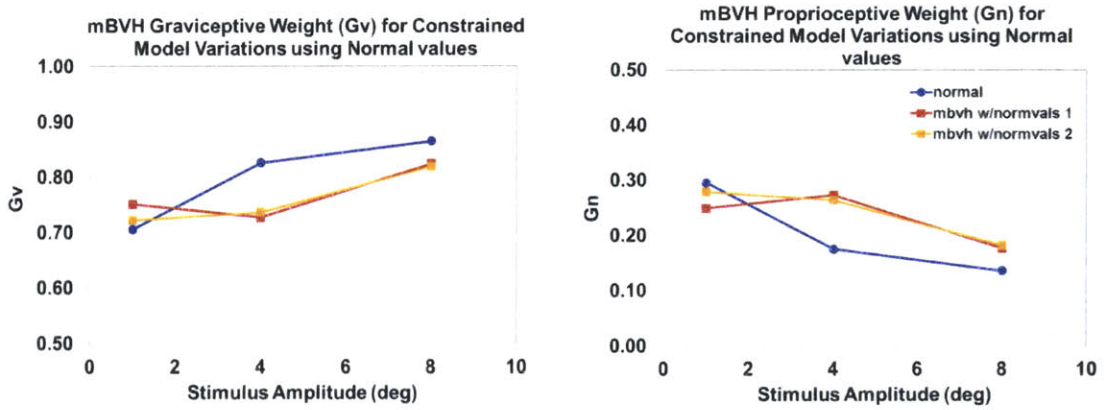

Figure 4.19 Three model configurations to estimate the graviceptive (Gv) and proprioceptive (Gn) weight as a function of stimulus amplitude. Normal model configuration with constrained Kp (blue), "mBVH w/normvals 1" model configuration with normal constrained value of Kp, and normal values for Kd, and τd at each amplitude (yellow), "mBVH w/normvals 2" model configuration constrained value of Kp, and normal value at each amplitude for τd (red). All illustrate clear reductions in graviceptive weight at higher stimulus amplitudes.

4.5.2.4 Time-domain model validation

In this chapter, we have almost exclusively discussed results in the frequency domain (e.g., measured transfer functions and model-predicted transfer functions). However, to illustrate how the model used above accounts for time-domain behavior, this section displays the model–predicted results in the form of a time-domain trace.

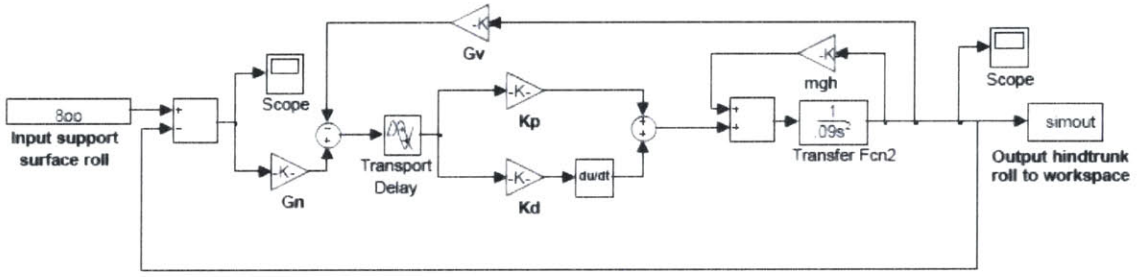

Figure 4.20 Simulink model schematic used for transfer function model validation.

The model (schematic shown in Figure 4.20) was built in Simulink (MATLAB, MathWorks, Natick, MA, version 2008b) and was used in conjunction with model

parameters derived from non-simultaneous model parameter estimation described above. The input to the model was the PRTS platform roll for the 8° pp stimulus. The model output was the simulated hindtrunk roll.

The simulated hindtrunk roll and (normal) measured hindtrunk roll are plotted in Figure 4.21. Since only the low frequency portion of the transfer function was used to estimate the model parameters, it is not surprising that the model predications are consistent with the overall shape of the measured data but do not capture the higher frequency components.

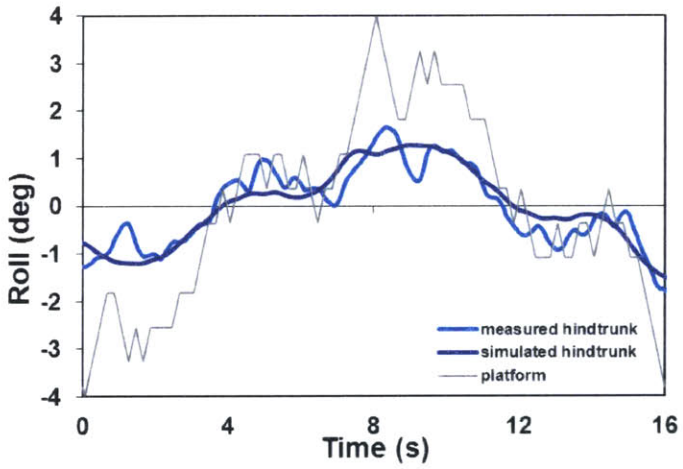

Figure 4.21 Model validation (e.g. normal 8°pp) of results.

4.5.3 Comparison to human work

The hindtrunk roll measured in the normal monkey as a function of stimulus amplitude (Figure 4.22) shows similar saturation to the COM sway measured in normal humans (Peterka 2002). The mBVH response curve also demonstrates sway saturation and is very different than the linear response curves measured in the humans with severe bilateral vestibular-loss.

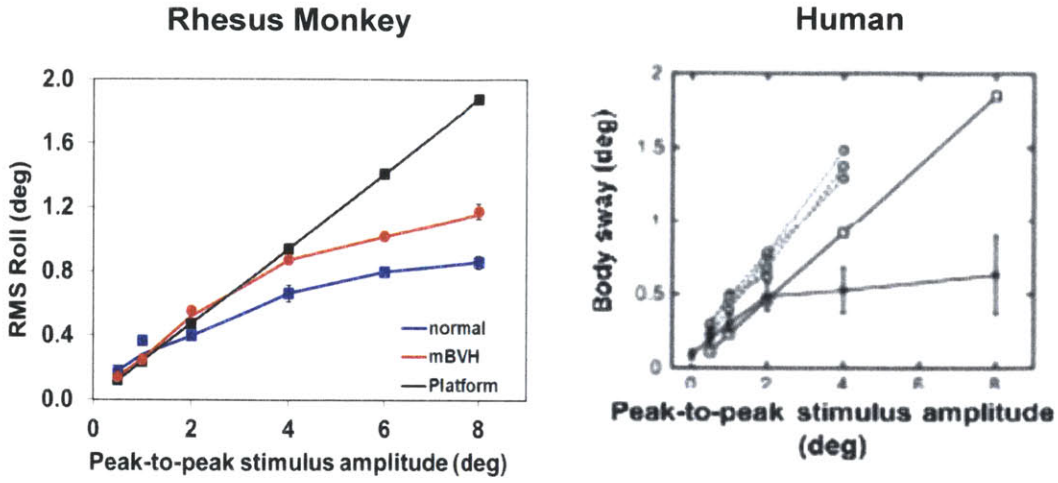

Figure 4.22 Human COM body sway as a function of stimulus amplitude (right) from Peterka (2002) for eyes-closed, support surface stimulus (Normal = closed circles, severe bilateral vestibular loss = open circles, platform = open square). Rhesus monkey hindtrunk roll (left) as a function of stimulus amplitude.

Figure 4.23 shows that sway saturation was seen for both the monkey and the human in that the rhesus hindtrunk and human COM gains decreased as stimulus amplitude increased (i.e., orientation with earth-vertical as opposed to platform surface). For stimulus amplitudes that were < 4° pp in the normal human, gains were usually > 1 between 0.1 and 1 Hz (Peterka 2002). In contrast, the normal rhesus monkey hindtrunk gains generally not > 1 except for the 1 and 2° pp stimulus amplitudes. As in humans, the rhesus hindtrunk showed increasing phase lag with increasing frequency and also decreased coherence with increased frequency.

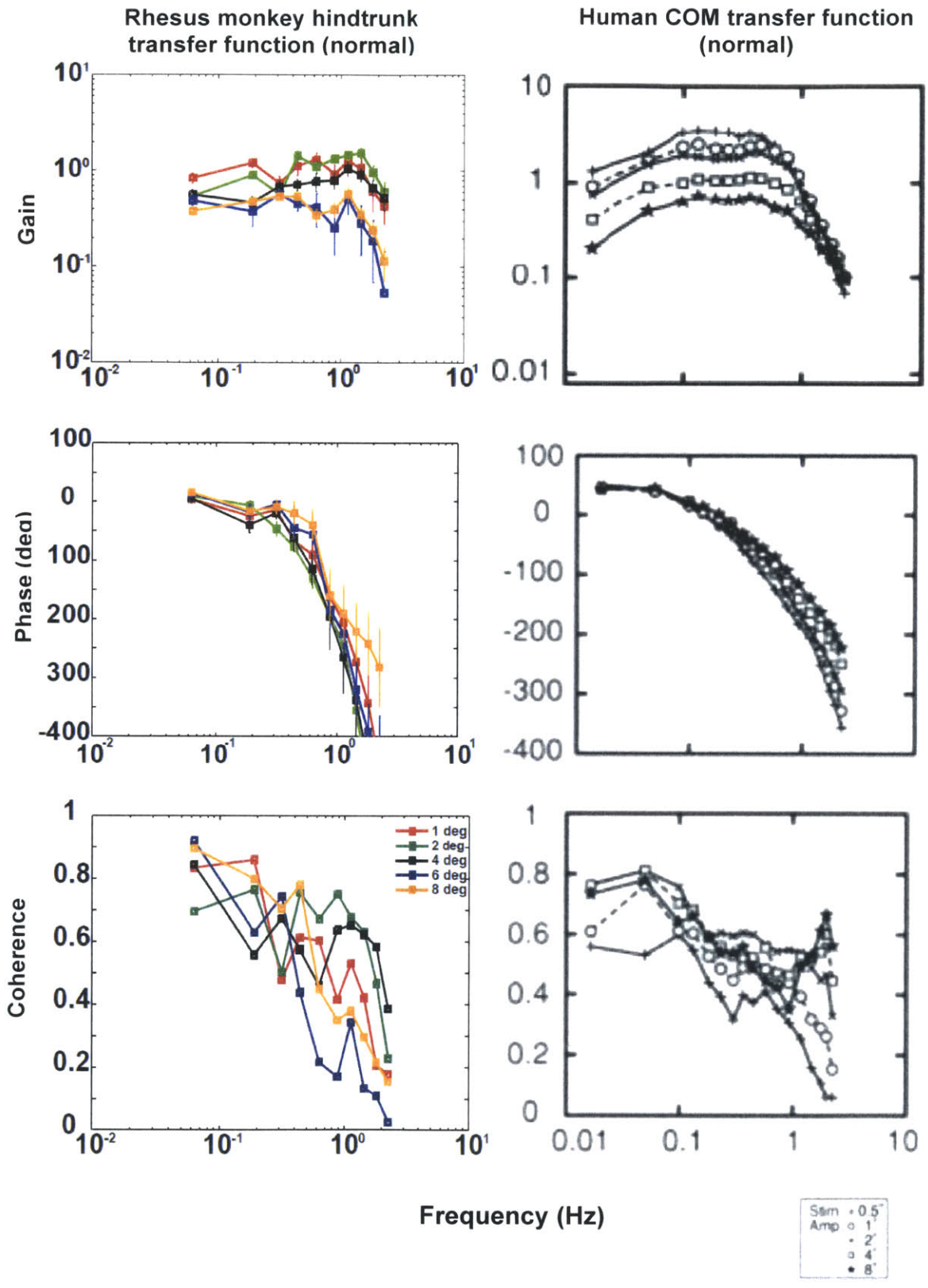

Figure 4.23 Normal rhesus hindtrunk transfer function with standard error bars (left) and normalhuman COM transfer functions (right) from Peterka (2002).

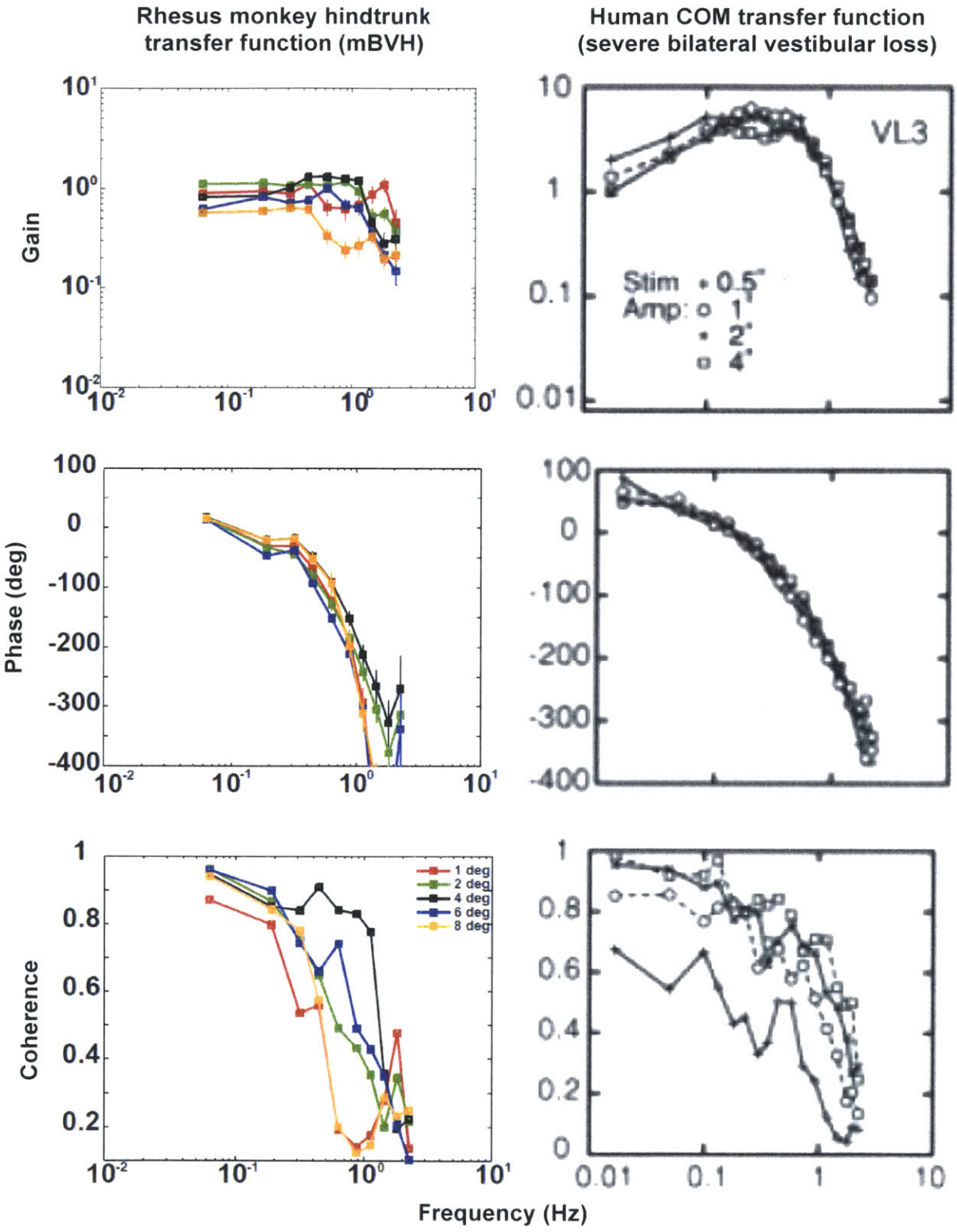

Figure 4.24 Mild bilateral vestibular-loss (mBVH) rhesus hindtrunk transfer function with standard error bars (left) and severe bilateral vestibular-loss human COM transfer function (right) from Peterka (2002).

Figure 4.24 shows that sway saturation was present in the mBVH state of the monkey, however, for the severe bilateral vestibular-loss human there was no sway saturation present and gain functions remained the same regardless of stimulus amplitude. Furthermore, gains in the severe vestibular-loss humans were much > 1 which indicated that the human COM tilt was greater than that of the platform tilt (e.g., as much as 5 times greater). In contrast, the monkey in the mBVH state had hindtrunk gains that were approximately <, or equal to, 1 for any stimulus amplitude. This greater stability of the monkey was potentially due to: 1) the animal was in its natural quadrupedal stance which allowed for a relatively larger base-of-support and lower COM than the bipedal human and 2) the rhesus monkey had only mild vestibular dysfunction and thus the ability to use graviceptive (e.g., vestibular) cues was still present.

Normal rhesus monkey hindtrunk model results for sensory weights were comparable to those seen in normal humans (Figure 4.25). The rhesus monkey hindtrunk proprioceptive weight was ~ 0.34 for the lowest stimulus amplitude and then decreased to ~ 0.15 at the higher amplitudes, and consequently the graviceptive gains increased as stimulus amplitude increased. For the human, there were similar trends in that proprioceptive weightings decreased for an increase in stimulus amplitude, and as such, graviceptive gains increased as stimulus amplitude increased.

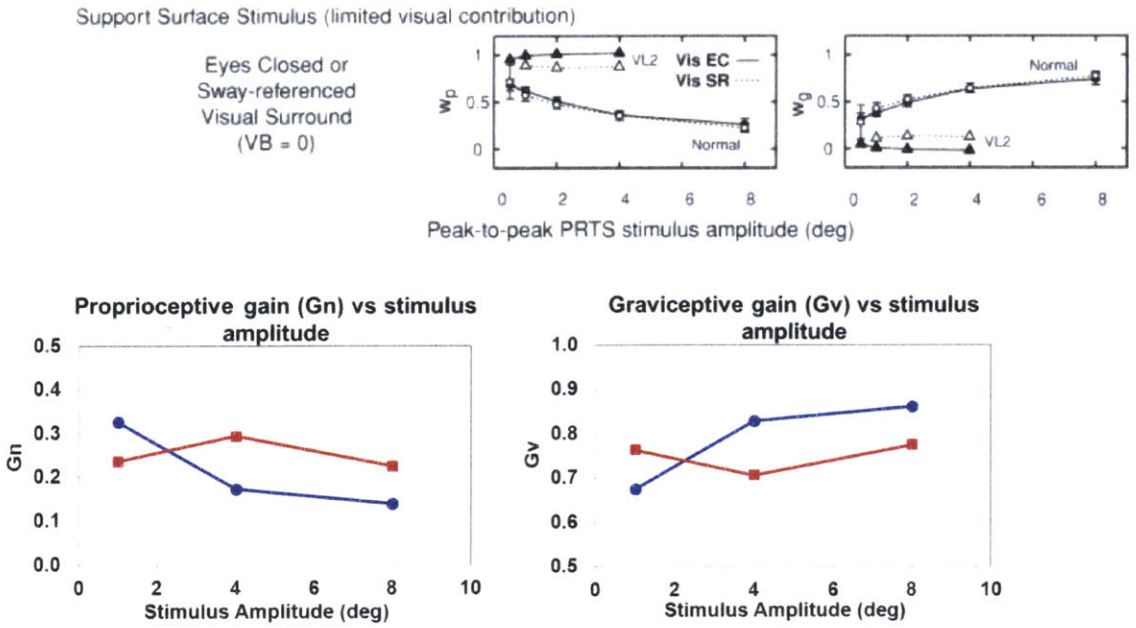

Figure 4.25 Model derived normal and severe bilateral vestibular-loss human sensory weights from Peterka (2002) with proprioceptive weight, Wp, and graviceptive weight, Wg (top). Mild bilateral vestibular-loss (mBVH) rhesus hindtrunk sensory weights from non-simultaneous model fits (bottom) for normal (blue) and mBVH (red).

The rhesus monkey results for the mBVH state showed that for the higher stimulus amplitudes, proprioceptive gains were weighted more than in the normal state. However, since the animal was only mildly impaired, sway saturation was still seen in the stimulus-response curves and transfer function results. Furthermore, the model results in the previous section showed that the monkey was still able to make use of some of its graviceptive (e.g., vestibular) cues though to a lesser extent than normal. For the severe bilateral vestibular-loss human, proprioceptive weights were ~ 1 and gravipcetive weights ~ 0 across stimulus amplitude. This stronger weighting of proprioceptive cues in the humans with severe bilateral vestibular-loss is consistent with their transfer function gains being much higher than the hindtrunk gains seen in the mild vestibular-loss rhesus monkey (Figure 4.24). Differences in levels of vestibular impairment were a likely source of the differences in the impaired humans and monkey results shown in Figure

4.25. Other potential sources include anatomical differences (e.g. rhesus monkey is a habitual quadruped and therefore has a relatively greater base-of-support than the bipedal human and more inherent stability).

4.5.4 Future work

The goal of the models used in this paper was to adapt and build on models previously applied to human posture while identifying the simplest model that still was able to capture the characteristics (via physiologic model parameter estimates) of rhesus monkey posture. Thus, while multiple segments and links allow for more complex motions and analysis of joint torques, they also lead to higher model complexity and often more model parameters. Given the apparent redundancy in certain model parameters already present in our simple single-link model, a future multi-link model will need to include higher resolution and more experimental data to reliable estimate a more complex model. Thus, the application of the single-link inverted pendulum analysis to a single monkey served as an appropriate first ever approach to modeling rhesus monkey posture in two different sensory states.

4.6 Conclusions

Through characterization of stimulus-response curves, transfer function analysis and modeling techniques, we found evidence that the animal in both the normal and mBVH sensory states exhibited forms of sensory reweighting in that graviceptive sensory cues were used to a greater extend with increasing stimulus amplitude while proprioceptive cues were used to a lesser extend with increasing stimulus amplitude. The normal animal's stimulus-response curve revealed saturating nonlinear increase in hindtrunk roll for an increase in stimulus amplitude (sway saturation). Transfer functions

showed that as stimulus amplitude increased, hindtrunk gains increased for the animal in the mBVH state (i.e., the vestibular-lesioned animal oriented more with the platform) than the normal animal that had decreased gains with increased stimulus amplitude (i.e., the normal animal oriented more with earth-vertical). These results were used in conjunction with a model to test the sensory reweighting hypothesis (i.e., increased weighting of gravipceptive cues for increases in stimulus amplitude). Parameter optimization based on normal and mBVH hindtrunk measured transfer functions led to model estimated parameters that were consistent with increased graviceptive sensory weighting (orientation to earth-vertical) for an increase in stimulus amplitude in both sensory states. Consistent with the mild vestibular impairment, the mBVH model predicted less sensory reweighting than in the normal state.

---

[1]Chapter II (Section 2.4.2) addresses animal training.
[2]Chapter II (Section 2.5.4) justifies the logic behind the outlier criteria used.

V. Stabilization by light-touch in vestibular loss rhesus monkeys

5.1 Abstract

Rhesus monkeys with vestibular dysfunction were provided an external sensory cue: light-touch to the tongue, mouth, and lips (via an earth-mounted juice reward dispenser). In order study the effects of the level of vestibular dysfunction on the animal's ability to make use of the light-touch cue, one rhesus monkey, R2, was studied in a state of mild bilateral vestibular hypofunction (mBVH) and the other, R1, in a state of severe bilateral vestibular hypofunction (sBVH). Two juice reward configurations were used in this study: 1) an earth-mounted (EM) juice reward configuration that provided a light-touch cue and a stationary reference, and 2) a head-mounted (HM) juice reward configuration in which the head was free to move and the stationary reference was unavailable. The quiet-stance test conditions used allowed for alteration of stance width as well as support surface cues. In comparing trunk sway from the HM and EM configurations, R1 in the sBVH state had greater benefit (observed as a greater reduction in trunk sway) from the EM light-touch cue than R2 in the mBVH state.

5.2 Introduction

It is well known that inputs to the visual, somatosensory, and vestibular systems combine through sensory integration to form an output postural response (e.g., Horak and Macpherson 1996). Subcutaneous touch and pressure receptors can be used to inform subjects of their position with respect to an external reference. For example, pressure receptors are stimulated in the feet when standing on a support surface or stimulated in the fingertip when touching a stationary object. In this study, we focused on varying

inputs to the animals' somatosensory systems (e.g., through altering footplate cues and light-touch cues) for mild and severe bilateral vestibular-impaired monkeys.

Stabilization of posture by a light-touch (< 1 N) has been previously investigated in both normal (Lackner et al. 2001) and severe bilateral vestibular-loss humans (Lackner et al. 1999). In the normal standing human, the index finger was lightly touching a stationary surface that allowed them to derive the information necessary to stabilize their body sway. Although having a stationary spatial reference (e.g., flat surface) was found to be the most effective in attenuating postural sway, light fingertip contact with various surfaces (e.g., both bendable and rigid filaments, or even an imagined spatial position) led to significantly decreased center-of-pressure (COP) sway. Fingertip contact was far below that to provide mechanical support (< 65 g and often as low as 5-10 g) and subjects spontaneously adopted a force level of ~ 0.4 N (~ 40 g). This force level was within the maximal dynamic sensitivity of somatosensory receptors in the fingertip (Johnasson and Magnusson 1991). Because the fingertip has rich sensory innervation, it is very responsive to deformation of its surface (i.e., displacement detection thresholds at the fingertip are around 1 mm). Therefore, in normal humans, sensory information from light fingertip touch has proven sufficient to allow for postural orientation.

The effects of light fingertip touch were also previously investigated in bilateral vestibular-loss humans (Lackner et al. 1999). They explored whether vestibular-loss human subjects could substitute contact cues (in place of the missing vestibular information) from the fingertip to balance in darkness. Bilateral vestibular-loss subjects were unable to stand without falling in the dark with no fingertip contact, but bilateral vestibular-loss subjects were significantly more stable in the dark with light-touch.

In addition to fingertip touch, studies that utilized the tongue to provide sensory information used for postural orientation have also been implemented. The tongue is densely innervated and has a large somatosensory cortical representation (Picard and Olivier 1983). In subjects with normal vestibular function, information about head orientation is sensed by the vestibular system. However, in those patients with vestibular dysfunction, one form of sensory substitution used to derive head position is electro-tactile stimulation of the (densely innervated) tongue (e.g., Bach-y-Rita and Kercel 2003; Vuillerme et al. 2011). For a vestibular-loss subject, the missing vestibular information that is replaced by a sensory substitute can lead to a more accurate estimation of body orientation needed for balance than if no sensory substitute were provided. This chapter addresses whether a simple light-touch cue to the mouth and lips of the rhesus monkeys with vestibular dysfunction can attenuate body sway.

We hypothesize that a rhesus monkey with severe vestibular-loss can utilize light-touch, via the mouth (i.e., tongue, lips, etc.), to attenuate its body sway in quiet-stance. Furthermore, we hypothesize that the severe vestibular-loss animal can stabilize itself using light-touch for quiet-stance conditions with both limited visual and support surface cues (a test condition that has previously proven difficult for human bilateral vestibular-loss subjects (Horak et al. 1990)).

5.3 Methods

5.3.1 Sensory states

Experiments were conducted under the approval of the Massachusetts Eye and Ear Infirmary (MEEI) Institutional Animal Care Committee and were in accordance with USDA guidelines. For these sets of experiments, two adult female rhesus monkeys, R1

and R2, (R1: 7 yrs, 7.9 kg and R2: 5 yrs, 6.7 kg) were used. R1 was surgically implanted with a vestibular prosthesis (discussed in Chapter VI) that may have caused minor vestibular damage. Baseline measurements for R1 were made in this "control" state. R2 was not instrumented with the device, and baseline measurements were made in this "normal" state. The baseline sensory state (i.e., the control state of R1 and normal state of R2) of each rhesus monkey was characterized by measuring its angular vestibuloocular reflex (VOR) at discrete frequencies. The VOR is a simple eye movement reflex used reflecting semicircular canal function.

After characterizing the baseline sensory state for R1 and R2, each monkey underwent a series of ototoxic treatments. The purpose of these treatments was to target and kill the vestibular hair cells while preserving a functioning eighth nerve. Intratympanic gentamicin (IT gent) kills vestibular hair cells and has been used to treat vertigo in Meniere's patients (e.g. Minor 1999). Initial surgery was conducted under anesthesia (ketamine (10 mL/kg) pre anesthesia and isoflurane (2 - 5% saturation with oxygen gas)) and consisted of tympanic membrane perforation and gentamicin injection (40 mg/mL) in each ear. Maximum damage cause by the drug was estimated to be approximately 2 weeks post-administration (i.e., 1 cycle of IT gent treatment = administration, then a 2 week waiting period). For both animals, the gentamicin treatments were followed by intramuscular streptomycin (IM strep) treatments (350 mg/mL per day for 21 days x 2) that were injected to each animal's muscle.

Figure 5.1 shows plots of the percentage decrease in VOR gain relative to the baseline for monkeys R1 (left panel) and R2 (right panel). R1 underwent 3 cycles of IT gent treatments and 2 IM strep treatments that resulted in severe bilateral vestibular

hypofunction (sBVH) as can be seen in the relatively large decrease in VOR gain relative to the control state. R2 underwent 5 cycles of IT gent treatment and 2 IM strep treatments that resulted in mild bilateral vestibular hypofunction (mBVH) as reflected in the relatively small decrease in VOR gain relative to its normal state.

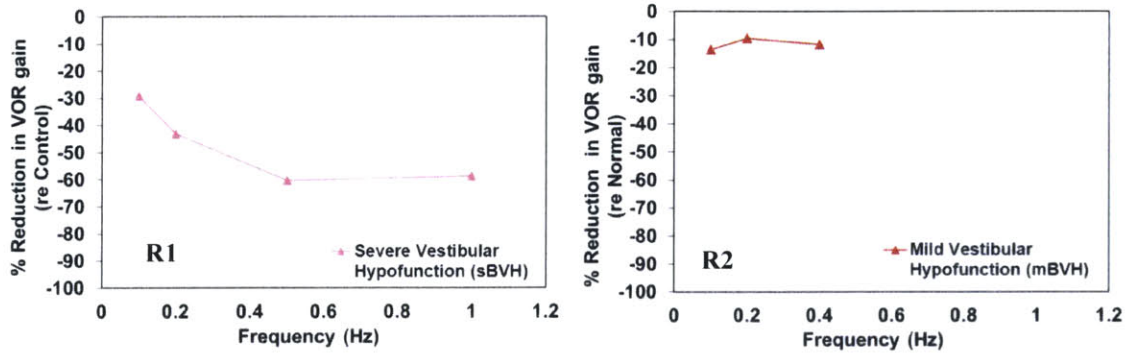

Figure 5.1 Reduction of VOR gain from baseline measurement as a function of frequency measured in R1 (left) and R2 (right).

5.3.2 Balance platform apparatus

The animal was trained by use of a juice reward system to stand free of human or mechanical restraint on the balance platform.[1] Figure 5.2 is a schematic illustrating the two different reward schemes used: an earth-mounted juice reward configuration (EM) wherein the animal's lips, mouth, and tongue made contact with a flexible, bendable tubing attached to a rod anchored to the ground (left) and a head-mounted juice reward configuration (HM) where the monkey had a juice tube clipped to its headcap and flexible tubing was routed to the monkey's mouth (right). The head-mounted reward system did not provide an earth-stationary reference cue and the monkey was able to freely move its head during the test session.

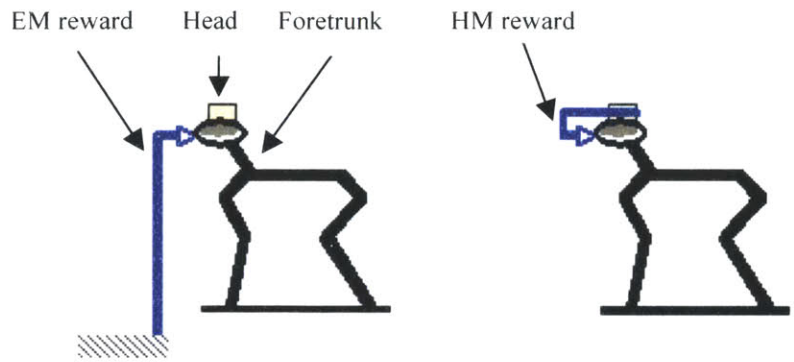

Figure 5.2 Earth-mounted (EM) reward configuration (left) and the head-mounted (HM) reward configuration (right).

The head and foretrunk body motion was measured using position sensors (miniBIRD, Ascension Technology Corporation, Milton, VT) sampled at 100Hz. In order to minimize visual cues, all test sessions were conducted in dim lighting with black tarp surround.

5.3.3 Quiet-stance training and testing

The monkey was trained to stand on the balance platform with each foot on the appropriate footplate to receive a juice reward. A more detailed description of animal training is provided in Chapter II (Section 2.4.2), and we will only discuss it briefly here. In order to motivate and encourage the rhesus monkey to stand on the platform, the animal was first trained to receive the reward from an EM juice dispenser. When the monkey was able to stand on the platform comfortably, the animal was trained using the HM dispenser. In order to maintain the animal's attention on the task, it was essential to provide a juice reward and hence a tubing configuration (i.e., either earth-mounted or head-mounted). Therefore, it was not possible to test the no dispenser condition.

By altering the footplate surface, platform somatosensory (i.e., footplate) cues

were varied. The gum rubber surface provided stronger and more reliable cues than the foam surface. Mediolateral stance width was varied to provide either a large base-of-support (wide stance) or small base-of-support (narrow stance). Four test conditions of varying levels of task difficulty were utilized (gum-wide, gum-narrow, foam-wide, and foam-narrow).

5.3.4 Data analysis

In a given test session, data was broken down into 15s trials. In order to remove the offset for a given trial, the mean was computed and was subtracted from each data point within the trial. The foretrunk RMS roll was then computed. Usable trials were defined as those sections in which the foretrunk RMS roll fell within specific movement criteria.[2] Table 5.1 shows the number of usable and unusable trials. All data analyses were conducted in MATLAB (MathWorks, Natick, MA).

Table 5.1 Number of usable and unusable data sections for R1 and R2.

	R1 in the sBVH state				R2 in the mBVH state			
	EM		HM		EM		HM	
	usable	*unusable*	usable	*unusable*	usable	*unusable*	usable	*unusable*
gum-wide	12	1	10	1	33	2	40	4
gum-narrow	15	4	15	4	19	2	53	6
foam-wide	13	1	13	2	24	1	27	6
foam-narrow	18	4	19	5	41	5	47	6

In regards to comparisons of the measured results, for the above analyses a student's t-test (assuming unequal variance, unequal sample size) was used to determine significance.

5.4 Results

The RMS roll measured for the quiet-stance test conditions are shown in Figure 5.3.

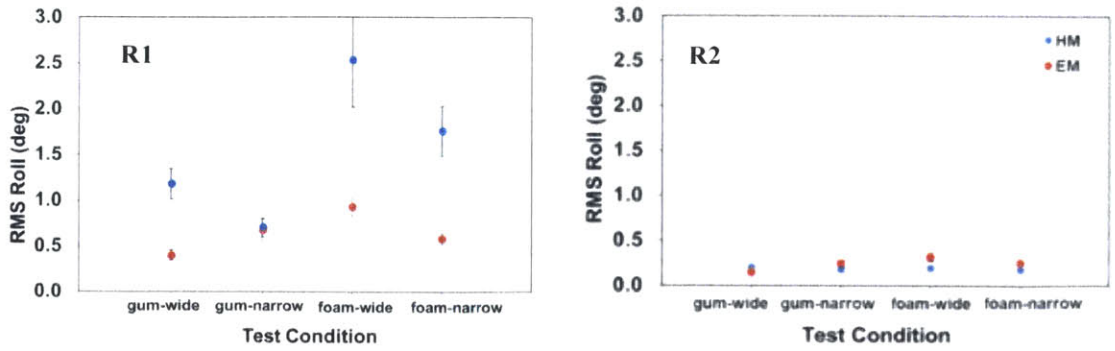

Figure 5.3 Foretrunk RMS roll with standard error bars as a function of quiet-stance test condition for R1 with severe bilateral vestibular-loss (sBVH) (left) and R2 with mild vestibular-loss (mBVH) (right) for earth-mounted (EM) and head-mounted (HM) dispensers.

R2 with mild vestibular-loss (Figure 5.3, right) showed no significant change for RMS roll between EM and HM configurations for the gum conditions, however, the RMS roll for the EM configuration in the wide and narrow foam conditions was significantly greater than the HM configuration ($df = 29$, $t = 3.01$, $p < 0.01$ and $df = 63$, $t = 2.95$, $p < 0.01$, respectively). We hypothesized that the small but significant increase in roll between HM and EM could be explained by the animal (R2) having to adjust its posture to attend to two tasks as opposed to one task (i.e., adjusting and changing its postural strategy to accomplish the goals of standing on the platform *and* keeping its mouth affixed to the juice reward (EM configuration) as opposed to just standing on the platform (HM configuration)).

In contrast, when comparing the EM and HM configurations for R1, the animal with a more severe vestibular impairment, the HM roll was significantly greater than the EM roll for three out of the four test conditions (e.g., $df = 11$, $t = 4.49$, $p < 0.001$ for the gum-wide and $df = 13$, $t = 3.04$, $p < 0.01$ for the foam-wide condition), showing that R1's sway decreased for the EM configuration where there was a light-touch, stationary reference cue provided.

When comparing the wide stance width to narrow stance width for both the gum and foam surface for the HM configuration, decreasing trends were seen. This was possibly due to the narrow stance width being more favorable to the animal in the HM configuration. This may explain why in the gum-narrow condition the roll for the HM configuration was not significantly different than the EM configuration.

5.5 Discussion

When provided a stationary, light-touch sensory cue (via an EM juice dispenser) the R1, in the sBVH state, demonstrated less RMS roll than when this cue was removed. However, when a light-touch cue was provided to R2 in the mBVH state, the differences in RMS roll between the EM and HM conditions were insignificant or changed only slightly. These findings imply that the severely-impaired animal, R1, achieved greater benefit from the external sensory (light-touch) cue and used that postural reference information to stabilize its trunk.

5.5.1 Mild versus severe vestibular loss

Since previous studies have only focused on the effects of providing light fingertip touch to normal and bilateral vestibular-loss humans (Lackner et al. 1999), there are no previous findings to compare the effects of light-touch in a mildly-impaired animal. Since a range of vestibular dysfunction exists clinically, it is important to know if subjects with mild vestibular impairment can benefit from using light-touch to stabilize themself.

The rhesus monkey, R1, in the severely impaired state was able to utilize lip, tongue, and mouth contact cues from the earth-mounted dispenser to orient its posture and reduce trunk sway (RMS roll) compared to the test configuration where it did not

receive these cues. This finding is consistent with previous findings that have shown that bilateral vestibular-loss humans are able to utilize light fingertip touch to provide stabilizing cues in darkness (Lackner et al. 1999) and that without light-touch humans with severe vestibular-loss were more unsteady. For three out of the four quiet-stance test conditions (i.e., gum-wide, foam-wide, and foam-narrow), the sBVH animal showed increased sway for the HM configuration in comparison to the light-touch EM configuration. This result showed that an animal with severe vestibular-loss can make use of external somatosensory contact cues (via the mouth), for even the most difficult quiet-stance test condition (foam-narrow).

R2 in the mBVH state showed only a small change in sway between the HM and EM configurations. This result was surprising given that even normal humans (with no vestibular dysfunction) were able to reduce their body sway when provided light fingertip touch (Lackner et al. 2001). Other results within this thesis (e.g., Chapter III) have shown that R2 in the mBVH state may have co-contracted its muscles to compensate for its vestibular loss, and thus, there was decreased sway compared to normal even in the more difficult (foam) conditions. We hypothesize that the animal was using a similar strategy here (i.e., muscle stiffening or co-contraction) as a mode of compensation for its mild vestibular lesion for both the EM and HM configurations and thus the added "benefit" of the additional light-touch contact cue provided was not used and therefore made little difference in terms of stability (i.e., the co-contraction strategy was a sufficient postural compensation mechanism to stabilize the animal).

For both HM and EM configurations and for all quiet-stance conditions, R2's sway was less than R1's. Because R2's sway magnitude was much smaller than R1's,

one hypothesis we propose is that R2 simply "out-performed" R1. More specifically, R2 may have already hit a performance plateau in that R2 simply had better balance compared to R1 and so it could not get any better (or more stable) with when provided an additional sensory cue.

Even in humans with intact vestibular function, there are still intersubject differences (e.g., age (Prieto et al. 1996; Cenciarini et al. 2010), different levels of experience (Horak and Macpherson 1996), and also body-type) can lead to different postural strategies and different levels of performance. Prieto et al. (1996) showed that elderly human adults have increased sway compared to young human adults. In our study, R1 was older (~ 7 yrs old) compared to R2 (~ 5 yrs old). Although there was about 2 years age difference between the two animals, both were considered young adults and therefore increased sway seen in R1 due to age-related effects may be possible but is unlikely. Another potential cause of differences between the two animals is level of experience. However, since both animals were trained using similar methodology, it is unlikely that experience level caused the discrepancies seen in sway between the two animals. Size and build of each animal was a likely source of intersubject differences. R1 was larger in size and weighed more than R2 (R1: 7.9 kg and R2: 6.7 kg). The differences in size and weight of the two animal's could have likely led to each animal using a different postural strategy to balance on the platform. R2 weighed less and was shorter in height than R1. Because R2 had a lower center-of-mass $(COM)^3$ height relative to the balance platform surface and weighed less than R1, it was inherently more stable. Furthermore, for a given goal or set of goals there are multiple postural strategies to

achieve them because the musculoskeletal system has more degrees of freedom than are necessary to achieve a specific task or goal.

In order to determine the (posture) effects of varied levels of vestibular function on an animal's ability to make use of light-touch cues, future work should attempt to limit intersubject variability as much as possible (i.e., utilize animals of similar age and size). Furthermore, testing a larger number of subjects would only further enhance our knowledge on the effects of vestibular dysfunction on posture while animals are receiving a light-touch cue.

5.6 Conclusion

This chapter showed that an animal, R1, with severe vestibular-loss can utilize non-vestibular cues (e.g., light-touch via the lips, tongue, and mouth) to provide orientation information that improves postural stability and reduces trunk sway. This improved stability was measured in conditions of weak visual cues, a condition shown to destabilize humans with severe bilateral vestibular-loss. When provided with a light-touch cue, a mildly-impaired animal, R2, did not decrease its trunk sway when provided the light-touch cue. We hypothesize that is due to R2 compensating for the mild impairment with increased muscle stiffening and that the resulting stability led to the light-touch cue being either ignored or not making a substantial difference when integrated by the animal's postural control system.

---

[1]Chapter II (Section 2.4.2) addresses animal training.
[2]Chapter II (Section 2.5.4) justifies the logic behind the outlier criteria used.
[3]Chapter I (Section 1.4.4) describes posture nomenclature (e.g., base-of-support, center-of-pressure, and center-of-mass).

VI. The postural sway evoked by head-turns in a severely vestibular-impaired rhesus monkey utilizing a semicircular canal prosthesis

6.1 Abstract

A rhesus monkey's posture in response to head-turns was measured in a severe bilateral vestibular hypofunction (sBVH) sensory state and also in a severe vestibular hypofunction state aided by prosthetic stimulation (sBVH + STIM-ON). We show that the prosthetic electrical stimulation (supplied by a prototype invasive vestibular prosthesis) in a severe vestibular-loss animal decreased trunk sway. We propose that the partially restored head velocity cues provided by the prosthesis could be integrated by the central nervous system (CNS) to allow the severely-impaired animal a more accurate estimate of head orientation. Furthermore, we hypothesized that this more accurate estimate of head orientation (in the sBVH + STIM-ON state) combined with neck proprioceptive information to provide the severely-impaired animal a more accurate estimate of trunk position.

6.2 Introduction

Vestibular loss can arise due to congenital anomalies, genetic diseases, exposure to ototoxic drugs, age-related hair cell degeneration, and other idiopathic causes. People suffering from severe vestibular dysfunction experience equilibrium disorders that can cause unsteady balance in daily activities such as walking in dim lighting or on uneven surfaces, bending to pick something up, or the simple task of turning one's head. Although some patients may develop compensatory strategies over time, vestibular-loss sufferers that are unable to do so are left with limited treatment options and can become

permanently debilitated. For those severe vestibular-loss subjects with intact eighth nerve function, an invasive vestibular prosthesis aimed at restoring vestibular function holds great potential as a possible rehabilitative solution.

Vestibular prostheses excite the neurons of the vestibular system and are aimed at restoring vestibular function. The vestibular system responds to head movements that are both angular (via the semicircular canals) and linear (via the otolith organs). Although a prosthesis that restores full vestibular function (i.e., to both the otoliths and the semicircular canals) would be ideal, this technology is not yet feasible. Directing electrical stimulation to the otoliths is hindered by the opposing polarities of the otolith hair cells, however each of the semicircular canals has uniform directional sensitivity that makes electrical stimulation more feasible. Past and current investigations have involved the development of semicircular canal prostheses aimed at restoring rotational cues. Although the semicircular canal prostheses transduced head velocity, there has been considerable evidence that canal cues can be used in conjunction with otolith cues to estimate head orientation relative to gravity (e.g. Angelaki et al. 1999; Merfeld et al. 1999).

Previous vestibular prosthesis studies have focused on eye movement responses of animals such as guinea pig (e.g., Gong and Merfeld 2002), chinchilla (e.g., Fridman et al. 2010), squirrel monkeys (e.g., Lewis et al. 2010; Merfeld et al. 2007) and rhesus monkeys (e.g., Dai et al. 2011) and have shown that the prosthesis can partially restore the vestibuloocular reflex (VOR) to subjects with severe vestibular loss. Although prosthetic vestibular stimulation has been extensively characterized in terms of eye

movements, postural responses have not been rigorously investigated in either animals or humans.

Although posture resulting from implementation of vestibular prostheses has not been fully characterized, it has been shown that electrical stimulation (of the vestibular afferents) can affect human posture. Galvanic vestibular stimulation (GVS), a simple method that allows for probing of the posture effects by altering the vestibular signal, has been studied in humans (e.g., Fitzpatrick et al. 2004). The galvanic stimulus is commonly delivered by an anodal electrode on the mastoid process behind one ear and a cathodal electrode behind the other ear (i.e., bilateral bipolar GVS). Bilateral monopolar GVS has electrodes of same polarity at both ears, while unilateral monopolar GVS has a stimulating electrode at just one ear. Fitzpatrick et al. (2004) had shown that GVS stimulation affected human body sway magnitude and direction. Greater stimulation current yielded higher amplitude tilt (of the head and trunk). In a standing subject, bilateral bipolar GVS resulted in movement of the body toward the side of the anodal electrode. The significance of this result is that it showed that vestibular afferents are sensitive to electrical stimulation and can cause postural responses. However, unlike natural stimuli, GVS has a large disadvantage in that it has no directionality and the entire population of susceptible afferents are stimulated (regardless of the alignment of the hair cells they innervate). This setback is overcome by direct stimulation of the individual ampullary nerve afferents via a (semicircular canal) vestibular prosthesis. Furthermore, observations were only for short-term stimulation (i.e., during the test session), therefore long-term effects (e.g., adaptation) were not observed

In both humans and non-human primates, some postural effects of the vestibular prostheses have been observed (as in Philips et al. 2013; Thompson et al. 2012, respectively). Phillips et al. 2013 implemented a unilateral vestibular prosthesis in humans that consisted of electrodes chronically implanted in each of the three semicircular canals in the right ear. Testing was conducted during quiet-stance (tandem foot placement) with eyes-open or eyes-closed. This study showed that the modulation of stimulation current modulated the amplitude of the postural responses (i.e., peak sway amplitude increased in both mediolateral and anterior-posterior planes for an increase in prosthetic stimulation current). Also, stimulation of a specific canal affected postural sway orientation in that sway was directed opposite to the stimulated canal (i.e., right posterior canal stimulation produced a sway response shifted in the left-anterior right-posterior (LARP) plane and right anterior canal stimulation produced a sway response shifted in the right-anterior left-posterior (RALP) plane). However, one observed problem was that all of the subject's eye movement responses to the stimulation were not consistent with observed postural responses. More specifically, in all subjects the direction of the elicited eye movements changed as a function of stimulation current level (possibly due to increases in current spread at higher current levels), but the direction of the postural response was not observed to change for an increase in stimulation current level. Furthermore, the prosthetic stimulation was only provided for a relatively short duration (e.g., during the test session). Therefore, the long-term effects (e.g., adaptation or habituation) of chronic prosthetic stimulation (e.g., days/months) on posture were not explored. Although the results were encouraging, they show that further development and characterization of the prosthesis is necessary in order to further explore its

rehabilitative potential. Phillips et al. (2013) measured the effects of prosthetic stimulation of human vestibular-loss subjects on quiet-stance body sway with tandem foot placement. In the work described here we employed a more challenging balance task for a severe vestibular-loss subject: head-turns to targets.

When humans with severe bilateral vestibular dysfunction turn their heads while walking, it can result in an ataxic gait, imbalance, and falls. Head-turns have also revealed instabilities in bilateral vestibular-loss (quadruped) cat subjects (Stapley et al. 2006). Normal cats trained to perform rapid, large-amplitude head turns to the left or right in yaw while standing on a balance platform, exhibited a strategy of pushing off the forelimb contralateral to the head-turn and all four limbs created a yaw rotational moment in the direction of the target. However, bilateral vestibular labyrinthectomized cats thrust their body to the ipsilateral side of the head-turn leading to imbalance and falls. Stapley et al. hypothesized that postural imbalance in the labyrinthectomized animals arose from the misperception that the trunk was rolling contralaterally (based on available neck proprioceptive information in absence of vestibular information).

It is widely accepted that head orientation inputs from the vestibular receptors (the otoliths and semicircular canals) and neck afferents (joint receptors and muscle spindles) combine via vestibulospinal and cervicospinal reflex pathways, respectively (Stapley et al. 2006). Furthermore, it has been suggested that vestibular ("head-in-space") inputs and neck proprioceptive ("head-on-trunk") inputs are combined to calculate the position and velocity of the trunk relative to earth-based coordinates such as the line of gravity ("trunk-in-space") (e.g., Mergner 1997). If this is correct, then the absence of either vestibular or neck proprioceptive information would lead to an erroneous estimate of

trunk position. Intact cats (and humans) receive both vestibular (head-in-space) signals and neck proprioceptive (head-on-trunk) signals. When neck proprioceptive signals are combined with vestibular signals, the result yields a reliable estimation of trunk orientation (Figure 6.1, top). Vestibular-lesioned test subjects, however, lack the head-in-space signal but are still receiving a reliable head-on-trunk signal. As a result, the vestibular-loss subject estimates an erroneous trunk position (trunk-in-space) leading to imbalance and falls (Figure 6.1, middle).

We propose that the electric stimuli delivered by the vestibular prosthesis will partially restore vestibular cues to the severely-impaired animal. Because of this, we hypothesize that an animal in a severely vestibular-impaired state aided by a vestibular prosthesis (sBVH + STIM-ON) will have a more accurate estimate of trunk position (Figure 6.1, middle and bottom). This would lead to reduced trunk sway in the sBVH + STIM-ON state compared to the sBVH state without stimulation.

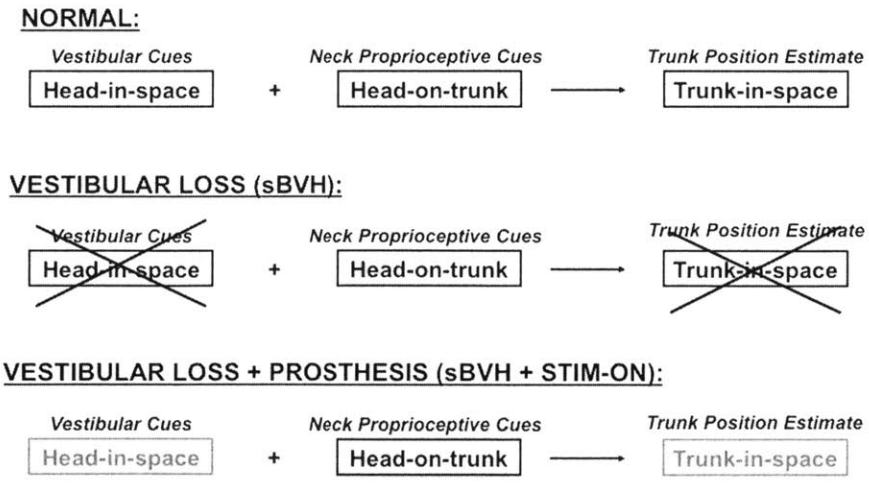

Figure 6.1 Schematic of normal, vestibular loss, and vestibular loss assisted by prosthesis trunk-in-space estimation. Gray text is to indicate a partial restoration.

The schematic shown in Figure 6.1 does not suggest that neck proprioceptive cues are the sole source of proprioception (e.g., bottom-up proprioception also plays a role in standing). However, because of the nature of the stimuli (i.e., relatively high velocity head-turns) meant to excite the semicircular canals, as opposed to those involving movements support surface (e.g., as in the platform roll-tilt stimulus described in Chapter IV), we assumed that neck proprioception cues combining with vestibular cues were dominant in estimating the trunk position during the head-turn..

6.3 Methods

6.3.1 Sensory states

Experiments were conducted with the approval of the Massachusetts Eye and Ear Infirmary (MEEI) Institutional Animal Care Committee and were in accordance with USDA guidelines. For these experiments, one adult female rhesus monkey R1 (7 yrs, 7.9 kg) was used. The animal was trained to stand free of restraint on a balance platform while receiving a juice reward.[1]

Using similar surgical procedures as described in Merfeld et al. 2007 for squirrel monkeys, the animal underwent surgery prosthesis implantation of its right posterior semicircular canal. After the surgical procedure, but before the treatments to compromise the vestibular system, the rhesus monkey's angular vestibuloocular reflex (VOR), a simple measure of semicircular canal function, was tested to define this baseline, or "control", state. After quantifying the control state, the monkey then underwent a series of ototoxic treatments that targeted and killed the vestibular hair cells while preserving eighth nerve function. Intratympanic gentamicin (IT gent) specifically kills vestibular hair cells and has been used to treat vertigo in Meniere's patients (e.g., Minor 1999).

Surgery was conducted under anesthesia (ketamine (10 mL/kg) pre anesthesia and isoflurane (2 - 5% saturation with oxygen)) and consisted of tympanic membrane perforation and gentamicin injection in each ear (i.e., 40 mg/mL in each ear). Maximum damage caused by the drug was estimated to be approximately 2 weeks post-administration (i.e., 1 cycle of IT gent treatment = administration, then 2 week waiting period). R1 underwent 3 cycles of IT gent treatments. In order to cause a greater level of vestibular dysfunction, the gentamicin treatments were followed by intramuscular streptomycin (IM strep) treatments (350 mg/mL per day for 21 days x 2). Following these sets of treatments, VOR gain was measured to characterize the severe bilateral vestibular hypofunction (sBVH) sensory state as shown in Figure 6.2 relative to control. Figure 6.2 also shows the VOR gain measured for the sBVH + STIM-ON state relative to control.

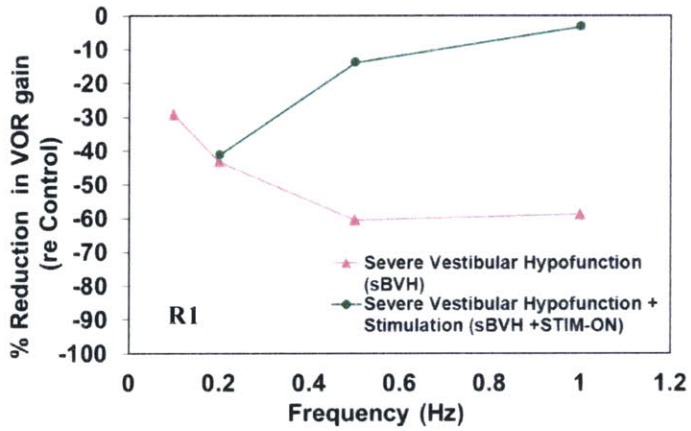

Figure 6.2 VOR gain reduction (re control sensory state) for the sBVH and sBVH + STIM-ON sensory states.

6.3.2 Vestibular prosthesis

The details of the prosthesis design and implementation have been previously published (Gong and Merfeld 2002; Lewis et al. 2010; Merfeld et al. 2007) and will only

be described briefly here. The study described in this chapter utilized a one-dimensional, semicircular canal prosthesis in which the electrode was placed in the ampulla of the right posterior canal in the rhesus monkey, R1. Although a one-dimensional prosthesis is described, current ongoing research involves the development of a three-dimensional prosthesis to simulate all three canals in each ear.

The one-dimensional prosthesis sensed head velocity that was high-pass filtered (~0.03 Hz cutoff frequency, time constant of 5 s), to mirror the system dynamics of the mechanisms associated with a normal rhesus monkey semicircular canal. The filtered head velocity was used to modulate the current pulse rate of the electric stimulus so that increasing (or decreasing) head velocity results in increases (or decreases) in spike rate (similar to the normal physiology of the canal and ampullary nerve). The tonic, baseline pulse rate was 250 Hz with pulse amplitude in the range of 90 microamperes, with 200 μs pulse duration. The rate was modulated to provide a bidirectional cue (i.e., head-turns that were ipsilateral to the stimulating electrode increased the rate of stimulation while head-turns that were contralateral to the stimulating electrode decreased rate of stimulation). The modulation itself was based on a hyperbolic tangent function that saturated at higher angular velocities, but was approximately linear for mid-range velocities (Figure 6.3, left). The prosthesis electronics housing was mounted to the animal's head and is shown in Figure 6.3, right.

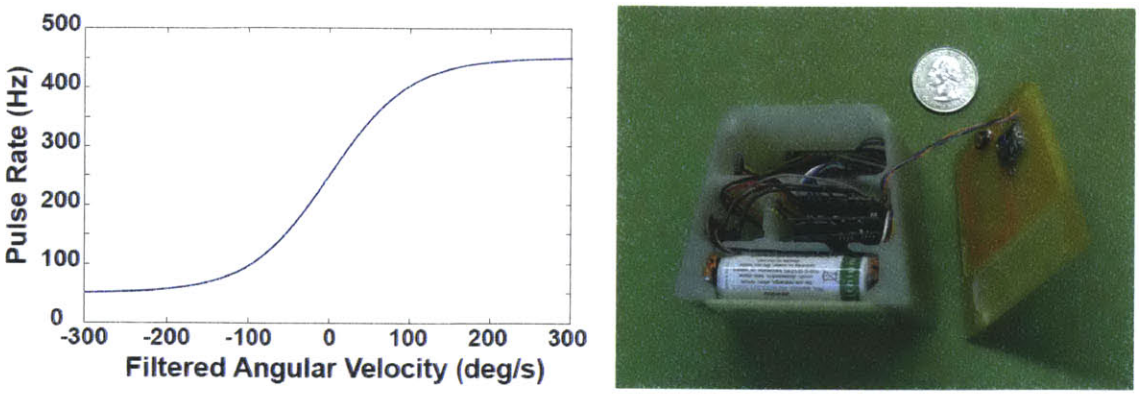

Figure 6.3 The hyperbolic tangent function (left) and electronics housing (right) for the rhesus monkey prosthesis.

Prior to the start of data collection, the animal was given only 8 days to adapt to the prosthetic simulation. There was a reduction in head movement due to (possibly) a behavioral response of the animal to the sensation of the electrical stimulation pulses. The time course necessary for the animal to become behaviorally adapted to the stimulation was not addressed in this study, but should be characterized in future work.

6.3.3 Overview of setup

Rhesus monkeys are habitual quadrupeds and were examined in their natural, quadrupedal stance. The animal was trained to stand free of human or mechanical restraint on the balance platform in order to receive a juice reward.[1] The head-mounted (HM) juice reward consisted of an acrylic clip attached to the monkey's head-cap (electronics housing) and a flexible tube that was routed to the monkey's mouth. This configuration was used so that the animal could freely rotate its head to illuminated targets (Figure 6.4).

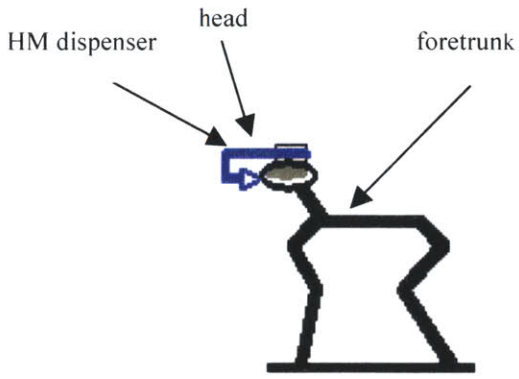

Figure 6.4 Schematic of the juice reward configuration: head-mounted, HM, dispenser.

In order to measure the motion of the head and foretrunk, position sensors (miniBIRD, Ascension Technology Corporation, Milton, VT) were sampled at 100 Hz. In order to limit environmental visual cues (e.g., of the surrounding wall and floor) all test sessions were conducted in dim lighting with a black tarp surround.

6.3.4 Head-turns to illuminated targets

Data were collected for R1 in the sBVH and sBVH + STIM-ON sensory states. For each state, the animal stood on a stationary platform and light-emitting diodes (LEDs) were positioned at 0° straight-ahead and $\sim 40^{\circ}$ oblique (in the plane of the right posterior canal) as shown in the schematic of Figure 6.5. A manual switch was pressed by the experimenter to illuminate the targets in the different positions. The animal was trained such that when it turned its head and fixated on the illuminated targets, it received a juice reward. When the animal was able to stand free of human restraint and make head-turns to the appropriate target, data were collected.

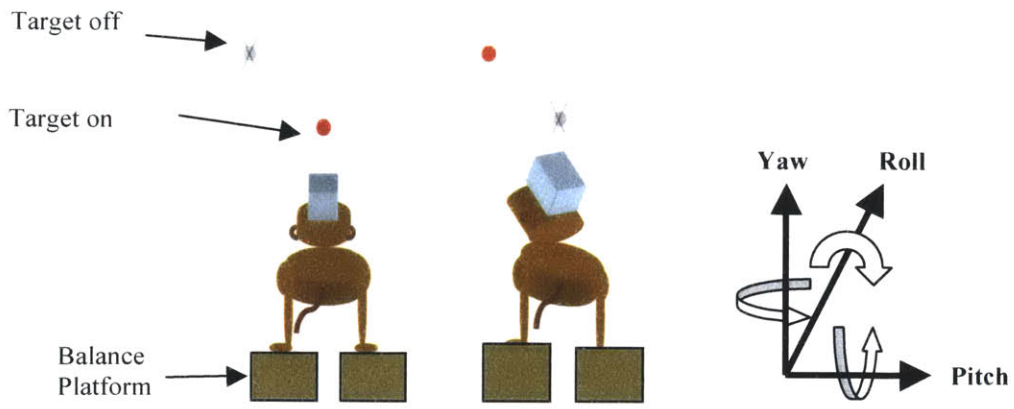

Figure 6.5 Schematic of the head-turn experimental condition (Lewis et al 2007). The left panel shows the monkey fixated on the 0° target while the monkey in the middle panel is fixate on the 40° target.

The experimenter pressed a manual switch to either illuminate the target in the 0 or the ~40° (oblique) position. During test sessions, the time of the manual switch press was recorded as a step in the digital output (value of either 0 (off) or 1 (on)). This was used to mark the onset of LED-on in the head measurement data record. After the test session, the head-turns to the oblique target were manually marked (by the data analyst). The digital output aided in determining the time just before the head-turn and just after the head-turn (the head-turn interval). The head-turn interval (or section) consisted of the following: start) the 0° target being illuminated and the animal facing forward; end) the 40° oblique target being illuminated and the animal turned its head. The initial maximum value of head yaw following the 40° oblique target being illuminated marked the end of the head-turn interval. The peak values of roll, pitch, and yaw displacement and velocity of the head and foretrunk were then computed for each head-turn interval. Equations 6.1 and 6.2 describe maximum displacement (MAXD) and maximum velocity (MAXV).

$$MAXD = \max(x(i)) - \min(x(i)) \tag{6.1}$$

where x(i) is position data for either the head or foretrunk within a given head-turn section for section number "i"

$$MAXV = \max(\dot{x}(i)) - \min(\dot{x}(i)) \tag{6.2}$$

where $\dot{x}(i)$ is derivative of the position data for either the head or foretrunk within a given head-turn section for section number "i"

Body position measurements in terms of the normalized percentage of peak foretrunk displacement for a given peak head displacement (nMAXD) were also computed (Equation 6.3), as well as body velocity measurements in terms of a normalized percentage of peak foretrunk velocity for a given peak head position velocity (nMAXV) (Equation 6.4). The purpose for normalizations (described in Equations 6.3 and 6.4) were to counteract the effects of the animal having variations in head-turn magnitude (to the illuminated target fixation point) on the animal's trunk motion.

$$nMAXD = \left| \frac{MAXD_{foretrunk}}{MAXD_{head}} \right| 100\% \tag{6.3}$$

$$nMAXV = \left| \frac{MAXV_{foretrunk}}{MAXV_{head}} \right| 100\% \tag{6.4}$$

Anchoring indices (Amblard et al. 1997), describing the relative angular deviations of a body segment relative to an inferior body segment (e.g., head relative to trunk), were calculated and analyzed.

$$AI = \frac{\sigma_r - \sigma_a}{\sigma_r + \sigma_a} \qquad (6.5)$$

where
AI = anchoring index
σ_r = standard deviation of the relative angular distribution (with respect to axes linked to inferior anatomical segment)
σ_a = standard deviation of absolute angular distribution of segment considered

Anchoring index (AI) was quantified to determine the movement of one body segment relative to an inferior body segment. An AI < 0 would, in theory, indicate that the body segment was more stable relative to the inferior body segment than in space, an AI > 0 would indicate that the body segment was more stable in space than relative to the inferior body segment, and an AI = 0 would indicate that the body segment was neither more stable in space or relative to the inferior body segment.

All data analyses were conducted using MATLAB (MathWorks, Natick, MA).

6.3.6 Usable data

Usable head-turn data were defined as those segments in which the head movements fell within specific movement criteria[2]: 1) all head-turn segments for a given test session were pooled and the sample minimum, lower quartile (Q1), median (Q2), upper quartile (Q3), and sample maximum were determined based on the MAXD head yaw and 2) outlier sections were defined as those with head MAXD yaw less than or greater than Q1-1.5*(Q3-Q1) and Q3+1.5*(Q3-Q1), respectively (as in Tukey 1977). The mean and standard deviations for Equations 6.1 through 6.5 were determined from the usable head-turn sections. For both sensory states, there were ample usable head-turn sections (i.e. sBVH sensory state: N = 70 usable *(9 unusable)* and sBVH + STIM-ON sensory state: N = 78 usable *(17 unusable)*).

In regards to comparisons of the measured results, for the above analyses a student's t-test (assuming unequal variance, unequal sample size) was used to determine significance.

6.4 Results

6.4.1 Head movements in sBVH and sBVH + STIM-ON sensory states

The peak foretrunk roll as a function of peak head yaw for all usable head-turns in the sBVH and sBVH + STIM-ON states are shown in Figure 6.6.

Figure 6.7 reveals that in the sBVH + STIM-ON compared to the sBVH state for all three axes of motion (i.e., yaw, pitch, and roll), the animal had significantly less head movement both in position and velocity (e.g., head pitch displacement and velocity: $df = 110$, $t = -3.428$, $p < 0.001$ and $df = 122$, $t = -2.117$, $p < 0.05$, respectively).

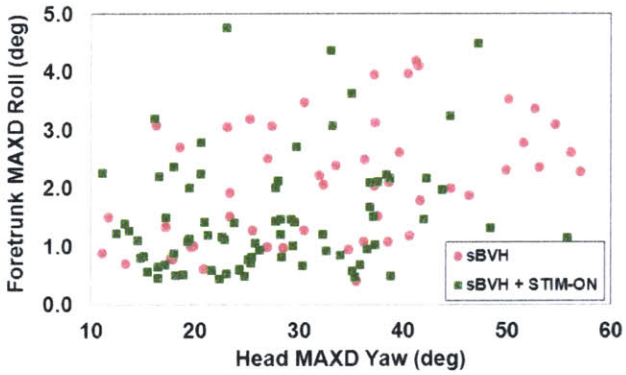

Figure 6.6 Foretrunk MAXD roll as a function of head MAXD yaw for all usable head-turns in sBVH and sBVH + STIM-ON states.

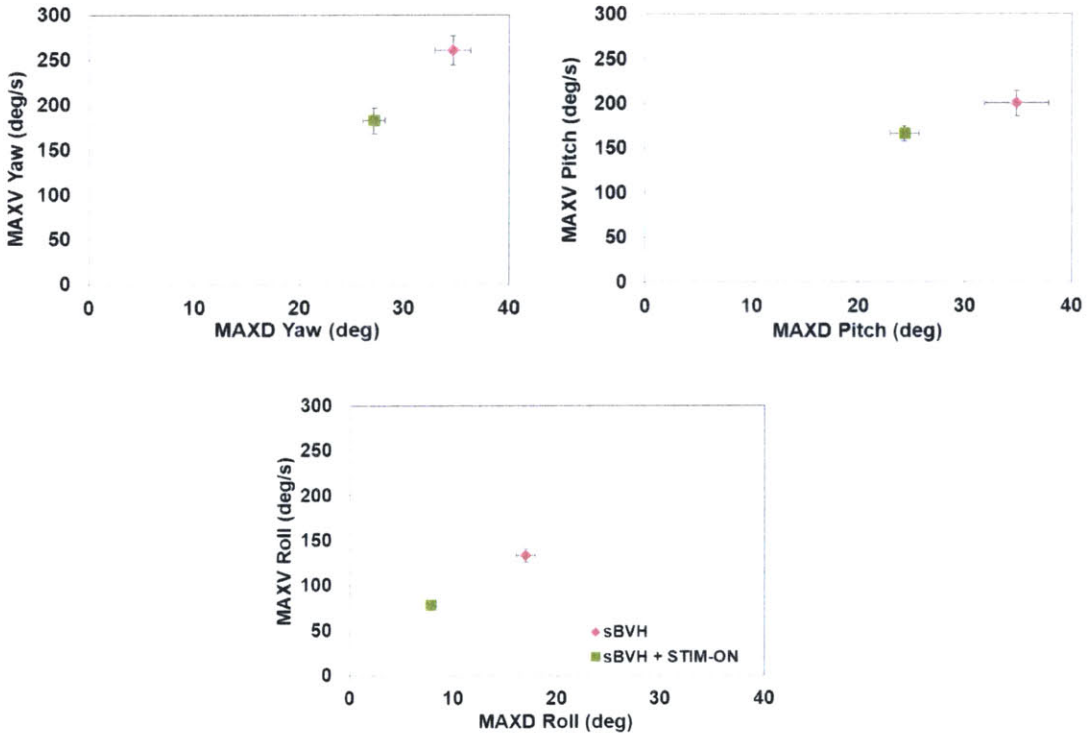

Figure 6.7 Head MAXD as a function of MAXV in yaw (left), pitch (right), and roll (bottom) for sBVH and sBVH + STIM-ON sensory states with standard error bars shown.

We accounted for the differences in head movement seen here by: 1) analyzing trunk motions for head motions that were similar in magnitude for the two states (Section 6.4.2) and 2) normalizing foretrunk position (or velocity) by head position (or velocity) (Section 6.4.3).

6.4.2 Foretrunk motions for comparable head-turn magnitudes

Because head-turn amplitude was smaller in the stimulated state (sBVH + STIM-ON) than the sBVH state, we aimed to determine if the decreases seen in foretrunk roll were a consequence of the smaller head-turns or increased stability due to the partially restored head orientation cues. In this section, we compared foretrunk roll between the sBVH and sBVH + STIM-ON sensory states for head-turns of similar amplitude.

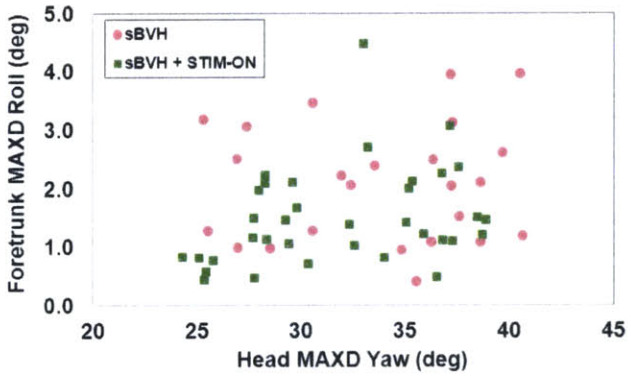

Figure 6.8 Foretrunk MAXD roll as a function of head MAXD yaw for comparable head-turn magnitudes in the sBVH and sBVH + STIM-ON states.

Figure 6.8 shows the range of head-turns (25-40° counter-clockwise in yaw) for the two sensory states (sBVH: N = 26; sBVH + STIM-ON: N = 36). This range was selected because there was overlap in head-turn magnitude between the two states. The mean and standard error were computed for each sensory state for this range of head-turn amplitudes (Figure 6.9).

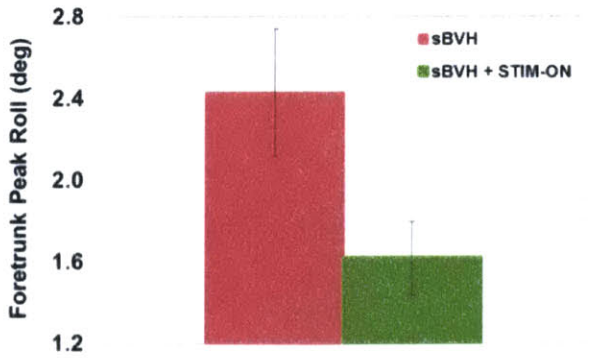

Figure 6.9 Foretrunk MAXD roll for sBVH and sBVH + STIM-ON states with standard error bars shown.

Figure 6.9 shows that between the two states there was a significant decrease (df = 42, t = -2.55, $p < 0.02$) in foretrunk roll in the sBVH + STIM-ON state relative to the sBVH state for an insignificant difference in head-turn yaw.

6.4.3 Absolute and normalized foretrunk motions

For all usable head-turns sections shown in Figure 6.7 (i.e., regardless of head-turn magnitude), both absolute and normalized foretrunk motions were pooled then compared for the sBVH and sBVH + STIM-ON sensory states.

Foretrunk MAXV yaw as a function of foretrunk MAXD yaw (Figure 6.10, left) showed no significant difference between sBVH and sBVH + STIM-ON foretrunk MAXD. There was a small but significant decrease in MAXV yaw in the sBVH + STIM- ON state (df = 96, t = -2.806, $p < 0.01$). Foretrunk MAXD roll and MAXV roll were both significantly less (df = 112, t = -12.350, $p < 0.001$ and df = 98, t = -3.324, $p < 0.002$, respectively) in the prosthesis on state (sBVH + STIM-ON) than the sBVH state (Figure 6.10, right).

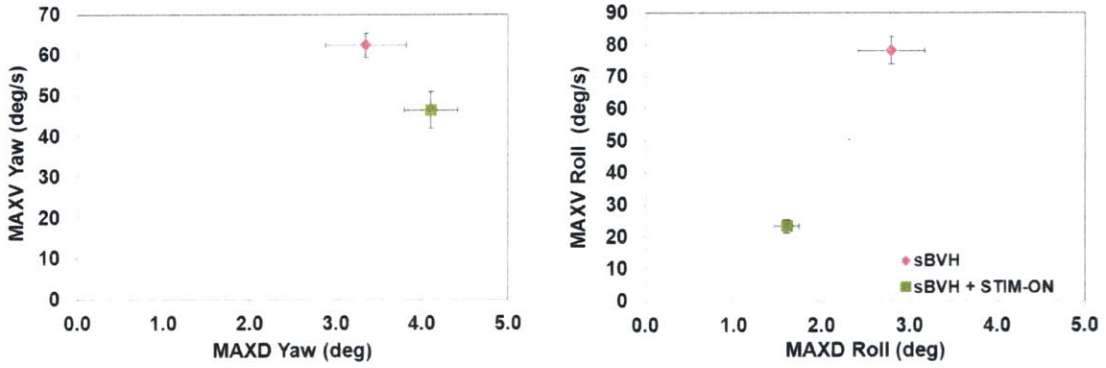

Figure 6.10 Foretrunk MAXD as a function of MAXV in yaw (left) and roll (right) for sBVH and sBVH + STIM-ON states with standard error bars shown.

The magnitude of the foretrunk roll normalized by head yaw and foretrunk roll velocity normalized by head yaw velocity (i.e., nMAXV foretrunk roll and nMAXD foretrunk roll) are shown in Figure 6.11 (left and right, respectively). When the prosthesis was turned on, there was a significant decrease ($df = 127$, $t = -5.603$, $p < 0.001$) in nMAXV foretrunk roll. Although insignificant, the nMAXD foretrunk roll also revealed a decreasing trend in comparing the sBVH to sBVH + STIM-ON states.

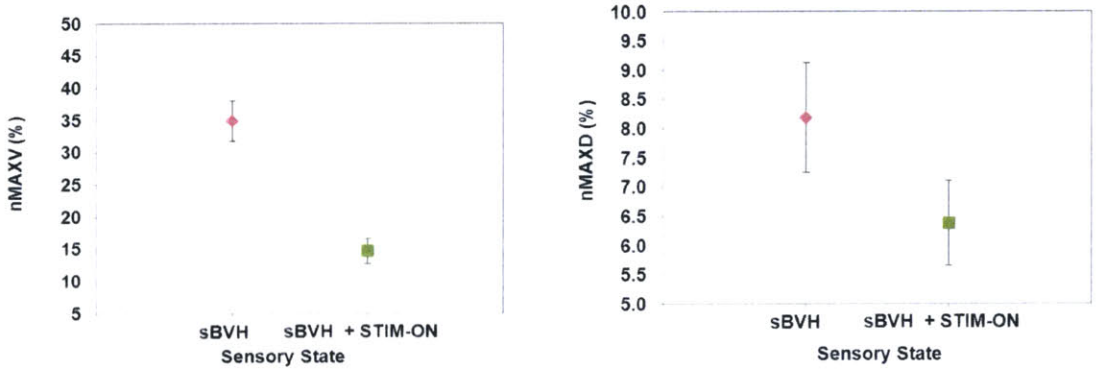

Figure 6.11 Ratio of foretrunk-to-head MAXV roll (left) and MAXD roll (right) for sBVH and sBVH + STIM-ON states with standard error bars shown.

6.4.4 Changes in postural strategy between sensory states

In order to determine if there were changes in postural strategy between the sBVH and sBVH + STIM-ON sensory states, roll AI was calculated (Figure 6.12). For both

sensory states the AI was negative, indicating that the head was more stable relative to the trunk than in space (i.e., the trunk was being "carried with" the head). Since the animal was performing head-turns to illuminated targets, this result was not surprising. The decrease in AI when the animal received prosthetic stimulation was not significant.

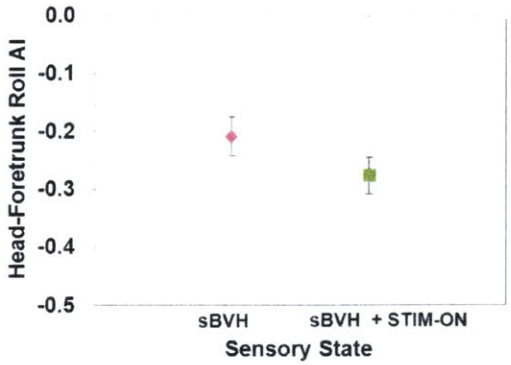

Figure 6.12 Head-foretrunk roll anchoring index for sBVH and sBVH + STIM-ON states with standard error bars shown.

6.5 Discussion

A rhesus monkey with severe bilateral vestibular loss exhibited a decrease in foretrunk roll when receiving vestibular prosthetic stimulation. We propose that the prosthetic electrical stimulation modulated by the animal's head velocity partially restored head velocity information. When the CNS integrated this information, it provided the severely-impaired animal more accurate head orientation cues than when the animal was without the stimulation. The more accurate estimate of head orientation allowed the severe vestibular-loss animal a better estimate of trunk position. This was observed as a reduction in trunk sway for the stimulated state (sBVH + STIM-ON) compared to the non-stimulated state (sBVH).

6.5.1 Animal's estimation of trunk position

A previous study conducted in normal and labyrinthectomized cats hypothesized that the combination of vestibular and neck afferent information contributed to trunk stability in space (Stapley et al. 2006). They proposed that the intact cat received both vestibular signals encoding velocity of head roll in space and neck proprioceptive signals of head roll with respect to trunk. The head-on-trunk signal combined with the head-in-space signal to indicate trunk position. Since the lesioned cat lacked the information of head roll in space, they suggested that the neck proprioceptive input of head-on-trunk, in the absence of an accompanying head-in-space input, was estimated by the animal as the body rolling under a stable head. This caused an illusion of falling in the roll plane as opposed to the head rolling on a stable trunk. This misperception caused an erroneous postural response leading to increases in sway and falls.

We showed that the severe vestibular-loss rhesus monkey's estimate of trunk position and/or velocity were improved (decreased or had a decreasing trend) when the animal was provided with partially restored head velocity cues via the prosthesis. More specifically, in comparing the sBVH state to the sBVH + STIM-ON state the animal showed significant decreases in foretrunk roll position for insignificantly different head-turn magnitudes (Figure 6.8). Furthermore, Figure 6.9 showed that foretrunk roll displacement (or velocity) normalized by head yaw displacement (or velocity) for the sBVH + STIM-ON and sBVH states revealed decreases in trunk motion. Taken together, these results are interpreted as the animal in the sBVH + STIM-ON state being able to utilize the partially restored canal cues from the prosthesis to obtain a more accurate estimate of trunk position (compared to the animal in the severely-impaired state).

6.6 Conclusions and Future Work

Here we show that the implementation of a vestibular prosthesis in a severely vestibular-impaired monkey led to a more stable trunk. Although the results shown here are for one-dimensional stimulation, future posture studies should continue with characterization of a vestibular prosthesis providing stimulation to all three semicircular canals. Also, to further test the utility of the prosthesis, balancing tasks that have proven to be difficult for vestibular loss subjects (e.g., head-turns while walking and balancing on a moving support surface) should be investigated. Furthermore, future work should incorporate electromyographic (EMG) measurements to allow for study of muscle activation patterns of the limbs and trunk to observe how those change with and without prosthetic stimulation. Also, eye movement measurements (e.g., via coil system) should be evaluated to quantify of the role of eye movements in conjunction with posture responses to balancing tasks (such as those listed above) both with and without the prosthetic stimulation.

---

[1] Chapter II (Section 2.4.2) discusses training methods used.
[2] Chapter II (Section 2.5.4) justifies the logic behind the outlier criteria used.

VII. Summary

The measured data and observed model results were consistent with the following: 1) the severity of vestibular dysfunction affects the postural mechanisms used to compensate, 2) severe vestibular-loss animals can utilize light-touch to improve postural stability, and 3) electric stimulation (via a vestibular prosthesis) in a severe vestibular-loss animal can aid in postural stability.

We observed that the severity of the vestibular dysfunction affects the postural compensation mechanisms used. For stationary support-surface conditions (e.g., quiet-stance and head-turns), we observed that a mild vestibular-impaired animal had decreased sway compared to its baseline condition but that a severe vestibular-impaired animal had increased sway relative to baseline. A feedback controller model was able to predict sway that was consistent with measured results. Furthermore, model parameters were consistent with the following: 1) the animal in the mildly impaired state increased its intrinsic/short-latency stiffness and damping in order to compensate and 2) the animal in the severely impaired state relied more on its long-latency neural mechanisms to compensate for the larger sways present.

For the tilting support surface, we examined a sensory reweighting hypothesis (i.e., there is increased weighting of graviceptive cues and decreased weighting of proprioceptive cues at larger platform tilts). In the normal animal, saturating trunk sway was observed at higher platform tilt amplitudes (sway saturation). The mild vestibular-loss animal also demonstrated sway saturation, but sway was generally elevated from normal. A feedback controller model was implemented and the model-predicted results

were consistent with the sensory reweighting hypothesis in that: 1) the normal model parameter results were consistent with greater weighting of graviceptive cues (and decreased weighting of proprioceptive cues) at larger platform tilts and 2) the model parameter results for the mildly impaired state showed that graviceptive weighting increased with platform tilt, but not to the extent seen in the normal state.

In this thesis, we have shown that sensory state (or level of vestibular impairment) can influence compensation strategy. The observations for mild and severe vestibular impairment can aid in determining rehabilitation strategies and also will serve as a baseline for future human (and non-human primate) research. Based on our observations, it is conceivable that different rehabilitative plans (e.g., patient training, non-invasive aids or vestibular prostheses) would be necessary based on the severity of vestibular loss, and that the type of assistive device (if any) could be influenced by the severity of vestibular dysfunction and best suited for a specific patient.

For a severe level of vestibular impairment without the aid of non-invasive, sensory cues (e.g., light-touch) or invasive, electric stimulation (via a vestibular prosthesis), the animal was unstable and had large trunk sways. We observed that an additional light-touch (proprioceptive) sensory cue aided the severe vestibular-loss animal in reducing its trunk sway compared to the configuration where it did not receive a light-touch cue. However, the animal with mild vestibular loss showed little change when provided the light-touch cue. We proposed that the animal in the severely impaired state was able to benefit from the light-touch cue, but that the animal in the mildly impaired state used other means (e.g., increases in intrinsic/short-latency stiffness) to compensate and, therefore, made little use of the additional sensory cue. These results

imply that severely vestibular-impaired subjects can benefit (i.e., enhance their stability) when an additional proprioceptive cue is provided. We also determined that prosthetic stimulation (via a prototype vestibular implant) in a severe vestibular-loss animal aided in postural stability. These findings indicate that prosthesis development and postural characterization should proceed. Future posture studies should include: 1) responses to multi-canal and bilateral prostheses and 2) continuation of non-human primate posture research with the aim of human vestibular prosthesis implementation.

Through measured and model-predicted results, we observed that sensory reweighting shown here in normal rhesus monkeys (and previously observed in normal humans), is used by the animal even for a mild level of vestibular impairment. The results suggest that modeling could be used to quantify vestibular contributions in a mildly impaired state, and also could be helpful in tracking a patient's rehabilitative progress following implantation of a vestibular prosthesis.

Overall, the results reported within this thesis establish the beginnings of a baseline database of primate postural responses to a wide variety of test situations for different levels of vestibular impairment against which rehabilitative techniques (e.g.., posture mechanisms used to compensate, non-invasive sensory substitutes, and invasive prototype vestibular prostheses) can be evaluated.

References

Angelaki DE, McHenry MQ, Dickman JD, Newlands SD, Hess BJM. "Computation of Inertial Motion: Neural Strategies to Resolve Ambiguous Otolith Information." *The Journal of Neuroscience* 19, no. 1 (1999): 316-327.

Angelaki DE, Wei M, Merfeld DM. "Vestibular Discrimination of Gravity and Translational Acceleration." *Annals of the New York Academy of Sciences* 942 (2001): 114-127.

Amblard B, Assaiante C, Fabre JC, Mouchnino L, Massion J. "Voluntary head stabilization in space during oscillatory trunk movements in the frontal plane performed in weightlessness." *Experimental Brain Research* 114, no. 2 (1997): 214-225.

Bach-y-Rita P, Kercel SW. "Sensory substitution and the human machine interface." *Trends Cogn Sci.* 7 (2003): 541-546.

Beloozerova IN, Zelenin PV, Popova LB, Orlovsky GN, Grillner S, Deliagina TG. "Postural Control in the Rabbit Maintaining Balance on the Tilting Platform." *Journal of Neurophysiology* 90, no. 6 (2003): 3783-3793 .

Black FO, Nashner LM. "Postural disturbance in patients with benign paroxysmal positional nystagmus." *Ann Otol Rhinol Laryngol.* 93, no. 6 (1984): 595-599.

Borel L, Harlay F, Magnan J, Chays A, Lacour M. "Deficits and recovery of head and trunk orientation and stabilization after unilateral vestibular loss." *Brain: A Journal of Neurology* 125, no. 4 (2002): 880-894.

Brookhart JM, Parmeggiani PL, Petersen WA, Stone SA. "Postural stability in the dog." *American Journal of Physiology* 208, no. 6 (1965): 1047-1057.

Camana PC, Hemami H, Stockwell CW. "Determination of feedback for human postural control without physical intervention." *Journal of Cybernetics* 7, no. 3-4 (1977): 199-225.

Carpenter MG, Frank JS, Silcher CP, Peysar GW. "The influence of postural threat on the control of upright stance." *Experimental Brain Research* 138, no. 2 (2001): 210-218.

Casadio M, Morasso PG, Sanguineti V. "Direct measurement of ankle stiffness during quiet standing: implications for control modelling and clinical application." *Gait & Posture* 21, no. 4 (2005): 410–424.

Cenciarini M, Loughlin PJ, Sparto PJ, Redfern MS. "Stiffness and damping in postural control increase with age." *IEEE Transactions on Biomedical Engineering* 57, no. 2 (2010): 267-275.

Cheung B. "Nonvisual Spatial Orientation Mechanisms." In *Spatial Disorientation in Aviation*, by Ercoline W Previc H, 37-94. Reston, VA: American Institute of Aeronautics and Astronautics, 2004.

Chiang B, Fridman GY, Chenkaii D, Rahman MA, Della Santina CC. "Design and performance of a multichannel vestibular prosthesis that restores semicircular canal sensation in rhesus monkey ." *Neural Systems and Rehabilitation Engineering, IEEE Transactions on* 19, no. 5 (2011): 588 - 598 .

Courtine G, Roy R, Hodgson J, McKay H, Raven J, Zhong H, Yang H, Tuszynski MH, Edgerton VR. "Kinematic and EMG Determinants in Quadrupedal Locomotion of a Non-Human Primate (Rhesus)." *J Neurophysiol* 93 (2005): 3127-3145.

Dai C, Fridman GY, Chiang B, Davidovics N, Melvin T, Cullen KE, Della Santina CC. "Cross-axis adaptation improves 3D vestibulo-ocular reflex alignment during chronic stimulation via a head-mounted multichannel vestibular prosthesis." *Experimental Brain Research.* no. 210 (2011): 595–606.

Davies WDT. *System identification for self-adaptive control.* Wiley-Interscience, 1970.

Della Santina CC, Migliaccio AA, Patel AH. "Electrical Stimulation to Restore Vestibular Function Development of a 3-D Vestibular Prosthesis." *Engineering in Medicine and Biology Society,27th Annual International Conference of the.* Shanghai: IEEE-EMBS 2005. , 2006. 7380 - 7385.

Dozza M, Chiari L, Horak F. "Audio-Biofeedback Improves Balance in Patients With Bilateral Vestibular Loss ." *Archives of Physical Medicine and Rehabilitation* 86, no. 7 (2005): 1401–1403.

Edin B. "Cutaneous afferents provide information about knee joint movements in humans." *Journal of Physiology* 531, Pt 1 (2002): 289-297.

Edin B. "Quantitative analyses of dynamic strain sensitivity in human skin mechanoreceptors." *Journal of Neurophysiology* 92, no. 6 (2004): 3233-43.

Fitzpatrick RC, Day BL. "Probing the human vestibular system with galvanic stimulation." *Journal of Applied Physiology* 96 (2004): 2301-2316.

Fridman GY, Davidovics NS, Dai C, Migliaccio AA, Della Santina CC. "Vestibulo-Ocular Reflex Responses to a Multichannel Vestibular Prosthesis Incorporating a 3D Coordinate Transformation for Correction of Misalignment." *Journal of the Association for Research in Otolaryngology* 11, no. 3 (2010): 367-381.

Fung J, Macpherson JM. "Determinants of postural orientation in quadrupedal stance." *The Journal of Neuroscience* 15, no. 2 (1995): 1121-1131.

Fung J, Jacobs R, Macpherson JM. "Strategies of postural orientation and equilibrium in quadrupedal stance." Edited by IEEE. *Strategies of postural orientation and equilibrium in quadrupedal stancee.* Portland, OR : Engineering in Medicine and Biology Society, 1995., IEEE 17th Annual Conference, 1995. 1219-1220 .

Golliday C, Hemami H. "Postural stability of the two-degree-of-freedom biped by general linear feedback ." *Automatic Control, IEEE Transactions on* 21, no. 1 (February 1976): 74 - 79.

Gong W, Merfeld DM. "System design and performance of a unilateral semicircular canal prosthesis." *Biomedical Engineering IEEE Transactions on* 49, no. 2 (2002): 175-181.

Goodworth AD, Peterka RJ. "Influence of Stance Width on Frontal Plane Postural Dynamics and Coordination in Human Balance Control." *Journal of Neurophysiology* 104, no. 2 (2010): 1103-1118 .

Goodworth AD, Wall C, and Peterka RJ. "Influence of Feedback Parameters on Performance of a Vibrotactile Balance Prosthesis." *Neural Systems and Rehabilitation Engineering, IEEE Transactions on* 17, no. 4 (2009): 397 - 408.

Gurfinkel VS, Lipshits MI, Mor S, Popov KET, 44, 473-486. "The state of stretch reflex during quiet standing in man." *Understanding the Stretch Reflex, Progress in Brain Research* 44 (1976): 473-486.

Gurfinkel VS. "Muscle afferentation and postural control in man." *Agressologie* 14 (February 1973): 1-8.

Herdman SJ. "Vestibular rehabilitation." In *Contemporary Perspectives in Rehabilitation*, by Wolf SL, 392. Philadelphia, PA: F.A. Davis, 1994.

Hodgson A, Wichayanuparp S, Recktenwald MR, Roy RR, McCall G, Day MK, Washburn D, Fanton JW, Kozlovskaya I, Edgerton VR. "Circadian Force and EMG Activity in Hindlimb Muscles of Rhesus Monkeys." *Journal of Neurophysiology* 86, no. 3 (2001): 1430-1444.

Horak FB. "Postural compensation for vestibular loss and implications for rehabilitation." *Restorative Neurology and Neuroscience* 28, no. 1 (2010): 57-68.

Horak FB, Macpherson JM. "Postural orientation and equilibrium." In *Comprehensive Physiology*, by R.S. Dow Neurological Sciences Institute Legacy Good Samaritan Hospital & Medical Center, 255–292. Portland, OR: American Physiological Society, 1996.

Horak FB, Nashner LM, Diener HC. "Postural strategies associated with somatosensory and vestibular loss." *Experimental Brain Research* 82, no. 1 (1990): 167-177.

Horak FB, Shupert CL, Dietz V, Horstmann G. "Vestibular and somatosensory contributions to responses to head and body displacements in stance." *Experimental Brain Research* 100, no. 1 (1994): 93-106.

Huterer M, Cullen KE. "Vestibuloocular Reflex Dynamics During High-Frequency and High-Acceleration Rotations of the Head on Body in Rhesus Monkey." *Journal of Neurophysiology* 88, no. 1 (2002): 13-28.

Johansson R, Magnusson M. "Human Postural Dynamics." *Critical Reviews in Biomedical Engineering* 18, no. 6 (1991): 413-437.

Kearney RE, Hunter IW. "Dynamics of human ankle stiffness: Variation with displacement amplitude." *Journal of Biomechanics* 15, no. 10 (1982): 753–756.

Kimura T. "Bipedal and quadrupedal walking of primates: comparative dynamics." *Primate morphophysiology, locomotor analyses and human bipedalism*, 1985: 81-104.

Kirsch Rf, Boskov D, Rymer WZ. "Muscle Stiffness During Transient and Continuous Movement of Cat Muscle: Perturbation Characteristics and Physiological Relevance." *IEEE Transactions of Biomedical Engineering* 41, no. 8 (August 1994): 758-770.

Koozekanani SH, Stockwell CW, McGhee RB, Firoozmand F. "On the Role of Dynamic Models in Quantitative Posturography." *Biomedical Engineering, IEEE Transactions on* 27, no. 10 (October 1980): 605 - 609 .

Kuo AD. "An optimal state estimation model of sensory integration in human postural balance." *Journal of Neural Engineering* 2, no. 3 (2005): 203.

Lackner JR, DiZio P, Jeka J, Horak F, Krebs D, Rabin E. "Precision contact of the fingertip reduces postural sway of individuals with bilateral vestibular loss." *Experimental Brain Research* 126, no. 4 (1999): 459-466.

Lackner JR, Rabin E, DiZio P. "Stabilization of posture by precision touch of the index finger with rigid and flexible filaments." *Experimental Brain Research* 139, no. 4 (August 2001): 454-464.

Lewis RF, Haburcakova C, Wangsong G, Karmali F, Merfeld DM. "Vestibuloocular Reflex Adaptation Investigated With Chronic Motion-Modulated Electrical Stimulation of Semicircular Canal Afferents ." *Journal of Neurophysiology* 103, no. 2 (2010): 1066-1079 .

Lewis RF, Haburcakova C, Gong W, Makary C, Merfeld DM. "Vestibuloocular Reflex Adaptation Investigated With Chronic Motion-Modulated Electrical Stimulation of Semicircular Canal Afferents ." *Journal of Neurophysiology* 103 (2010): 1066-1079.

Lewis RF et al. "Vestibular Influences on Spatial Orientation." National Institutes of Health (NIH) Research Grant Proposal (2007).

Loram I, Maganaris C, Lakie M. "The passive, human calf muscles in relation to standing: the non-linear decrease from short range to long range stiffness." *The Journal of Physiology* 584, no. 2 (2007): 661-675.

Loram ID, Lakie M. "Direct measurement of human ankle stiffness during quiet standing: the intrinsic mechanical stiffness is insufficient for stability ." *The Journal of Physiology* 545 (2002): 1041-1053.

Macpherson JM, Everaert DG, Stapley PJ, Ting LH. "Bilateral vestibular loss in cats leads to active destabilization of balance during pitch and roll rotations of the support surface." *Journal of Neurophysiology* 97, no. 6 (2007): 4357-4367.

Macpherson JM. "Changes in a postural strategy with inter-paw distance." *Journal of Neurophysiology* 71, no. 3 (1994): 931-940.

Macpherson JM. "Strategies that simplify the control of quadrupedal stance. II. Electromyographic activity." *Journal of Neurophysiology* 60, no. 1 (1988): 218-231 .

Macpherson JM, Lywood, DW, Van Eyken A. "A system for the analysis of posture and stance in quadrupeds." *Journal of Neuroscience Methods* 20, no. 1 (1987): 73-82.

Matthews, PBC. "Proprioceptors and their contribution to somatosensory mapping: complex messages require complex processing." Can. J. Physiol. Pharmacol. no. 66 (1988): 430-438.

McGhee RB, Kuhner MB. *On the Dynamic Stability of Legged Locomotion Systems.* University of Southern California Los Angeles Dept. of Electrical Engineering, 1970.

Merfeld DM, Zupan L, Peterka RJ. "Humans use internal models to estimate gravity and linear acceleration." *Nature* 398, no. 6728 (1999): 615-618.

Merfeld DM, Haburcakova C, Wangsong G, Lewis RF. "Chronic Vestibulo-Ocular Reflexes Evoked by a Vestibular Prosthesis ." *Biomedical Engineering, IEEE Transactions on* 54, no. 6 (2007): 1005-1015.

Mergner T, Huber W, and Becker W. "Vestibular–neck interaction and transformation of sensory coordinates." *J Vestib Res* 7 (1997): 347–367.

Minor LB. "Intratympanic Gentamicin for Control of Vertigo in Meniere's Disease: Vestibular Signs That Specify Completion of Therapy." *American Journal of Otology* 20, no. 2 (1999): 209-219.

Nashner LM. "Adapting reflexes controlling the human posture." *Experimental Brain Research* 26, no. 2 (1976): 59-72.

Nashner LM. *Sensory feedback in human posture control.* Massachusetts Institute of Technology. Dept. of Aeronautics and Astronautics, Cambridge, MA: Massachusetts Institute of Technology, 1970.

Peterka RJ, Wall C, Kentala E. "Determining the effectiveness of a vibrotactile balance prosthesis." *Journal of Vestibular Research* 16 (2006): 45-56.

Peterka RJ. "Sensorimotor integration in human postural control." *Journal of Neurophysiology* 88, no. 3 (2002): 1097-1118 .

Phillips C, DeFrancisci C, Ling L, Nie K, Nowack A, Phillips JO, Rubinstein JT. "Postural responses to electrical stimulation of vestibular end organs in human subjects." *Experimental Brain Research*, June 2013.

Picard C, Olivier A. "Sensory cortical tongue representation in man." *J Neurosurg* 59 (1983): 781-789.

Previc FH. "Visual Illusions in Flight." In *Spatial Disorientation in Aviation*, by Ercolin WR FH Previc, 283-321. Reston, VA: American Institute of Aeronautics and Astronautics, 2004.

Prieto TE, Myklebust JB, Hoffman RG, Lovett EG, Myklebust BM. "Measures of postural steadiness: differences between healthy young and elderly adults." *Biomedical Engineering, IEEE Transactions on* 43, no. 9 (1996): 956 - 966 .

Qu X, Nussbaum NA. "Evaluation of the roles of passive and active control of balance using a balance control model." *Journal of Biomechanics* 42, no. 12 (2009): 1850-1855.

Sienko KH, Balkwill MD, Oddsson LIE, Wall C. "Effects of multi-directional vibrotactile feedback on vestibular-deficient postural performance during continuous multi-directional support surface perturbations." *Journal of Vestibular Research* 18, no. 5-6 (2008): 273-285.

Stapley PJ, Ting LH, Kuifu C, Everaert DG, Macpherson JM. "Bilateral vestibular loss leads to active destabilization of balance during voluntary head turns in the standing cat." *Journal of Neurophysiology* 95, no. 6 (2006): 3783-3797.

"The Balance Center of Maryland." *http://www.balancemaryland.com/balance-system.* 2013.

Thompson LA, Haburcakova C, Gong W, Lee DJ, Wall C, Merfeld DM, Lewis RF. "Responses evoked by a vestibular implant providing chronic stimulation." *Journal of Vestibular Research* 22, no. 12 (2012):11-15.

Thomson DB, Inglis JT, Schor RH, Macpherson JM. "Bilateral labyrinthectomy in the cat: motor behaviour and quiet stance parameters." *Experimental Brain Research* 85, no. 2 (1991): 364-372.

Tukey JW. *Exploratory Data Analysis.* Reading, MA: Addison-Wesley, 1977.

Tyler M, Danilov Y, Bach-y-Rita P. "Closing and open-loop control system: Vestibular substitution through the tongue." *Journal of Integrative Neuroscience* 2, no. 2 (2003): 159-164.

van der Kooij H, Jacobs R, Koopman B, van der Helm F. "An adaptive model of sensory integration in a dynamic environment applied to human stance control." *Biological Cybernetics* 84, no. 2 (2001): 103-115.

Vilenksy JA. "Masses, Centers-of-Gravity, and Moments-of-Inertia of the Rhesus monkey (Macaca Mulatta)." *AM. J. PHYS. ANTHROP.* 50 (1979): 57-66.

Vuillerme N, Hlavackova P, Franco C, Diot B, Demongeot J, Payan Y. "Can an electro-tactile vestibular substitution system improve balance in patients with unilateral vestibular loss under altered somatosensory conditions from the foot and ankle?" *Engineering in Medicine and Biology Society,EMBC, 2011 Annual International Conference of the IEEE*, 2011: 1323 - 1326 .

Winter DA, Patla AE, Prince F, Ishac M, Percsak KG. "Stiffness Control of Balance in Quiet Standing." *Journal of Neurophysiology* 80 (1998): 1211–1221.

Winter DA. "Human balance and posture control during standing and walking." *Gait & Posture* 3, no. 4 (1995): 193–214.